Of Genes and Patients: Stochastic Dynamic Causal Modelling of the Prefrontal-Hippocampal Network

David Bernal Casas

Dissertation
submitted to the
Combined Faculties for the Natural Sciences and for Mathematics
of the Ruperto-Carola University of Heidelberg, Germany
for the degree of
Doctor of Natural Sciences

presented by

David Bernal Casas, M.Sc. Eng., Lic. Phys.
born in: Barcelona, Spain
Oral-examination:

Of Genes and Patients: Stochastic Dynamic Causal Modelling of the Prefrontal-Hippocampal Network

Referees: Prof. Dr. Rainer Spanagel
Prof. Dr. Peter Kirsch

Statement of Originality

I hereby declare that this dissertation is my own work and has been written independently, with no other sources and aids than quoted in the text, references and acknowledgements.

Heidelberg, May 2013

David Bernal Casas

Es con todo mi corazón que dedico
esta disertación doctoral a la
memoria de mis abuelos

Asimismo, le tributo este esfuerzo
a todos aquellos seres queridos
que me han apoyado en
este arduo camino

Concluiré simplemente
con lo siguiente:

“Somos un equipo”

Abstract

The research field of functional magnetic resonance imaging (fMRI) has made possible a remarkable progress in the understanding of the human brain enabling neuroscientists to study spatio-temporal alterations in the healthy and the diseased brain. While current theories of schizophrenia stress the critical role that plays aberrant connectivity among brain regions in major psychiatric disorders, other theories point towards the crucial role that plays functional excitation-inhibition (E-I) balance within the neural microcircuitry. Indeed, recent neuroscientific research has revealed increasing evidence that taking functional brain connectivity into account is essential to understand how the human brain works. Particularly, when trying to understand the brain pathology of schizophrenia, it becomes mandatory to study the connectivity among brain regions. The connection between the dorsolateral prefrontal cortex (DLPFC) and the hippocampal formation (HF) during working memory (WM) has been found to be increased in carriers of genetic risk variants for schizophrenia and schizophrenic patients. However, less is known about causality, i.e. which region drives the altered connection. Stochastic dynamic causal modelling (sDCM) is a novel mathematical algorithm for studying causal connectivity from fMRI data among higher cognitive brain regions. In this study, we focus on identifying alterations on genetic risk carriers and schizophrenia patients from the prefrontal-hippocampal network estimated with sDCM. We strive on giving a plausible biological interpretation to the sDCM parameter estimates by linking the concepts of causal connectivity and functional (E-I) balance. Furthermore, we ask whether sDCM parameter estimates contain sufficiently rich information to predict behavior and how these alterations on the prefrontal-hippocampal network have an impact on performance and reaction time. The final goal of this study is to describe how genetic risk variants for schizophrenia contribute to the phenotype expressed in patients in relation to the underlying neurobiology and behavior and thus help identifying potential blanks for the development of effective treatments.

Zusammenfassung

Die Forschung mittels funktioneller Magnetresonanztomographie (fMRT) hat wesentlich zum Verständnis des menschlichen Gehirns beigetragen, indem sie den Neurowissenschaftlern das Erforschen temporär- räumlicher Veränderungen sowohl im gesunden als auch im erkrankten Gehirn ermöglicht. Während aktuelle pathophysiologische Theorien der Schizophrenie den Veränderungen der Konnektivität innerhalb der Hirnregionen eine wesentliche Rolle zuschreiben, betonen andere Theorien die Bedeutung der funktionellen Balance zwischen Excitation und Inhibition (E-I) in neuronalen Mikroschaltkreisen. In der Tat zeigen die jüngsten neurowissenschaftlichen Forschungsergebnisse, welchen wichtigen Beitrag die Konnektivität zwischen Hirnregionen zum Verständnis der Arbeitsweise des gesunden und auch des erkrankten Gehirn leistet. Insbesondere für das Verständnis von pathologischen veränderten Hirnfunktionen bei der Schizophrenie scheint die Berücksichtigung der Konnektivität unabdingbar. So wurde eine verstärkte Konnektivität zwischen dem dorsolateralen präfrontalen Kortex (DLPFC) und der Hippocampusformation (HF) sowohl bei Trägern genetischer Risikovarianten als auch bei Schizophrenie-Patienten während der Bearbeitung von Arbeitsgedächtnisaufgaben (working memory, WM) entdeckt. Trotzdem bleibt vieles in Bezug auf die Kausalität unklar. Zum Beispiel bleibt die Frage offen, welche Region für die verstärkte Konnektivität verantwortlich ist. Moderne Ansätze wie das stochastic dynamic causal modelling (sDCM) nutzen neue mathematische Algorithmen zur Erforschung kausaler Konnektivität zwischen Hirnregionen auf der Basis von fMRT-Daten. Fokus dieser Studie ist die Identifizierung von Veränderungen im präfrontal-hippocampalen Netzwerk bei Trägern genetischer Risikovarianten und Schizophrenie-Patienten mittels sDCM. Anschließend wird versucht, die mittels sDCM geschätzten Parameter auf neurobiologischer Ebene zu erklären, indem die Konzepte der kausalen Konnektivität und der funktionellen Balance (E-I) verknüpft werden. Weiterhin wird untersucht, ob die durch sDCM geschätzten Parameter genügend Informationen beinhalten, um Vorhersagen über das Verhalten der Probanden treffen zu können und inwiefern Veränderungen im präfrontalen-hippocampalen Netzwerk einen Einfluss auf die Leistung und die Reaktionszeit während der Ausführung einer Arbeitsgedächtnis-Aufgabe haben. Das Endziel dieser Studie besteht darin, unter Einbeziehung der zugrundeliegenden Neurobiologie und des Verhaltens, besser zu verstehen, wie genetische Risikovarianten zum Phänotyp der Schizophrenie beitragen und dadurch potenzielle Ansatzpunkte für neue Therapiemöglichkeiten zu identifizieren.

Contents

Chapter 1: Introduction

"Whether you think you can or whether you think you can't, you're right"
Henry Ford

1.1. Background of the problem

The main goal of neuroscience is the better understanding of how the brain works. This can be performed at very different description levels, from the molecular level up to the system level. Functional neuroimaging is a technique that describes brain function at the system level. The research framework presented here uses neuroimaging methods to identify the causal dynamics within a particular macroscopic system: the prefrontal-hippocampal network, which is known to play a fundamental role in the pathophysiology of one of the most severe mental disorders: schizophrenia.

The next section will cover the research themes that are relevant for understanding this dissertation. This is not meant to be an exhaustive review of the themes, but it will pinpoint the basic research assumptions of this study. This literature review introduces the three main aspects of the research problem: functional neuroimaging, schizophrenia, and genetic studies.

1.1.1. Introduction to functional neuroimaging: measuring effective connectivity and functional excitation-inhibition (E-I) balance in fMRI

In the last decades, functional neuroimaging has made possible a remarkable progress in the understanding of the human brain enabling neuroscientists to study spatio-temporal alterations in the healthy and the diseased brain as a function of various stimuli. During these years, researchers have brought into the field of functional neuroimaging a large number of mathematical concepts i.e. functional and effective connectivity, with the purpose of addressing some of the issues in neuroscience i.e. functional organization of the brain.

Functional neuroimaging techniques significantly evolved during this process. The current state of non-invasive functional neuroimaging techniques has been classified according to underlying hemodynamic and electrophysiological principles. Hemodynamic principles concern the measure of biological signals generated by the cardiovascular system. The currently available functional neuroimaging techniques based on hemodynamic principles are positron emission tomography (PET) or single-photon emission computed tomography (SPECT), functional magnetic resonance imaging (fMRI), and near-infrared spectroscopy (NIRS). Electrophysiological principles concern the measure of electrical signals emanating from the central nervous system. The currently available

electrophysiological techniques include electroencephalography (EEG), magnetoencephalography (MEG), and transcranial magnetic stimulation (TMS) (Shibasaki, 2008).

Among these functional imaging techniques, fMRI measures the blood-oxygenation-level-dependent (BOLD) signal correlated to neural activity in the brain during perceptual and higher-cognitive tasks. The first successful fMRI study was published in Science Journal by (Belliveau et al., 1991). This new MRI technique was developed for quantitative imaging of cerebral hemodynamics, enabling for measuring the regional cerebral blood volume during both resting and task states by using a visual stimulus paradigm. The study showed the first magnetic resonance maps of human task activation. During photic stimulation, increases in cerebral blood volume were reported in the primary visual cortex (32 ± 10 percent, n = 7 subjects).

Nowadays, BOLD-based fMRI is a powerful technique for studying brain function not only locally but also at the systems level. The field of fMRI became central in neuroimaging research due to its relatively low invasiveness, wide availability, and absence of radiation exposure. More specifically, the field of fMRI for studying cognitive processes to examine how brain function supports mental activities literally exploded. While the first fMRI study exclusively focused on localized brain activation, soon after its publication the first attempts were made to identify functional networks in the brain by means of fMRI.

A landmark study in this context was a methodological review article published in Human Brain Mapping Journal by (Friston, 1994). Friston reviewed the primary difference between functional and effective connectivity and their role in addressing various aspects of functional brain organization. These concepts were initially formulated in the analysis of separable spike trains acquired from multiunit recordings (Aertsen and Preissl, 1991; Gerstein et al., 1989; Gerstein and Perkel, 1969; Gochin et al., 1991). At this microscopic level, correlations arise from stimulus-locked transients, driven by a common afferent input, or oscillations induced by input stimuli, mediated by synaptic connections (Gerstein et al., 1989). Thus, in this view, functional connectivity is the analysis about the observed covariations but it does not provide any direct insight in the origin of such observed variability. Thus, the focus has been displaced from functional connectivity studies, concerning static interactions among nodes to effective connectivity studies, encompassing dynamically distributed brain connectivity. Effective connectivity closely resembles the intuitive notion of connection, and can be defined as the influence on neural system exerts over another, mediated by synaptic efficacy or at the systems level. For instance, in electrophysiology, there is a close relationship between effective connectivity and synaptic efficacy (Gerstein et al., 1989). Moreover, it has also been proposed in the literature that effective connectivity in electrophysiology is defined as the simplest

time-dependent circuit that replicates the observed temporal interactions between the recorded neurons (Aertsen and Preissl, 1991).

Recently developed data analysis techniques where used for measuring effective connectivity in the human brain using fMRI data. A relevant study within this context is a methodological article published in NeuroImage Journal by (Friston et al., 2003). In this article, the authors introduced Dynamical Causal Modelling (DCM) for the first time. They developed this approach for the effective connectivity analysis using fMRI responses and experimentally designed inputs. The ensuing framework allowed one to make inferences about, the connectivity among brain regions and how these connectivity estimates are influenced by changes in experimental context.

DCMs are state space models formulated as ordinary differential equations. The basic idea is to implement a plausible neuronal model of interacting brain areas. This neuronal model is followed by a hemodynamic forward model that describes how neuronal or synaptic activity is transformed into observed fMRI responses. This hierarchical model consisting of two layers enables the parameters of the neuronal model (i.e., effective connectivity estimates) to be estimated from measured fMRI data. By using a bilinear approximation to the dynamics of interactions among neuronal populations, the parameter estimates of the implicit causal model reduce to three different sets. The three different sets of parameters are: (1) parameters that mediate intrinsic coupling among brain areas (intrinsic parameters), (2) bilinear parameters that allow experimentally designed inputs to influence the connectivity among brain areas (modulatory parameters), and (3) parameters that mediate the influence of experimentally designed inputs on brain areas (extrinsic parameters or driving inputs). The estimation proceeds in a Bayesian framework given known, deterministic inputs and the observed responses of the brain system.

DCM represented a completely different focus from existing approaches to effective connectivity: It uses a more plausible generative model of measured brain responses and takes into consideration their nonlinear and dynamic nature. Such nonlinear models of neural ensemble dynamics have been used to infer on effective connectivity between brain regions in multiple studies.

During last years, DCMs for fMRI responses have been limited largely to deterministic DCMs, where uncertainty about the states is ignored (Friston et al., 2003). These models assume that there are no random variations in the hidden neuronal and physiological states that mediate the effects of known experimental inputs on observed fMRI data. However, many studies suggested that physiological noise due to stochastic fluctuations in neuronal and vascular responses need to be taken into consideration (Biswal et al., 1995; Kruger and Glover, 2001; Riera et al., 2004). For instance, working memory (WM) tasks activate or deactivate regions that are susceptible to elicit

task-independent activity i.e. regardless the specific task. Recently, there has been an increasing interest in estimating both the parameters and hidden states of DCMs based upon differential equations that include state-noise (Daunizeau et al., 2009; Friston et al., 2008).

A relevant study within this context is a methodological article published in NeuroImage Journal by (Friston et al., 2011). In this article, the authors introduced stochastic DCM (sDCM) for the first time. The work focuses on discovering the functional integration of brain systems using fMRI time series. The algorithm enables to overcome Markovian assumptions – which were implausible – about the serial independence of random fluctuations. It can be applied to experimentally evoked responses (task state) or endogenous activity (resting state) fMRI studies. The authors envisaged that this novel mathematical algorithm would provide a meaningful complement to current functional connectivity analyses for both task and resting-state studies. This work established the methodological framework of the present study (see Section 1.4).

Although functional and effective connectivity can be cited at a conceptual level in both neuroimaging and electrophysiology techniques they differ essentially at a practical level. This is because the time-scales and nature of these neurophysiological measurements are very different (seconds vs. milliseconds and hemodynamic vs. spike trains). Nonetheless, new emerging studies have started to link findings between fMRI and electrophysiological techniques to locate specific brain functions (Logothetis and Wandell, 2004).

An influential study within this context is a review article published in Nature Journal by (Logothetis, 2008). In this article, the author provided an overview of the actual state of fMRI, and draw on fMRI and physiological data to describe the current understanding of the hemodynamic signals and the limitations they impose on fMRI data interpretation. As displayed in Figure 1.1.1.1, the author depicted a scheme of a canonical cerebral microcircuit and described the four different types of excitation-inhibition (E-I) changes and their plausible effect on the hemodynamic responses.

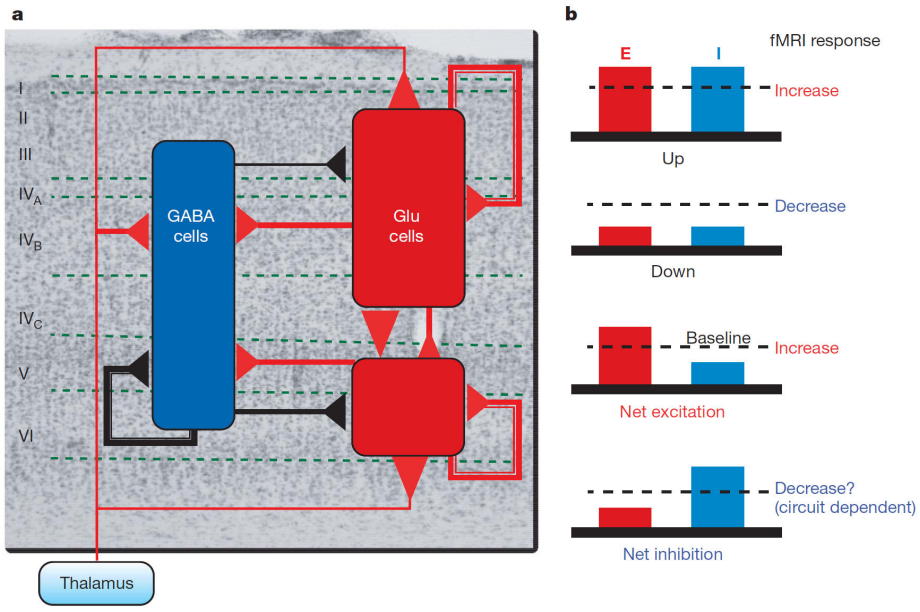

Figure 1.1.1.1. Principles of excitation-inhibition circuits. *Figure courtesy of (Logothetis, 2008)*

This canonical microcircuit comprises three different neuronal populations: supragranular-granular and infragranular glutamatergic spiny neurons (Glu cells), and GABAergic cells. All neuronal populations interact with each other and potential proportional and opposite-direction changes of cortical (E-I) activity are likely to strongly affect the hemodynamic responses. A very simple explanation of the fMRI responses assumes that observed increases of the BOLD signal occurs as a result of increases in the excitatory activity, and observed decreases of the BOLD signal occurs as a result of decreases in the excitatory conductances.

However, increases of the BOLD signal may also occur as a result of balanced proportional increases in the excitatory and inhibitory conductances, but without a net excitatory activity. Furthermore, an increase in recurrent inhibition with concomitant decreases in excitation may result in reduction of the BOLD signal, but the response to this question seems to be dependent on the specific brain region that is inhibited.

The author concluded that the limitations of fMRI are caused by the structural and functional brain organization, and these limitations are improbable to be solved in the future by improving the power of the scanners. Furthermore, the author stated that the fMRI signal may potentially lead to confusion about excitation and inhibition and therefore, complicates the precise definition of functional (E-I) balance.

Once introduced the elements of effective connectivity analyses and functional (E-I) balance in BOLD-fMRI, the next section will introduce the disconnection hypothesis and dysfunctional excitation-inhibition (E-I) balance in schizophrenia.

1.1.2. Introduction to schizophrenia: disconnection hypothesis and dysfunctional excitation-inhibition (E-I) balance

Schizophrenia is a severe mental disease characterized by withdrawal from reality, illogical patterns of thinking, hallucinations, and delusions, and accompanied in varying degrees by other behavioral, emotional, or cognitive deficits. The notion that schizophrenia is not caused by localized pathophysiology of brain areas, but arises from pathophysiological connectivity among brain regions, has been an influential thought. In addition to this idea, other pathophysiological theories point towards the critical role that plays functional excitation-inhibition (E-I) balance within the neural microcircuitry. It seems that schizophrenia results from abnormal regulation of functional (E-I) balance in neocortical networks.

Over the last century, disrupted interactions among brain areas have been proposed to underlie schizophrenia. This pathophysiological theory was originally presented by (Wernicke, 1906), who postulated that schizophrenia arises from anatomical disruption of association fiber tracts, and reformulated five years later in terms of psychopathology by (Bleuler, 1911), who coined the term schizophrenia for the first time to indicate the "splitting" of different mental domains. In the last decades, this influential theme re-emerged in neurophysiologic and functional neuroimaging studies revealing aberrant distributed activity and functional connectivity in schizophrenia (Hoffman et al., 1991; Volkow et al., 1988; Weinberger et al., 1992).

An influential study on this re-emerging topic is the article published in Clinical Neuroscience Journal by (Friston and Frith, 1995). In this PET study of language in 6 healthy subjects and 3 groups of 6 schizophrenic subjects, scientists reviewed the evidence for pathophysiological changes in the prefrontal and temporal cortices of schizophrenia patients and abnormal integration of the physiological dynamics between these brain regions. The main message of this study is that although local brain abnormalities, i.e., DLPFC, may be a sufficient explanation for some signs of schizophrenia, they do not provide a convincing explication for some symptoms such as hallucinations and delusions. These symptoms are better understood at a physiological level as altered functional connectivity and at a cognitive level as impairment to integrate perception and action. Their findings revealing consistently reduced prefronto-temporal connectivity in patients in comparison to controls indicate that altered prefrontal-temporal coupling is a well described endophenotype for schizophrenia.

In an attempt to explain these observations, (Friston, 1998) reviewed evidence for the disconnection hypothesis and presented a mechanistic model of how dysfunctional brain integration

among neuronal populations might result. This hypothesis suggests that psychosis can be understood as an impaired control of neuronal plasticity that manifests as inappropriate functional integration of brain systems. The mechanistic model is based on the crucial role that plays synaptic plasticity in shaping the connectivity dynamics that underlie human brain function. The assumption is that the pathophysiology is expressed at the level of modulation of associative plasticity in those neural systems in charge of memory and emotional learning, in the post-natal period. This modulation is mediated by ascending neurotransmitter systems that: (1) have been associated with schizophrenia; and (2) are known to be implicated in consolidating synaptic connections during learning.

Indeed, there is increasing evidence that analysing functional brain connectivity is essential to elucidate how the human brain works (Biswal et al., 2010). Particularly, when trying to understand brain pathology in major psychiatric disorders like schizophrenia, it is mandatory to study the connectivity between different brain regions (Fornito et al., 2012; Friston and Frith, 1995; Stephan et al., 2009a).

More specifically, the prefrontal-hippocampal network has been found to play a crucial role in pathophysiological theories of schizophrenia (Barch, 2005; Fletcher, 1998; Weinberger et al., 1992), and their connectivity has been studied in numerous studies on the disorder. Impaired PFC-HF connectivity has been described in mouse models of schizophrenia (Sigurdsson et al., 2010) as well as in individuals with increased psychosis risk and in first episode patients (Benetti et al., 2009; Crossley et al., 2009). In schizophrenia patients, altered PFC-HF coupling was found both under resting conditions (Zhou et al., 2007; Zhou et al., 2008) and during WM tasks (Crossley et al., 2009; Wolf et al., 2009).

WM concerns the maintenace and on-line manipulation of information; and is an essential component of executive control for guiding behavior. WM processes temporary store contents; which are continually updated, scanned and manipulated in response to immediate processing demands (Baddeley, 1992). WM deficits in schizophrenia have been consistently described (Forbes et al., 2009; Lee and Park, 2005), they are known to be resilent to the treatment and thus may underlie many of the cognitive deficits and symptoms in the disorder (Silver et al., 2003). These deficits cause longer reaction time and less accurate performance in schizophrenic subjects, especially when memory load increases (Goldman-Rakic, 1994; He et al., 2012; Manoach et al., 1999; Park and Holzman, 1992).

A landmark study within the context of prefrontal-hippocampal connectivity and WM is the article published in Archives of General Psychiatry Journal by (Meyer-Lindenberg et al., 2005). In this PET study of WM in 22 medication-free schizophrenic subjects and 22 performance-, age-, and sex-

matched healthy volunteers, the researchers investigated the functional coupling between the HF and the DLPFC in the healthy and the diseased brain. Their analysis indicated a specific alteration of HF-DLPFC functional connectivity. The authors demonstrated an unmodulated persistence of coupling between these brain areas during a working memory load condition; which occurred in schizophrenia patients but not in healthy subjects. Figure 1.1.2.1 illustrates their findings by showing a significant coupling during both the 2-Back and 0-Back tasks in patients; which in controls was only present during the 0-Back task.

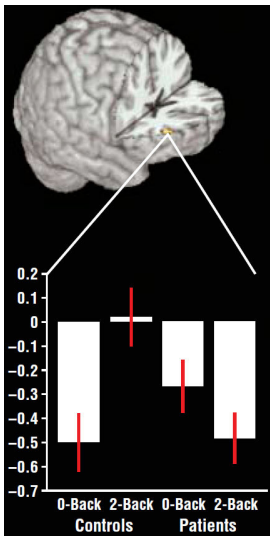

Figure 1.1.2.1. Mean values for covariation with left HF in the right DLPFC. *Figure courtesy of (Meyer-Lindenberg et al., 2005)*

This discovery suggested a plausible causal mechanism of the development of the pathophysiology of schizophrenia from HF dysfunction. Such a sequence of events would lead from an early developmental insult to the HF via impairment of the HF-DLPFC connectivity and induced maturational deficits in DLPFC circuitry to DLPFC dysfunction, which accounts for the core neuropsychology of the disease and is related to dopaminergic disinhibition. Therefore, a mechanism by which HF dysfunction may manifest in schizophrenia is by inappropriate reciprocal connectivity with the DLPFC.

This influential functional neuroimaging study is one of the mainstays of our research together with (Esslinger et al., 2009; Meyer-Lindenberg and Weinberger, 2006). It is worth highlighting that while some functional interactions between prefrontal and temporal cortices seem to be reduced in schizophrenic subjects (Friston and Frith, 1995), other functional interactions between temporal and prefrontal regions may be abnormally increased (Meyer-Lindenberg et al., 2005). To avoid any potential confusion, neuroscientists started to use the term “dysconnectivity” to describe these observations. This term emphasizes the idea that there is “abnormal” (rather than decreased) functional integration among brain areas in the disorder.

More recently, in a literature review article, (Stephan et al., 2006) reviewed the evidence for current theories of schizophrenia stressing the crucial role of abnormal connectivity among brain regions and focusing on the modulation of synaptic plasticity as a plausible mechanistic account for explaining how dysconnectivity arises. In particular, they discussed how dysconnectivity among brain regions associated with schizophrenia (Friston and Frith, 1995; Meyer-Lindenberg et al., 2005), could result from altered modulation of (NMDA)-dependent plasticity by other neurotransmitter systems; and further examined current discoveries provided by recent genome-wide linkage and allelic association studies supporting abnormal synaptic plasticity in schizophrenia (Harrison and Weinberger, 2005).

As displayed in Figure 1.1.2.2, they depicted a simplified diagram of the hierarchical relation among synaptic strength, synaptic plasticity and its modulation at glutamatergic synapses. The efficacy of a glutamatergic synapse largely depends on the number and functional state of postsynaptic AMPARs. The AMPARs are quickly inserted into and removed from the cell membrane (Malinow and Malenka, 2002; Montgomery and Madison, 2004). Both the trafficking and state-dynamics of AMPARs are mostly under the control of NMDARs. The function of NMDARs is affected by mGluRs as well as by various neurotransmitters, including acetylcholine (ACh), norepinephrine (NE), serotonine (5-HT), and dopamine (DA) (Gu, 2002). Some of these neurotransmitters, i.e. dopamine (Wolf et al., 2003) and acetylcholine (Massey et al., 2001), can also influence AMPAR function independently of NMDARs. Six out of seven candidate genes for schizophrenia identified by (Harrison and Weinberger, 2005), encode proteins that play a role in synaptic plasticity and its modulation. It should be stressed that the vast majority of these candidate genes affect NMDAR function directly.

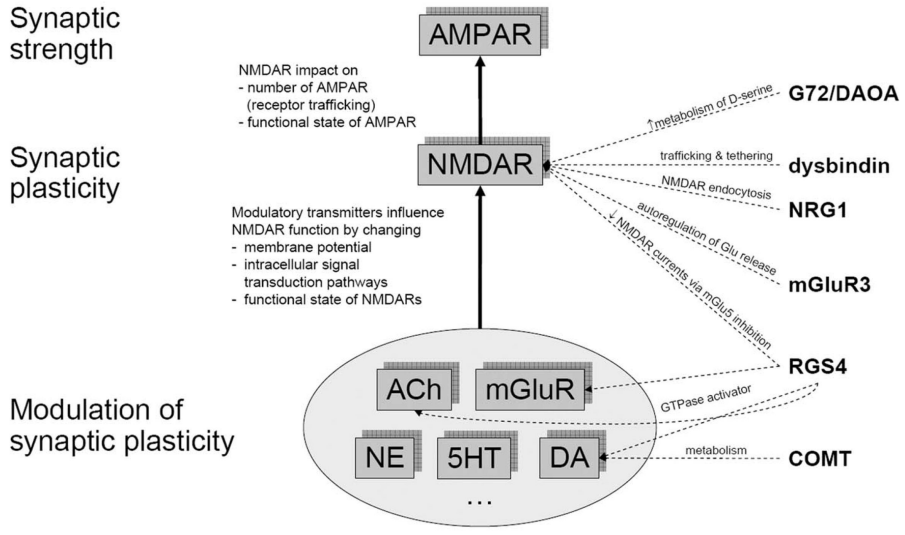

Figure 1.1.2.2. Simplified diagram of the hierarchical relation among synaptic strength, synaptic plasticity, and its modulation at glutamatergic synapses. *Figure courtesy of (Stephan et al., 2006)*

To conclude the article, (Stephan et al., 2006) illustrated the implication of the dysconnectivity hypothesis for functional neuroimaging studies reviewing recent data analysis techniques for measuring plasticity in the human brain using fMRI and EEG. The authors predicted that theoretical and causal models of brain responses for these data modalities, i.e. DCM, will potentially provide a mechanistic understanding of synaptic plasticity in schizophrenia.

In addition to these pathophysiological theories of schizophrenia highlighting the crucial role of abnormal connectivity among brain regions, other pathophysiological theories point towards the crucial role that plays functional (E-I) balance within the neural microcircuitry. Abnormal regulation of (E-I) balance in neocortical networks seems to underlie severe neuronal disorders including schizophrenia. This concept will serve as a guide for the discussion of our research findings.

A relevant article within this context is a literature review paper published in Frontiers In Molecular Neuroscience Journal by (Kehrer et al., 2008). The main message of this review is that the fundamental neurotransmitter pathology of schizophrenia remains poorly understood, despite tremendous advances over the last decades in discovering neurochemical and pathophysiological abnormalities in the disorder. The researchers stated that originally the dopamine/serotonin hypothesis supported most of the neurochemical research in schizophrenia; however, in the last years, the focus has turned to the glutamate system, the major excitatory neurotransmitter in the central nervous system, and towards the concept of functional (E-I) imbalance at the network level in specific brain areas associated with schizophrenia. Recent findings suggesting a crucial role for the NMDA-receptor in the aetiology of the disorder have led to the NMDA-hypofunction model opening a research field which allows study the disease in vitro at the cellular and network level. The researchers review evidence that changes in the (E-I) balance within the NMDA-hypofunction model leads to alterations in network behaviors, particularly in oscillatory activity within the gamma frequency band.

Despite all these findings on the disconnection hypothesis and dysfunctional excitation-inhibition (E-I) balance, we do not know what causes some individuals to develop this severe mental disorder and is still a major challenge. Indeed, recent studies report a robust evidence of a strong genetic component involved in the development of the disease. Thus, the next section will introduce some genetic mechanisms of dysconnectivity in schizophrenia.

1.1.3. Introduction to genetic studies: genetic mechanisms of dysconnectivity and dysfunctional excitation-inhibition (E-I) balance in schizophrenia

There is overwhelming evidence of a strong genetic influence to develop schizophrenia; nonetheless, genes alone do not completely explain the disease. In fact, a series of studies suggest that genes do not cause schizophrenia directly, but do make a person vulnerable to developing the disorder, as will be discussed in short.

The frequency of schizophrenia in the general population is less than 1%. However, being related to someone with schizophrenia extremely increases the risk of developing the disorder. For instance, if your sibling has the illness your chance of having schizophrenia is 9%. If your identical twin has schizophrenia, you have a 28% likelihood of developing the disease. If both of your parents have the illness, you have a 36% chance of developing the disorder. However, genes alone do not cause the disease. If they did, then identical twins, who share virtually the same genetic code, would have close to 100% likelihood of sharing the illness, rather than 28%.

Recently, significant risk genes for psychotic disorders have been discovered affording an excellent opportunity to establish neural mechanisms linked to genetic risk variants for schizophrenia. A landmark study within this context is an opinion article published in Nature Journal by (Meyer-Lindenberg and Weinberger, 2006). The researchers illustrated recent progress on linking genes to structural and functional variation in neural systems related to cognition and emotion, using imaging genetics as an example. They proposed the intermediate phenotype as a meaningful strategy for describing the brain systems affected by genetic risk variants to characterize quantitatively mechanistic aspects of brain function involved in mental disorders. The main hypothesis of the intermediate phenotype strategy is that gene effects are a more direct effect of genetic variation at the level of neural systems than is complex behavior, and will reveal association in genetic risk carriers even if the carriers do not show clinical symptoms.

As displayed in Figure 1.1.3.1, many genetic risk associations to brain-based phenotypes are even observed in healthy subjects. To the significant degree that susceptibility genes contribute to psychiatric risk, this approach offers a potential bottom-up strategy to discover biologically meaningful knowledge about unknown mechanisms. Therefore, imaging genetics becomes a guideline to the discovery of neural systems that translates genetic effects into behavior.

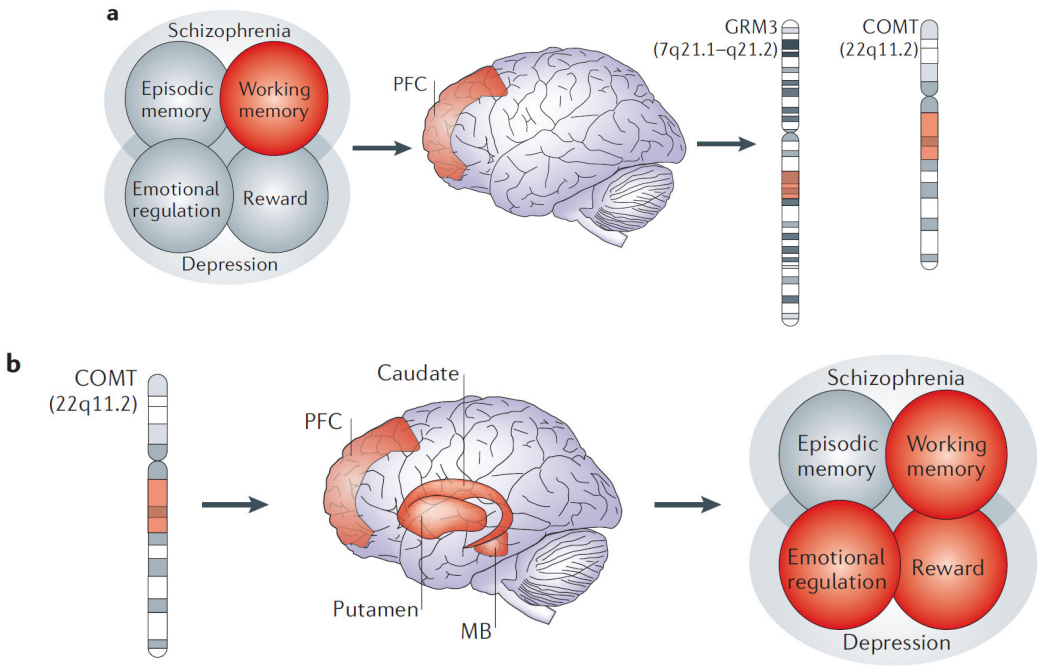

Figure 1.1.3.1. Intermediate phenotype tools for gene discovery versus neural mechanism characterization. *Figure courtesy of (Meyer-Lindenberg and Weinberger, 2006)*

Figure 1.1.3.1 illustrates the intermediate phenotype strategy by showing two different approaches for the detection of genetic risk variants linked to mental disorders: **a**) In the gene discovery approach, behavioral or brain systems phenotypes are used to diminish genetic complexity and increase penetrance to discover genes involved in mental disorders. **b**) In the neural mechanism approach, risk genes known to be associated with mental disorders or behavioral traits are used to identify neural mechanisms mediating their complex emergent phenotypic associations, implicating these mechanisms in the mental disorders to which they have been related.

This excellent opinion article is one the mainstays of our research together with (Esslinger et al., 2009; Meyer-Lindenberg et al., 2005), since in our study we adopted the neural mechanism characterization approach. The review of the literature continues with genome-wide association studies (GWAS) of schizophrenia.

GWAS have emerged as a new approach for investigating the genetic basis of schizophrenia. Recently, in a GWAS of schizophrenia, (O'Donovan et al., 2008) discovered the single-nucleotide polymorphism (SNP) rs1344706, in intron 2 of ZNF804A on chromosome 2q32.1, a gene coding for a protein of unknown function but potential gene regulatory ability, to be one of the most compelling candidate SNPs for schizophrenia. Their GWA cases (Table 1.1.3.1; Combined UK samples, 642 cases, 2937 controls) were drawn meeting criteria for schizophrenia. In a first replication sample (Table 1.1.3.1; Replication 1, 1664 cases, 3541 controls), they replicated the association observed in the GWA sample for 6 of the 12 SNPs. In a second replication sample, they did genotype these 6 SNPs

(Table 1.1.3.1; Replication 2, 4143 cases, 6515 controls). The full replication dataset (Table 1.1.3.1; Replication 1 + 2) provided strong independent support for schizophrenia susceptibility variants at 2q32.1 in ZNF804A ($p = 9.25 \times 10^{-5}$). Finally, they combined the data across all samples (Table 1.1.3.1; Meta SZ), and discovered that the ZNF804A locus provided the highest evidence for association to schizophrenia ($p = 1.61 \times 10^{-7}$). Therefore, the ZNF804A is very possibly a true susceptibility locus for schizophrenia; albeit one that confers a small increment in risk.

			Combined UK samples					Replication 1		Replication 1+2		Meta SZ			
			Cases $n = 642$ Controls $n = 2,937$					Cases $n = 1,664$ Controls $n = 3,541$		Cases $n = 6,666$ Controls $n = 9,897$		Cases $n = 7,308$ Controls $n = 12,834$			
Chr./Mb	SNP	Risk allele	SZ	CON	ATT(P)	Adj(P)	OR	CMH(P)	OR	CMH(P)	OR	CMH(P)	Meta-Adj	OR	Locus
2/185.5	rs1344706	T	0.66	0.59	7.08×10^{-7}	1.83×10^{-6}	1.38	0.026	1.09	9.25×10^{-5}	1.09	1.61×10^{-7}	1.95×10^{-7}	1.12	*ZNF804A*
11/29.1	rs1602565	C	0.15	0.11	7.81×10^{-6}	1.70×10^{-5}	1.49	0.005	1.19	3.22×10^{-4}	1.12	2.99×10^{-6}	3.02×10^{-6}	1.16	Intergenic
16/13.0	rs7192086	T	0.30	0.24	3.32×10^{-5}	6.52×10^{-5}	1.33	0.018	1.11	5.10×10^{-4}	1.09	6.08×10^{-6}	1.34×10^{-5}	1.12	Intergenic
11/132.1	rs3016384	C	0.56	0.49	5.82×10^{-5}	1.10×10^{-4}	1.29	0.012	1.10	0.016	1.05	5.63×10^{-4}	1.11×10^{-4}	1.08	*OPCML*
16/52.2	rs9922369	A	0.05	0.03	8.05×10^{-7}	2.05×10^{-6}	2.06	0.015	1.31	0.029	1.14	4.54×10^{-4}	5.01×10^{-6}	1.24	*RPGRIP1L*
12/116.2	rs6490121	G	0.40	0.34	4.33×10^{-6}	9.82×10^{-6}	1.33	0.044	1.08	0.992	1.00	0.109	5.51×10^{-3}	1.04	*NOS1*
2/144.3	rs2890738	A	0.41	0.33	4.96×10^{-9}	1.83×10^{-8}	1.44	0.249	1.03	–	–	–	–	–	Intergenic
3/134.5	rs7624858	A	0.44	0.37	1.15×10^{-4}	2.07×10^{-4}	1.27	0.113	1.06	–	–	–	–	–	*TMEM108*
5/138.5	rs17131938	A	0.07	0.04	2.94×10^{-4}	4.94×10^{-4}	1.64	0.091	0.81	–	–	–	–	–	*SIL1*
10/5.6	rs4750519	T	0.48	0.41	1.07×10^{-4}	1.93×10^{-4}	1.27	0.612	0.98	–	–	–	–	–	Intergenic
15/94.0	rs8031294	T	0.51	0.42	2.29×10^{-5}	4.62×10^{-5}	1.30	0.311	1.02	–	–	–	–	–	Intergenic
18/9.0	rs1893146	A	0.16	0.11	5.40×10^{-7}	1.42×10^{-6}	1.55	0.102	0.89	–	–	–	–	–	Intergenic

SZ and CON; allele frequency in schizophrenia and controls. ATT(P), trend test P value; Adj(P), genomic control adjusted P value; CMH(P), Cochran-Mantel-Haenszel P value; Meta-Adj, genomic control adjusted meta-analysis P value.

Table 1.1.3.1. Loci selected for follow-up analysis. *Table courtesy from (O'Donovan et al., 2008)*

Common risk factors between schizophrenia and bipolar disorder as shown by (Craddock et al., 2005), motivated the authors to investigate also the association with the latter disease. Therefore, in a second analysis, they included genotypes from the bipolar cases (Table 1.1.3.2; UK BP, 1865 cases) to the UK schizophrenia cases to make a large UK psychosis sample for inclusion in the meta-analysis. Table 1.1.3.2 shows that this association strengthened when the affected phenotype included bipolar disorder ($p = 9.96 \times 10^{-9}$), indicating that alleles in the vicinity of ZNF804A influence risk to a larger psychosis phenotype. In summary, the authors demonstrated that ZNF804A is probably a true susceptibility locus not only for schizophrenia but also for bipolar disorder.

						UK SZ		UK BP		Meta SZ + BP	
			Allele freq.			Cases $n = 642$, Controls $n = 2,937$		Cases $n = 1,865$, Controls $n = 2,937$		Cases $n = 9,173$, Controls $n = 12,834$	
Chr./Mb	SNP	Risk allele	SZ	BP	CON	ATT(P)	OR	ATT(P)	OR	CMH(P)	OR
2/185.5	rs1344706	T	0.66	0.62	0.59	7.08×10^{-7}	1.38	4.07×10^{-4}	1.16	9.96×10^{-9}	1.12
11/29.1	rs1602565	C	0.15	0.12	0.11	7.81×10^{-6}	1.49	0.055	1.14	4.26×10^{-6}	1.15
12/116.2	rs6490121	G	0.40	0.35	0.34	4.33×10^{-6}	1.33	0.168	1.06	0.124	1.03
16/52.2	rs9922369	A	0.05	0.03	0.03	8.05×10^{-7}	2.06	0.261	1.15	0.002	1.20
16/13.0	rs7192086	T	0.30	0.25	0.24	3.32×10^{-5}	1.33	0.206	1.06	2.56×10^{-5}	1.10
11/132.1	rs3016384	C	0.56	0.51	0.49	5.82×10^{-5}	1.29	0.057	1.08	4.43×10^{-4}	1.07

SZ, schizophrenia; BP, bipolar; CON, control; ATT(P), trend test P value; meta SZ+BP, meta-analysis for all schizophrenia and bipolar samples reported in this study; CMH(P), Cochran-Mantel-Haenszel P value.

Table 1.1.3.2. Combined schizophrenia and bipolar disorder analysis. *Table courtesy from (O'Donovan et al., 2008)*

As demonstrated by some follow-up studies (Riley et al., 2010; Steinberg et al., 2011; Williams et al., 2011), there is a strong association between ZNF804A (rs1344706) and schizophrenia being the A allele the risk allele. This association was also replicated in two studies among Han Chinese population (Xiao et al., 2011; Zhang et al., 2011) but not a third one (Li et al., 2011b). These replication studies corroborated that ZNF804A (rs1344706) is a relatively strong candidate susceptibility gene for schizophrenia; albeit one that confers a small increment in risk. However, the possible molecular mechanism responsible for enhancing risk for psychosis remained unknown for a while.

In this context an influential immunochemistry study was very recently published in PLoS ONE Journal by (Girgenti et al., 2012). Results confirmed that ZNF804A directly contributes to transcriptional control by regulating the expression of four schizophrenia associated genes: PRSS16, COMT, PDE4B, and DRD2. In particular, they demonstrated that expression of ZNF804A leads to a significant increase in transcript levels of PRSS16 and COMT, relative to GFP-transfected controls, and a statistically significant decrease in transcript levels of PDE4B and DRD2. Furthermore, they revealed that both epitope-tagged and endogenous ZNF804A directly interacts with the promoter regions of PRSS16 and COMT, suggesting a direct up-regulation of transcription by ZNF804A on the expression of these genes. In summary, these findings were the first to confirm that ZNF804A may modulate a transcriptional network of schizophrenia associated genes.

In addition to these outstanding findings, ZNF804A (rs1344706) has been correlated with increased ZNF804A transcript levels in adult tissue (Riley et al., 2010; Williams et al., 2011), and the risk allele has a lower affinity for nuclear proteins compared to the common allele (Hill and Bray, 2011). Furthermore, RNAi knockdown of ZNF804A in an immortalized human neuroepithelium cell line revealed abnormal expression of genes involved in cell adhesion (Hill et al., 2012). Despite the fact we do not know the function of the protein yet, in the last few years imaging genetics studies have started to characterize the prefrontal-hippocampal network linking ZNF804A (rs1344706) genotype to schizophrenia.

The first study within this new research field was published in Science Journal by (Esslinger et al., 2009). In this fMRI genetic study of WM in 115 healthy volunteers, researchers validated the intermediate phenotype strategy described by (Meyer-Lindenberg and Weinberger, 2006), indicating that mechanisms underlying genetic discoveries supported by genome-wide association studies (O'Donovan et al., 2008) are highly penetrant in the human brain, consistent with the pathophysiology of the mental disorder, and mirror candidate gene effects.

In this study, researchers map ZNF804A (rs1344706) effects on activation and connectivity across the brain. Local activation within the DLPFC was not significantly related to genotype but connectivity of the most activated DLPFC locale was strongly altered.

Figure 1.1.3.2 illustrates their findings by showing: (1) the risk allele (A allele) reduces interhemispheric DLPFC connectivity (red bars); and (2) the left HF is uncoupled from the right DLPFC in non-risk allele carriers but shows a dose dependent increased connectivity in risk-allele carriers (grey bars).

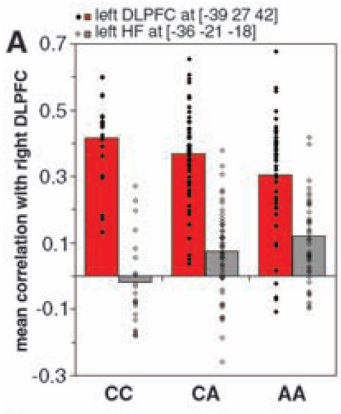

Figure 1.1.3.2. Functional connectivity results of the right DLPFC within the left DLPFC and the left HF for each genotype group: CC, CA, and AA. *Figure courtesy of (Esslinger et al., 2009)*

Their findings revealed that ZNF804A (rs1344706) or a variant in linkage-disequilibrium is functional in the human brain. Nonetheless, molecular changes leading up to abnormal brain systems function remain to be discovered. They speculated that, because genetic variation in dopaminergic and glutamatergic neurotransmission affects DLPFC or HF connectivity, examination of ZNF804A (rs1344706) in those neurotransmitter cascades is assured, as is its role in white matter development and plasticity. Finally, they concluded that abnormal connectivity arises as part of the core neurogenetic architecture of schizophrenia and probably bipolar disorder, identifying novel blanks for effective treatments.

In this dissertation, we follow up this article and previous ones (Meyer-Lindenberg and Weinberger, 2006; Meyer-Lindenberg et al., 2005), by examining the prefrontal-hippocampal network with sDCM and investigating relations between sDCM parameter estimates, ZNF804A (rs1344706), and behavior. The review of the literature continues with an fMRI genetic study.

Another interesting study in connection with this gen was published two years later in Archives of General Psychiatry Journal by (Rasetti et al., 2011). In this fMRI genetic study of WM in 153 healthy volunteers, 171 healthy siblings of schizophrenia patients, and 78 schizophrenia patients, the researchers studied the DLPFC-HF coupling in genetic risk carriers, siblings of patients, and patients.

This work analysed fMRI data using two connectivity analyses: seeded connectivity analysis and psychophysiological interaction (PPI) analysis. Their analyses revealed that altered DLPFC functional connectivity with the HF and, to a lesser degree, the rest of the PFC, is observed in patients and siblings when compared with healthy volunteers. The ZNF804A (rs1344706) genotype significantly modulates DLPFC coupling with the HF and PFC but not DLPFC activity in the healthy group. Similarly, ZNF804A (rs1344706) genotype modulates right DLPFC-HF connectivity in siblings and patients.

Figure 1.1.3.3 illustrates their findings across different groups: controls, siblings, and patients; by showing a statistically significant effect on the right DLPFC-left HF connectivity estimate across each group using both connectivity analyses.

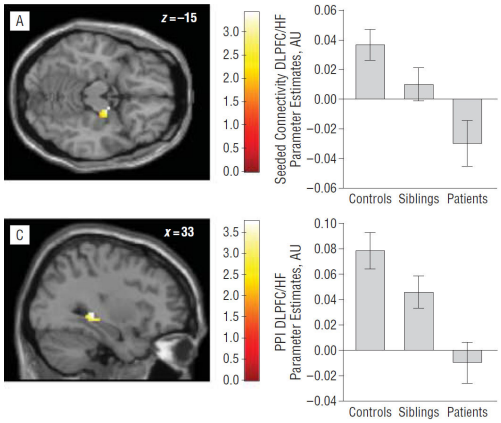

Figure 1.1.3.3. Seeded connectivity and PPI analyses for each group: controls, siblings, and patients. *Figure courtesy of (Rasetti et al., 2011)*

Figure 1.1.3.4 illustrates their findings across different genotype groups: CC, CA, and AA; showing a gene-dose effect on the right DLPFC-left HF connectivity estimate across each genotype group using both connectivity analyses.

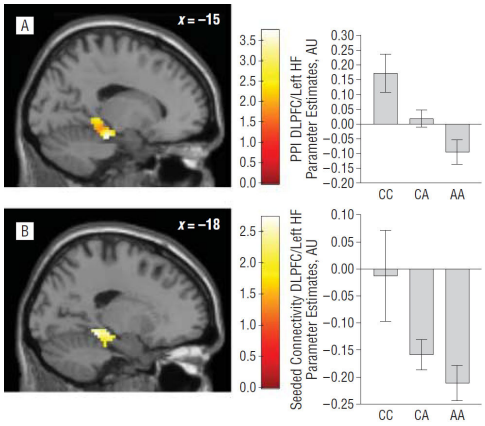

Figure 1.1.3.4. PPI and seeded connectivity analyses for each genotype group: CC, CA, and AA. *Figure courtesy of (Rasetti et al., 2011)*

It is important to highlight that these discoveries go in the opposite direction in comparison to the results obtained by (Esslinger et al., 2009; Meyer-Lindenberg et al., 2005). Nonetheless, the authors

stated over the article that this measurement needs to be interpreted cautiously (Rasetti et al., 2011).

The third study within this field was published in Human Brain Mapping Journal by (Paulus et al., 2013). In this fMRI imaging genetic study of WM in 94 healthy volunteers genotyped for ZNF804A (rs1344706), researchers aimed at replicating findings previously found by (Esslinger et al., 2009; Rasetti et al., 2011).

Analyses did not indicate further support for a decrease in the interhemispheric DLPFC functional connectivity at higher ZNF804A (rs1344706) risk status. Nonetheless, the analysed data show the previously described alteration in functional connectivity between the right DLPFC and the HFs, albeit with weaker effects. Decoupled by default, the functional coupling between the right DLPFC and anterior HFs increased with the number of ZNF804A (rs1344706) risk alleles. Therefore, the current data supported fronto-hippocampal dysconnectivity as intermediate phenotype linking ZNF804A (rs1344706) genotype to psychosis.

Figure 1.1.3.5 illustrates their findings by showing a gene-dose effect on the right DLPFC-left HF coupling consistent with (Esslinger et al., 2009).

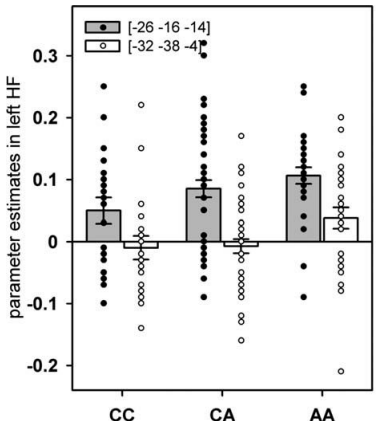

Figure 1.1.3.5. Means and standard errors of connectivity estimates of the right DLPFC within the left HF at two different coordinates for each genotype group: CC, CA, and AA. *Figure courtesy of (Paulus et al., 2013)*

To conclude the article, the authors discussed the difficulties in replicating the bilateral DLPFCs functional connectivity in light of the effect sizes ZNF804A (rs1344706) genotype has on human brain function, concluding that further replication studies in independent samples are needed to investigate the role that ZNF804A (rs1344706) plays in the functional integration of brain systems.

In summary, comparing healthy volunteers with either no, one, or two ZNF804A (rs1344706) risk alleles, (Esslinger et al., 2009; Paulus et al., 2013) found that the number of risk alleles predicted higher prefrontal-hippocampal functional coupling during the N-back WM task, just as had been observed earlier in patients (Meyer-Lindenberg et al., 2005), supporting the fact that higher

functional coupling (especially with a dysfunctional PFC, as in schizophrenia), not only less, can be the risk phenotype. Albeit limited to three studies (Esslinger et al., 2009; Paulus et al., 2013; Rasetti et al., 2011), these discoveries contributed to establish the "dysconnectivity" hypothesis as an intermediate phenotype linking ZNF804A (rs1344706) genotype to schizophrenia. The review of the literature continues with the importance of using optogenetic tools for the understanding of genetic mechanisms responsible of dysfunctional (E-I) balance within the neural microcircuitry.

An outstanding article within this topic is an optogenetic study in mice published in Nature Journal by (Yizhar et al., 2011). The researchers reviewed that serious behavioral impairments in mental disorders such as schizophrenia and autism result from increases in the cellular (E-I) balance within the neural microcircuitry as previously shown by (Kehrer et al., 2008). They proposed that this assumption may provide a unified approach encompassing physiological and genetic research. In this work, the authors implemented a variety of novel optogenetic tools to causally investigate the cellular (E-I) balance hypothesis in freely moving mice, and explored the associated circuit physiology. They discovered that elevation, but not reduction, of cellular (E-I) balance within the mouse medial prefrontal cortex impaired information processing at the cellular level. This was associated with specific behavioral deficits and increased power in the 30-80 Hz frequency band; findings already observed in clinical human populations. Furthermore, consistent with the (E-I) balance hypothesis, they found that compensatory elevation of inhibitory cell excitability partially rescued social impairments caused by (E-I) balance elevation.

With this section we have finished the review of fMRI genetic studies for understanding the genetic mechanisms of dysconnectivity in schizophrenia by means of functional connectivity analyses. Moreover, we have introduced the use of optogenetic tools to causal investigate dysfunctional (E-I) balance in schizophrenia. The next step is to precisely define the original problem that will be addressed in this dissertation.

1.2. Statement of the problem

As discussed above, an obvious limitation in fMRI is that neural function is not measured directly. It is inferred from hemodynamic measurements. A major improvement in fMRI is possible by the establishment of direct connections between hemodynamic measurements and neural function. To do this, it is necessary to establish the neural basis of hemodynamic functional connectivity which has been attempted with the so-called hemodynamic model. In this study, we will analyse our fMRI data with sDCM which includes a hemodynamic forward model (Stephan et al., 2007).

Functional connectivity is defined as a correlation between remote neurophysiological events (Friston, 1994; Friston et al., 1993b). In turn, effective connectivity is defined as the influence that one neuronal population exerts over another (Friston, 1994; Friston et al., 1993a). Functional connectivity among brain regions has been used to delineate the functional anatomy in health and schizophrenia (Meyer-Lindenberg et al., 2005) and the impact of genetic variation (Meyer-Lindenberg and Weinberger, 2006). Nonetheless, due to the fact that in fMRI the neural function is not measured directly, functional connectivity is an indirect measure of neuronal connectivity and therefore, reflects indirectly anatomic connectivity and synaptic efficiency (Buckner, 2010). In other words, this measure does not make any explicit reference to an underlying structural model or to specific directional effects. Furthermore, functional connectivity between two variables, e.g. brain regions, does not necessarily imply that one causes the other (Aldrich, 1995). Therefore, by using functional connectivity, we do not know anything about causality, i.e. which region drives the altered connection. In this study, we will analyse or fMRI data with sDCM which estimates the causality among brain regions.

As discussed in previous section, in simple terms, a brain system can be described by three different sets of parameters: a) intrinsic connections – within and between brain regions –, b) modulatory inputs of the task on the intrinsic connections, and c) driving inputs of the task into the brain regions (Friston et al., 2003). By functional connectivity, we might reveal modulatory effects of genetic risk variants on the connectivity estimates but we cannot reveal the contributions these genes make to the workings of these three set of parameters describing any brain system. In this study, we will describe the prefrontal-hippocampal network in terms of these three set of parameter estimates.

Moreover, a reoccurring difficulty in the field of psychiatric genetics is the non-replication of initially promising findings, partly caused by the small effects of single genes. The replication of imaging genetic results is therefore crucial for the long-term assessment of genetic effects on neural connectivity parameters. In this study, we will examine the effect of a genetic risk variant for schizophrenia on the prefrontal-hippocampal network in a large sample from three different locations.

As we indicated previously, the exact meaning of these set of parameter estimates in terms of functional excitation-inhibition (E-I) balance within and between brain regions is still poorly unknown. Furthermore, we do not know whether these parameters contain information concerning behavior or whether behavior is modulated by genotype or disease. In this study, we will strive on giving a plausible biological interpretation to the parameter estimates in terms of functional (E-I)

balance. Moreover, we will illustrate some causal relations between these set of parameters, genotype, and behavior in the healthy and the diseased brain.

Therefore, there is critical demand of new methods for understanding the contribution these genes make to the functioning of particular brain networks, and how changes in the structure and/or the expression of these genes impact on these distributed brain networks and behavior. In this study, we focus on applying and building mathematical algorithms which identify alterations on genetic risk carriers and schizophrenia patients from neural connectivity dynamics estimated with sDCM for fMRI responses and describe how these alterations have an effect on the behavior.

1.3. Purpose of the study

As discussed above, altered cortical connectivity is a well described endophenotype for schizophrenia. Thus, the main goal of this study is to identify alterations on genetic risk carriers and schizophrenia patients from the prefrontal-hippocampal network estimated with sDCM and describe how these alterations have an effect on the behavior. In other words, sDCM for fMRI responses are explored and brought into the specific prefrontal-hippocampal network to investigate relations between sDCM parameter estimates, genotype, and behavior. Towards this goal, we divided this study into four analyses:

a. In a first stage: Multi-site reproducibility of prefrontal-hippocampal connectivity estimates by sDCM in healthy volunteers; we focused in the prefrontal-hippocampal modelling in healthy volunteers. The method will be validated along three different data-sets, furnishing a robust meta-analysis study. In general terms, the aim of this analysis was to test whether the method is stable and reliable independent of the particular research setting, i.e., scanner, participants, experimenter.

b. In analysis second stage: Investigation of relations between sDCM parameter estimates, ZNF804A (rs1344706), and behavior in healthy volunteers; the links between prefrontal-hippocampal effective connectivity estimates, a genome-wide risk genetic variant for schizophrenia, and behavior in healthy volunteers were analyzed. We also studied the alterations on genetic risk carriers within the prefrontal-hippocampal network estimated with sDCM. To conclude, we evaluated whether these sDCM parameter estimates contain sufficiently rich information to predict the behavior.

c. During the third stage: Investigation of relations between sDCM parameter estimates and behavior in pair-wise matched healthy volunteers and schizophrenia patients; we analyzed the links between prefrontal-hippocampal effective connectivity estimates and behavior in pair-wise matched healthy control subjects and schizophrenia patients. The aim of

this third stage was to identify potential differences between controls and patients within the prefrontal-hippocampal network estimated with sDCM and test whether these sDCM parameter estimates contain sufficiently rich information to predict the behavior.

d. In the fourth and final project stage: Comparison of two-group genetic models and healthy vs. schizophrenia model; each of the two-group genetic models (recessive, co-dominant, and dominant) was compared to the new healthy vs. schizophrenia model. Our goal was to reveal which of the two-group genetic models contributes to the phenotype expressed in schizophrenia patients.

With these four analyses, we hope to illustrate how sDCM for fMRI responses can be used to identify alterations on risk genetic carriers and schizophrenic subjects within distributed brain systems in relation to the underlying neurobiology and behavior.

1.4. Theoretical framework

The theoretical framework used in this study is stochastic DCM for fMRI responses. Importantly, stochastic DCMs allow for uncertainty about both the states and parameters of the model. Critically, previous DCM studies of neuroimaging time series have been limited largely to deterministic DCMs, where uncertainty about the states is ignored (Friston et al., 2003).

These previous approaches, based on ordinary differential equations, assumed that there are no random variations in the hidden neuronal and physiological states that mediate the effects of known experimental inputs on observed fMRI responses. This may be a limitation in some instances, because several studies suggest that physiological noise due to stochastic fluctuations in neuronal and vascular responses may need to be taken into account (Biswal et al., 1995; Kruger and Glover, 2001; Riera et al., 2004). As a consequence, there has been growing interest in estimating both the parameters and hidden states of DCMs based upon stochastic differential equations with state noise. Examples of different inversion schemes have been in the DCM literature for a while (Daunizeau et al., 2009; Friston et al., 2008), including a “generalised filtering” scheme (Friston et al., 2010).

Moreover, we used Bayes model selection (BMS) to compare sDCMs in order to select the winning model, statistical tests to examine potential differences in the sDCM parameter estimates, and linear regression to investigate relations between sDCM parameter estimates and behavior.

1.5. Research hypotheses

As stated above, we divided this study into four analyses. Next we will give an overview of the research hypotheses for each analysis.

1.5.1. Multi-site reproducibility of prefrontal-hippocampal connectivity estimates by sDCM in healthy volunteers

A robust method might consistently reveal the same causal prefrontal-hippocampal network in healthy volunteers across the sites of the multi-center study. Furthermore, statistical tests on sDCM parameter estimates should not reveal statistically significant differences across the sites.

1.5.2. Investigation of relations between sDCM parameter estimates, ZNF804A (rs1344706), and behavior in healthy volunteers

Detecting the modulatory effect of ZNF804A (rs1344706) on the prefrontal-hippocampal network in healthy volunteers, will help to reveal the functionality of this genetic polymorphism on the workings of this particular brain system. All genetic models will be explored in order to reveal some phenotypic variants. Furthermore, sDCM parameter estimates containing sufficiently rich discrimination information might permit to predict the mean performance and reaction time and provide us some insights about the impact of this genetic polymorphism on the neurobiology of the causal prefrontal-hippocampal network and behavior.

1.5.3. Investigation of relations between sDCM parameter estimates and behavior in pair-wise matched healthy volunteers and schizophrenia patients

Estimating the causal prefrontal-hippocampal network in pair-wise matched healthy volunteers and schizophrenia patients will provide some insights about the underlying neuronal connectivity within this particular brain system in the healthy and the diseased brain. In case of having a different causal model, we will reveal a difference in the causal structure between these two regions in controls and patients; in case of having the same, we will reveal that these brain areas interact identically independently of the disorder and the pathophysiology of schizophrenia manifests on sDCM parameter estimates. Testing for potential differences on sDCM parameter estimates between healthy volunteers and schizophrenia patients might reveal some abnormalities within this particular brain system. To conclude, investigating relations between sDCM parameter estimates and behavior might permit to show the impact of the disease on the neurobiology of the prefrontal-hippocampal network and behavior.

1.5.4. Comparison of two-group genetic models and healthy vs. schizophrenia model

Comparing each of the two-group genetic models to the healthy vs. schizophrenia model, might reveal which of the phenotypes observed by each of the two-group genetic models reproduce the schizophrenia phenotype. The similarities and dissimilarities between these models might help us to hypothesize the functionality of this particular brain system.

1.6. Importance and scope of the study

This dissertation investigates the applicability of computational models like sDCM to identify causal biological mechanisms associated with psychiatric disorders like schizophrenia. The importance of the study lies on estimating reliable connectivity estimates with neurobiological interpretability and investigating relations between connectivity estimates, a risk genetic variant for schizophrenia, and behavior in healthy volunteers and schizophrenia patients.

The scope of the study is to establish the functional significance of a specific genetic polymorphism for disease mechanisms and thus help identifying potential blanks for the development of effective treatments. Rather than illustrating new evidence for intermediate phenotypes of a specific genetic risk variant, with this work we demonstrate that for meaningful studies in imaging genetics detailed information about the analysis process should be presented and the reliability of the results and their interpretation should be taken into consideration.

Chapter 2: Research methods

"Let me tell you the secret that has led me to my goal. My strength lies solely in my tenacity."
Louis Pasteur

This chapter presents a detailed description of the methods designed to analyze the fMRI data-sets and address the research questions of this study. It begins with an overview of the research methods, and then goes into the details of the research design, participants, instrumentation, data analysis, and assumptions and limitations of study.

2.1 Introduction to research methods

Next section will give an overview of Dynamical Causal Modelling (DCM), stochastic DCM (sDCM), Bayes model selection (BMS), statistical tests, and linear regression with further details in later sections of this chapter.

2.1.1. Summary of Dynamical Causal Modelling (DCM)

DCM models the brain as a dynamic system of interconnected regions; while, an experiment is defined as a designed perturbation of the system's dynamics (Friston et al., 2003; Stephan et al., 2010). Any given DCM represents a particular mechanistic model for explaining experimentally obtained measures of brain activity. Even though the mathematical formulation of DCMs differs significantly across different techniques, common neural mechanisms modeled by all DCMs include synaptic connection strengths and their experimental modulation. In contrast to purely statistical models of effective connectivity which characterize inter-regional connectivity in a phenomenological fashion, DCMs strive for neurobiological interpretability of their parameters and this is a core feature which distinguishes them from alternative approaches.

DCMs for fMRI responses are hierarchical models, consisting of two layers. The first layer is a neuronal model that describes the dynamics of interacting neuronal populations in the context of experimental inputs. The second layer is a hemodynamic forward model that characterizes how a given neuronal state translates into observed fMRI responses and serves to account for variations in neurovascular coupling across brain regions and individual subjects. Experimental inputs $u(t)$ enter the model in two different ways: they can elicit responses through direct influences on specific regions (driving inputs), or they can modulate the strength of coupling among regions (modulatory inputs).

Assuming, for simplicity, a single input $u(t)$, the state and measurement equations of a conventional deterministic DCM for fMRI are:

Neuronal state model: $$\frac{dx(t)}{dt} = f(x(t), \theta_n, u(t)) = (A + Bu(t))x(t) + Cu(t) \quad (1)$$

Hemodynamic forward model: $$y(t) = g(\theta_h) * x(t) + \varepsilon(t) \quad (2)$$

where $x(t)$ represents the neuronal state, $\theta_n = (A, B, C)$ are the neuronal parameters, A is a matrix of endogenous connection strengths, B is a matrix of modulatory input strengths, C denotes the strength of direct (driving) inputs, $g(\theta_h)$ is a nonlinear convolution operator that links the neuronal state $x(t)$ to a predicted BOLD signal $y(t)$ via changes in vasodilatation, blood flow, blood volume, and deoxyhemoglobin content (Stephan et al., 2007), θ_h are the hemodynamic parameters, and $\varepsilon(t)$ denotes Gaussian measurement error.

Critically, the neuronal parameters θ_n have some degree of neurobiological interpretability, representing, for instance, synaptic weights and their context-specific modulation. The hemodynamic parameters θ_h are not of scientific research interest because they exhibit strong interdependencies and thus high posterior covariances and low precision, which make it difficult to determine the distinct contribution provided by each parameter.

To summarize, DCM for fMRI responses provides a generative model for explaining measured BOLD time series as the outcome of hidden dynamics in an interconnected network of neuronal populations and its experimentally induced perturbations. Inverting such a model refers to estimate the posterior distribution of the parameters of both the neuronal and the hemodynamic model from observed fMRI responses of an individual subject. See (Brodersen et al., 2011) for a comprehensive overview.

2.1.2. Stochastic Dynamical Causal Modelling (sDCM)

Stochastic DCMs differ from conventional deterministic DCMs by allowing for endogenous or random fluctuations in unobserved (hidden) neuronal and physiological states, i.e., system or state-noise. Practically, this means the states are free to fluctuate, in addition to the parameter estimates, to model spontaneous and experimentally induced responses. The mathematical form we use here corresponds to that introduced in (Li et al., 2011a) which extend of Eq. 1 and 2 by including fluctuation terms for both states and causes:

Neuronal state model: $$\frac{dx(t)}{dt} = f(x(t), \theta_n, v(t)) + \omega^{(x)} = (A + Bv(t))x(t) + Cv(t) + \omega^{(x)} \quad (3)$$

Hidden causes model: $$v(t) = u(t) + \omega^{(v)} \quad (4)$$

Hemodynamic forward model: $$y(t) = g(\theta_h) * x(t) + \varepsilon(t) \quad (5)$$

The variables have the same meaning as in Eq. 1 and 2 above. Additionally, $\omega^{(x)}$ are random neural fluctuations, and $\omega^{(v)}$ are the hidden cause's fluctuations. Importantly, both types of stochastic innovations are assumed to be non-Markovian but show a degree of temporal smoothness; this is a typical feature of biological systems (Friston et al., 2011). In other words, the random state fluctuations $\omega^{(x)}$ are characterized by two hyperparameters π, σ which describe their precision (inverse variance) and smoothness, given a particular temporal autocorrelation function V (Li et al., 2011a):

$$\omega^{(x)} = N\left(0, V(\sigma) \otimes \sum\left(e^{-\pi}\right)\right) \quad (6)$$

The same sort of parameterization applies to the random fluctuations of the causes $\omega^{(v)}$. States, parameters and hyperparameters from Eq. 3, 4, and 5 are inferred using generalised filtering, a triple-estimation scheme that employs variational Bayesian techniques (Friston et al., 2010). Notably, the presence of stochastic innovations makes sDCMs applicable to both task-driven and "resting-state" fMRI data. In this study, we used sDCM based on generalised filtering, to investigate the prefrontal-hippocampal network in healthy volunteers and schizophrenia patients.

2.1.3. Bayes Model Selection (BMS)

In this study, we used BMS to compare sDCMs that are applied to empirical fMRI data (Penny et al., 2004a; Stephan et al., 2009b). Deciding between several competing models cannot only consider the relative fit to the data but also needs to take into account differences in model complexity; i.e., the number of free parameters and the functional form of the generative model which, for example, determines parameter interdependencies (Pitt and Myung, 2002). Penalizing for model complexity is important: as complexity increases, so does model fit (monotonically). At some point, however, the model will start fitting noise that is specific to a particular measurement (i.e., "over-fitting"). In other words, overly complex models are less generalisable across multiple realizations of the same underlying generative process. Therefore, assuming that all models are equally likely *a priori*, searching for an optimal model (given a set of alternatives) corresponds to searching the model that represents the best balance between fit and complexity. This is the model that maximizes the model evidence or marginal likelihood which integrates out uncertainty about hidden parameters and states:

$$p(y \mid m) = \int p(y \mid \theta, m) p(\theta, m) d\theta \quad (7)$$

In this study, we use an estimate of the negative free-energy as an approximation to the log model evidence (Friston et al., 2007) and employ a random effects BMS scheme at the group level that accounts for potential heterogeneity across subjects (Penny et al., 2010; Stephan et al., 2009b).

2.1.4. Statistical tests

Statistical tests provide a mechanism for making quantitative decisions about an effect. The goal is to determine whether there is enough evidence to reject a conjecture about the effect. This conjecture is called the null hypothesis. Not rejecting may be a good result if we want to continue to act as if we believe the null hypothesis is true. Or it may be an unsatisfactory result, maybe indicating we may not yet have enough data to demonstrate something by rejecting the null hypothesis. In this study, we used statistical tests to investigate potential differences in the sDCM parameter estimates of the winning model across different groups.

2.1.5. Linear regression

In statistics, linear regression is an approach for modelling the relationship between a scalar dependent variable y, i.e., performance and reaction time; and one or more explanatory variables denoted by X, i.e., sDCM parameter estimates of the winning model. Linear regression analysis can be very helpful for making forecasts and predictions. In this study, we used linear regression analysis to investigate relations between sDCM parameter estimates of the winning model and behavior across different groups.

2.2. Research design

This study utilized several quantitative methods: sDCM, BMS, statistical tests, and linear regression, and a qualitative method comparison. A brief overview of the methods used to address each of the four research objectives is presented; please find more details in later sections of this chapter.

To address Objective One: Multi-site reproducibility of prefrontal-hippocampal connectivity estimates by sDCM in healthy volunteers, we investigate the applicability and robustness of stochastic Dynamic Causal Modelling (Daunizeau et al., 2012; Friston et al., 2011; Li et al., 2011a) to investigate DLPFC-HF effective connectivity during WM in healthy volunteers. 180 healthy subjects were measured by fMRI during a standard working memory N-Back task at three different sites

(Mannheim, Bonn, Berlin; each with 60 participants). The reproducibility of regional activations in key regions for working memory (DLPFC; HF) was evaluated using conjunction analyses across locations. The effective connectivity between DLPFC and HF was analysed using a simple two region sDCM. For each subject, we evaluated twenty-two alternative sDCMs and compared their relative plausibility using Bayes model selection (BMS). We examined potential differences in the parameter estimates of the winning model by performing statistical tests.

To address Objective Two: Investigation of relations between sDCM parameter estimates, ZNF804A (rs1344706), and behavior in healthy volunteers, we investigate relations between prefrontal-hippocampal effective connectivity estimates, a risk genetic variant for schizophrenia: ZNF804A (rs1344706), and behavior in healthy volunteers. We further investigate the modulatory effect of this genetic polymorphism on the prefrontal-hippocampal network (Esslinger et al., 2009; Paulus et al., 2013; Rasetti et al., 2011). Furthermore, we ask whether specific directed connections strengths within the prefrontal-hippocampal network, contain sufficiently rich information to enable to predict behavior. All genetic models (additive, recessive, co-dominant, and dominant) were explored in order to estimate underlying phenotypic variants:

a. Additive model: “AA vs. AC vs. CC” model. Homozygous risk allele carriers versus heterozygous risk allele carriers versus non-risk allele carriers.

b. Recessive model: “AA vs. AC+CC” model. Homozygous risk allele carriers versus heterozygous plus non-risk allele carriers.

c. Co-dominant model: “AC vs. AA+CC” model. Heterozygous risk allele carriers versus homozygous risk carriers plus non-risk allele carriers.

d. Dominant model: “CC vs. AA+AC” model. Non-risk allele carriers versus homozygous plus heterozygous risk allele carriers.

AA stands for homozygote Adenine, AC stands for heterozygote, and CC stands for homozygote Cytosine, with the A allele being the risk allele. We designed a battery of statistical tests for detecting statistically significant differences on sDCM parameter estimates and behavior for each genetic model. We also performed linear regression of behavior on sDCM parameter estimates to see whether we can predict subject’s behavior from sDCM parameter estimates for each genetic model.

To address Objective Three: Investigation of relations between sDCM parameter estimates and behavior in schizophrenia patients and pair-wise matched healthy control subjects, we applied the same methodology described above to 33 schizophrenia patients and 33 pair-wise matched healthy control subjects. For each individual, we evaluated the same twenty-two alternative sDCMs and compared their relative plausibility using BMS. Then, we investigate statistically significant

differences on sDCM parameter estimates and behavior between healthy control subjects and schizophrenia patients (Meyer-Lindenberg et al., 2005). Furthermore, we investigated relations between the new set of sDCM parameter estimates and behavior in healthy control subjects and schizophrenia patients. Basis on these results, we defined a healthy vs. schizophrenia model.

To address Objective Four: Comparison of two-group genetic models and healthy vs. schizophrenia model, we qualitatively compare each of the two-group genetic models: additive, recessive, co-dominant and dominant to the healthy vs. schizophrenia model.

2.3. Participants

We applied the methodology described in this Chapter to two fMRI data sets.

2.3.1. First fMRI data set

In a first fMRI sample, a total of 180 healthy German participants from three different locations: Mannheim (60), Bonn (60), and Berlin (60), were analyzed. All participants gave written informed consent, and the study had ethics committee approval by the Universities of Heidelberg, Bonn, and Berlin.

Table 2.3.1.1 shows the demographics and behavioral data of participants across the three sites. We tested for potential systematic differences between subjects examined at the three different locations using a one-way ANOVA or a Kruskal-Wallis test depending on the distribution of the variables previously assessed by a Lilliefors Test. Regarding age, gender, and education (years of study), no significant differences were found. Concerning the behavior, no significant differences in performance and reaction time were found either.

	Mannheim	Bonn	Berlin	p-value
Age [years]	33.95 ± 9.64 range 19-49	31.47 ± 9.60 range 18-50	34.88 ± 8.72 range 18-50	No significant; p= 0.1384**
Sex [Male/Female]	27/33	29/31	29/31	No significant; p = 0.9151**
School education [years]	15.40 ± 2.43	15.48 ± 2.93	15.57 ± 2.57	No significant; p = 0.8978**
Performance on the 2-Back [%]	81.42 ± 17.22	77.67 ± 21.28	74.58 ± 19.45	No significant; p = 0.1351**
Reaction time on the 2-Back [ms]	472.02 ± 262.93	461.66 ± 297.70	577.08 ± 350.21	No significant; p = 0.1309**

Table 2.3.1.1. Demographics and behavior of healthy volunteers grouped according to the site
*One-way ANOVA; **Kruskal-Wallis test

Table 2.3.1.2 focuses participants grouped according to the "AA vs. AC vs. CC" model. Similarly as in previous table, no significant differences were found across variables regarding demographics and behavior.

	AA (67)	AC (79)	CC (34)	p-value
Age [years]	33.76 ± 9.16 range 18-50	32.44 ± 9.38 range 18-50	33.32 ± 10.01 range 18-50	No significant; p = 0.6206**
Sex [Male/Female]	30/37	38/41	17/17	No significant; p = 0.8655**
School education [years]	15.36 ± 2.77	15.51 ± 2.44	15.69 ± 2.86	No significant; p = 0.8554**
Performance on the 2-Back [%]	78.30 ± 17.26	77.50 ± 21.10	78.00 ± 20.25	No significant; p = 0.8904**
Reaction time on the 2-Back [ms]	517.96 ± 309.19	526.39 ± 328.71	429.47 ± 237.90	No significant; p = 0.4374**

Table 2.3.1.2. Demographics and behavior of healthy volunteers grouped according to the "AA vs. AC vs. CC" model
*One-way ANOVA; **Kruskal-Wallis test

Analyses of participants grouped according to the "AA vs. AC+CC" model are shown in Table 2.3.1.3. Two-sample t-test or Wilcoxon rank sum test were used depending on the verification of normality assumptions as in previous analyses. Regarding age, gender, education, performance, and reaction time no significant differences were found either.

	AA (67)	AC+CC (113)	p-value
Age [years]	33.76 ± 9.16 Range 18-50	32.71 ± 9.54 Range 18-50	No significant; p = 0.3954**
Gender [male/female]	30/37	55/58	No significant; p = 0.6149**
School Education [years]	15.36 ± 2.77	15.56 ± 2.56	No significant; p = 0.8515**
Performance on the 2-Back [%]	78.30 ± 17.26	77.65 ± 20.76	No significant; p = 0.6352**
Reaction time on the 2-Back [ms]	517.96 ± 309.19	497.23 ± 306.46	No significant; p = 0.5760**

Table 2.3.1.3. Demographics and behavior of healthy volunteers grouped according to the "AA vs. AC+CC" model
*Two sample t-test; **Wilcoxon rank sum test

Table 2.3.1.4 focuses participants grouped according to the "AC vs. AA+CC" model. Similarly as in previous table, no significant differences were found across variables regarding demographics and behavior.

	AC (79)	AA+CC (101)	p-value
Age [years]	32.44 ± 9.38 range 18-50	33.61 ± 9.41 Range 18-50	No significant; p = 0.3529**
Gender [male/female]	38/41	47/54	No significant; p = 0.8363**
School Education [years]	15.51 ± 2.44	15.47 ± 2.79	No significant; p = 0.7989**
Performance on the 2-Back [%]	77.50 ± 21.10	78.20 ± 18.22	No significant; p = 0.7894**
Reaction time on the 2-Back [ms]	526.39 ± 328.71	488.17 ± 289.03	No significant; p = 0.6426**

Table 2.3.1.4. Demographics and behavior of healthy volunteers grouped according to the "AC vs. AA+CC" model
*Two sample t-test; **Wilcoxon rank sum test

To conclude, Table 2.3.1.5 shows demographics and behavior of participants grouped according to the "CC vs. AA+AC" model. No significant differences were found regarding age, gender, education, performance, and reaction time as in previous analyses.

	CC (34)	AA+AC (146)	p-value
Age [years]	33.32 ± 10.01 range 18-50	33.05 ± 9.27 Range 18-50	No significant; p = 0.8996**
Gender [male/female]	17/17	68/78	No significant; p = 0.7210**
School Education [years]	15.69 ± 2.86	15.44 ± 2.59	No significant; p = 0.5778**
Performance on the 2-Back [%]	78.00 ± 20.25	77.87 ± 19.37	No significant; p = 0.8062**
Reaction time on the 2-Back [ms]	429.47 ± 237.90	522.52 ± 318.84	No significant; p = 0.2002**

Table 2.3.1.5. Demographics and behavior of healthy volunteers grouped according to the "CC vs. AA+AC" model
*Two sample t-test; **Wilcoxon rank sum test

2.3.2. Second fMRI data set

In a second fMRI sample, a total of 33 schizophrenia patients from Mannheim were analyzed. All patients gave written informed consent, and the study had ethics committee approval by the University of Heidelberg.

We performed pair-wise matching between the 33 schizophrenia patients and the first fMRI sample (see above) to control for factors which may be confounded with the neuropathology.

Table 2.3.2.1 shows the demographics and behavioral data of pair-wise matched healthy control (HC) subjects and schizophrenia (SZ) patients. 33 healthy participants were pair-wise matched by location (p = 1.000), gender (p = 1.000), age (p = 0.6988), and school education (p = 0.3451).

Concerning the behavioral data, significant differences in performance were found. No significant differences in reaction time were found.

	HC (33)	SZ (33)	p-value
Age [years]	34.24 ± 8.42 Range 19-48	33.42 ± 8.67 Range 18-50	No significant; p = 0.6988*
Gender [male/female]	23/10	23/10	No significant; p = 1.000**
School Education [years]	15.64 ± 2.45	14.92 ± 3.03	No significant; p = 0.3451**
Performance on the 2-Back [%]	83.04 ± 18.70	57.45 ± 20.32	**Significant; p = 4.3565e-6****
Reaction time on the 2-Back [ms]	519.67 ± 247.86	609.51 ± 249.53	No significant; p = 0.1472*

Table 2.3.2.1. Demographics and behavior of pair-wise matched healthy volunteers and schizophrenia patients
*Two sample t-test; **Wilcoxon rank sum test

2.4. Instrumentation

2.4.1. fMRI data acquisition and preprocessing

At all three sites, fMRI data sets were acquired at 3 Tesla using a Trio TIM (Siemens, Erlangen) whole-body MRI system. 128 contiguous multi-slice images were obtained with a gradient echo-planar sequence (orientation = AC-PC line, number of slices = 28; slice thickness = 4 mm; slice gap = 1 mm; FOV = 192 mm; TE = 30 ms; TR = 2.00 s; flip angle = 90°; matrix size = 64×64×28; voxel size = 3.0×3.0×5.0 mm^3).

The fMRI data sets were analyzed using procedures implemented in Statistical Parametric Mapping (SPM8, Welcome Trust Centre for Neuroimaging, London, UK; http://www.fil.ion.ucl.ac.uk/spm). All functional images and the structural image of each subject were preprocessed prior to the statistical analyses. We conducted rigid body motion correction of the functional time-series and "unified segmentation" (Ashburner and Friston, 2005) of the structural image. After co-registration of the realigned functional images to the subject specific structural image, the images were normalized to MNI space using the warping parameters obtained from the unified segmentation procedure applied to the structural image. Finally the functional images were smoothed by applying a 6 mm full-width at half maximum Gaussian kernel.

2.4.2. WM paradigm: N-Back task

We utilized the N-Back task (Owen et al., 2005), which requires the temporal tagging and updating of information on each trial, and therefore has a steep difficulty slope with increasing

demand (i.e., from 0-Back to 2-Back). Our N-Back paradigm used a block design with two conditions: 0-Back condition and 2-Back condition. In the 0-Back condition (a baseline condition requiring no WM), subjects were asked to press the button of the number that they were seeing. In the 2-Back condition, subjects were asked to press the button of the number that they saw two trials before. The study comprised a sequence of 0-Back blocks alternating with 2-Back blocks. Subjects performed four 0-Back blocks and four 2-Back blocks with 15 trials per block.

2.5. Data analysis

2.5.1. fMRI analyses using the General Linear Model (GLM)

Following preprocessing, we specified a voxel-wise general linear model (GLM) with two conditions of interest for each participant (0-Back and 2-Back). Each regressor was convolved with a canonical hemodynamic function and its temporal and dispersion derivatives. Contrasts of interest were defined as [2-Back - 0-Back] for identifying WM activations in the right DLPFC and [0-Back - 2-Back] contrast for identifying deactivations of the left HF.

At the group level, the first-level contrast images were entered into a full factorial design. To identify regions that were consistently (de)activated in participants from all three sites, we used a conjunction analysis (i.e., a "logical AND" analysis based on the conjunction null hypothesis; (Nichols et al., 2005)). Given our a priori hypothesis, based on the rich literature of N-back fMRI studies (see above), of activation in the right DLPFC and deactivation of left HF during 2-Back vs. 0-Back, we restricted this analysis to our regions of interest which were anatomically defined using the PickAtlas software (WFU PickAtlas, ANSIR Laboratory, Winston-Salem, NC, USA; http://fmri.wfubmc.edu/software/PickAtlas). Significant results were corrected for multiple comparisons using family wise error correction based on Gaussian random field theory.

The significant conjunction results within these anatomical masks were used to specify functionally defined region-of-interest masks for subsequent time series extraction in each subject. Specifically, time series were extracted for each subject by computing the first eigenvariate across all voxels within 6 mm radius from his/her maximum within the functionally defined ROIs from the group level.

2.5.2. sDCM analysis

The time series extracted from individual maxima within the ROIs defined at the group level were used to fit a set of twenty-two alternative sDCMs per subject. In relation to the experimental input

(cognitive set associated with working memory) we considered two classes of model. In the first set (models 1-7), experimental inputs exerted a driving effect on one or both regions. In the second set (models 8-22) the experimental input changed extrinsic or intrinsic connectivity - such that observed memory related responses were modelled by an interaction between hidden neuronal activity and the connection strengths that shape this activity. The structure of these twenty-two sDCMs is shown by Figure 2.5.2.1.

In models 1-7, we systematically examine all combinations of directed connections between DLPFC and HF (from DLPFC to HF, from HF to DLPFC, or both) and where driving inputs enter (in DLPFC, HF, or both). Driving inputs encode the influence of task on the DLPFC-HF network (set to 1 during 2-Back and 0 during 0-Back). Together with the stochastic innovations whose precision and temporal smoothness are estimated separately for each area (see above), the driving inputs represent and absorb influences from unknown (hidden) regions (Daunizeau et al., 2012; Friston et al., 2011; Li et al., 2011a) that change their inputs to the DLPFC-HF network depending on WM load. In other words, in these models, we are not modelling WM load dependent changes in DLPFC-HF connectivity by (bilinear) modulation of activity induced by any condition (i.e., a driving input representing any trial), as is often the case in DCM, but via changes in input to the network. The reason for this choice is that in our experimental design 0-Back and 2-Back blocks are continuously following each other, which means that a driving input representing all task conditions would simply correspond to a constant.

In models 8-22, we consider another type of mechanism. These additional models do not consider the 2-Back WM condition as driving input to HF or DLPFC, instead these regions are purely driven by the stochastic innovations and the 2-Back WM condition modulates all possible combinations of inter-regional and self-connections. In other words, DLPFC and HF are not directly affected by changes in working memory load (in terms of load-dependent driving inputs as in models 1-7 above), but we are modelling WM dependent changes in DLPFC and HF activity through (bilinear) modulation of their connectivity by the 2-Back condition.

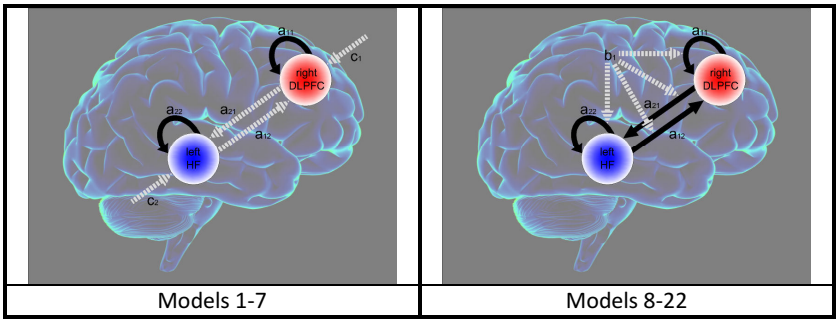

Figure 2.5.2.1. Space-state model

For the analyses presented in this study, we used stochastic DCM for fMRI as implemented in DCM10 in the software package SPM12 (alpha version), code release 4579.

2.5.3. Statistical tests and linear regression analysis

Concerning the first analysis, we examined potential differences in the sDCM parameter estimates of the winning model across the three sites by performing a one-way ANOVA or a Kruskal-Wallis test depending on the distribution of the sDCM parameter estimates previously assessed by a Lilliefors test.

Regarding the second analysis, we examined potential differences in the sDCM parameter estimates and behavior depending on the genetic model. For the additive model, we performed a one-way ANOVA or a Kruskal-Wallis test depending on the distribution of the sDCM parameter estimates and behavior previously assessed by a Lilliefors test. For the two-group genetic models: recessive, co-dominant, and dominant, we performed a two-sample t-test or a Wilcoxon rank sum test depending on the distribution of the sDCM parameter estimates and behavior previously assessed by a Lilliefors test. We performed linear regression of behavior on sDCM parameter estimates across different genetic models to see whether we can predict subject's behavior from sDCM parameter estimates for each genetic model.

Concerning the third stage, we examined potential differences in the sDCM parameter estimates and behavior by performing a two-sample t-test or a Wilcoxon rank sum test depending on the distribution of the sDCM parameter estimates and behavior previously assessed by a Lilliefors test. We performed linear regression of behavior on sDCM parameter estimates for healthy control subjects and schizophrenia patients to see whether we can predict subject's behavior from sDCM parameter estimates for healthy control subjects and schizophrenia patients.

2.6. Assumptions and limitations of the study

The connection between the DLPFC and the HF during WM has been found to be increased in carriers of schizophrenia risk genes (Esslinger et al., 2009; Paulus et al., 2013; Rasetti et al., 2011) and schizophrenia patients (Meyer-Lindenberg et al., 2005). In this study, we characterized the influence that a neuronal population exerts over the other driven by the 2-Back condition, the cognitively demanding condition of the N-Back task, with sDCM.

The main assumption of the study is that during the 2-Back condition, we can observe statistically significant differences on the dynamics of this particular brain system across healthy volunteers with

different genotype and between healthy controls subjects and schizophrenia patients. Moreover, we assumed that prefrontal-hippocampal connectivity estimates contain sufficiently rich discrimination information to enable to predict behavior. In other words, we assumed that we can predict subject's behavior from sDCM parameter estimates in healthy subjects and schizophrenia patients.

The main limitation of the study is that in our experimental design 0-Back and 2-Back blocks are continuously following each other. Therefore, we can only model the dynamics of one condition: the 2-Back task; because a driving input representing all task conditions would simply correspond to a constant.

Chapter 3: Research findings

> "There are 2 possible outcomes: If the result confirms the hypothesis, then you've made a measurement. If the result is contrary to the hypothesis, then you've made a discovery."
> Enrico Fermi

The purpose of this study is to identify alterations on genetic risk carriers and schizophrenia patients from the prefrontal-hippocampal network estimated with sDCM and describe how these alterations have an effect on behavior. Towards this goal, we divided this study into four analysis or research questions. This chapter is divided into four sections each of which describes the findings of each research question.

3.1. Multi-site reproducibility of prefrontal-hippocampal connectivity estimates by sDCM in healthy volunteers

We divided this section into four subsections: SPM for each site, BMS for each site, sDCM parameter estimates for each site, and statistical tests on sDCM parameter estimates across the three sites.

3.1.1. SPM for each site

The conjunction maps depicted in Figures 3.1.1.1 and 3.1.1.2 show the common (de)activation pattern across three locations in our anatomically constrained regions of interest. These conjunction analyses showed a consistent activation in the right DLPFC (x, y, z = 45, 41, 20; T = 8.94; p = 0.05, FWE-corrected) and consistent deactivation in the left HF (x, y, z = -27, -31, -10; T = 8.99; p = 0.05, FWE-corrected) across all three sites.

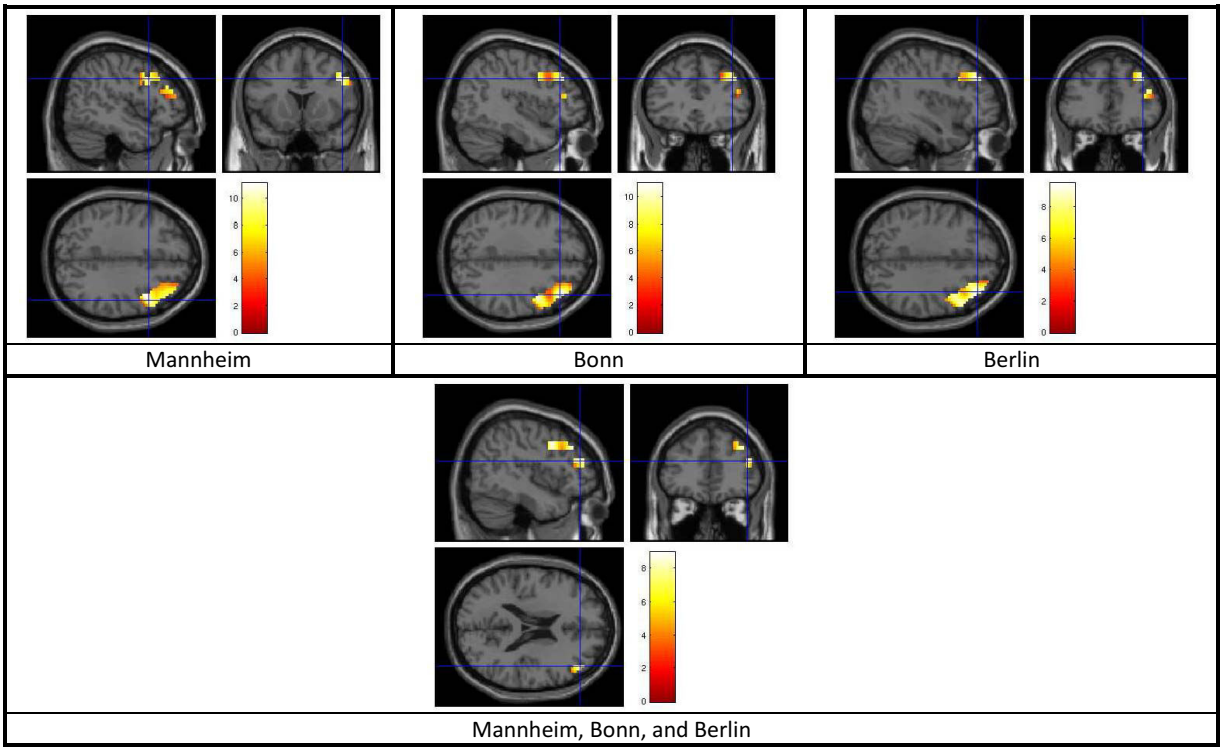

Figure 3.1.1.1. Activation maps for each site and conjunction map in the right DLPFC

As described in Chapter 2, these conjunction results were subsequently used as group-level functional ROIs to guide the subsequent time series extraction in the right DLPFC and left HF of each individual subject.

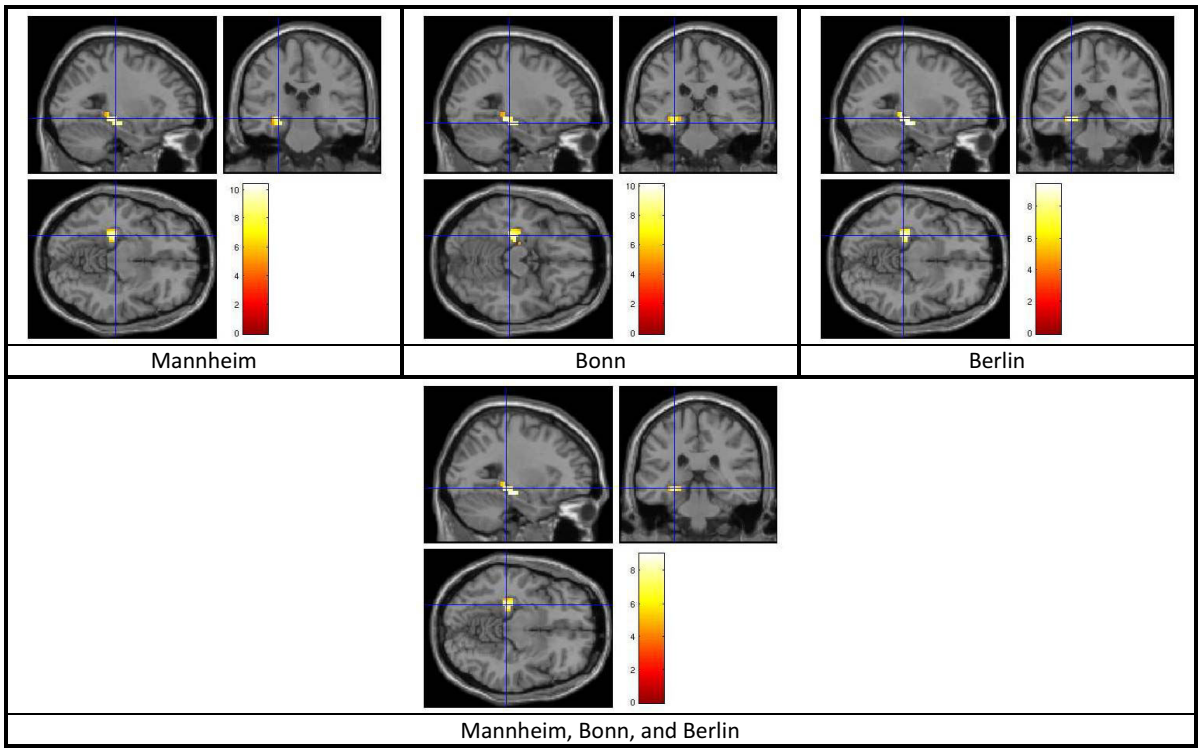

Figure 3.1.1.2. Deactivation maps for each site and conjunction map in the left HF

3.1.2. BMS for each site

We used random effects BMS to determine, from our model space of twenty-two alternative sDCMs (Figure 2.5.2.1), the model that provided the best balance between accuracy and complexity for explaining the measured data. The results were fully consistent across the three sites, revealing the same winning model (model 2; Figure 2.5.2.1) in Mannheim, Bonn, and Berlin. This model includes a driving influence of the 2-Back condition on both DLPFC and HF, and a unidirectional influence from DLPFC to HF.

Figure 3.1.2.1 shows the results of BMS Random Effects (RFX) for each location. The exceedance probability of model 2 (i.e., the probability that this model is a more likely model than any other model considered) was 0.97 (for the Mannheim cohort), 1.00 (for the Bonn cohort), and 0.93 (for the Berlin cohort), respectively.

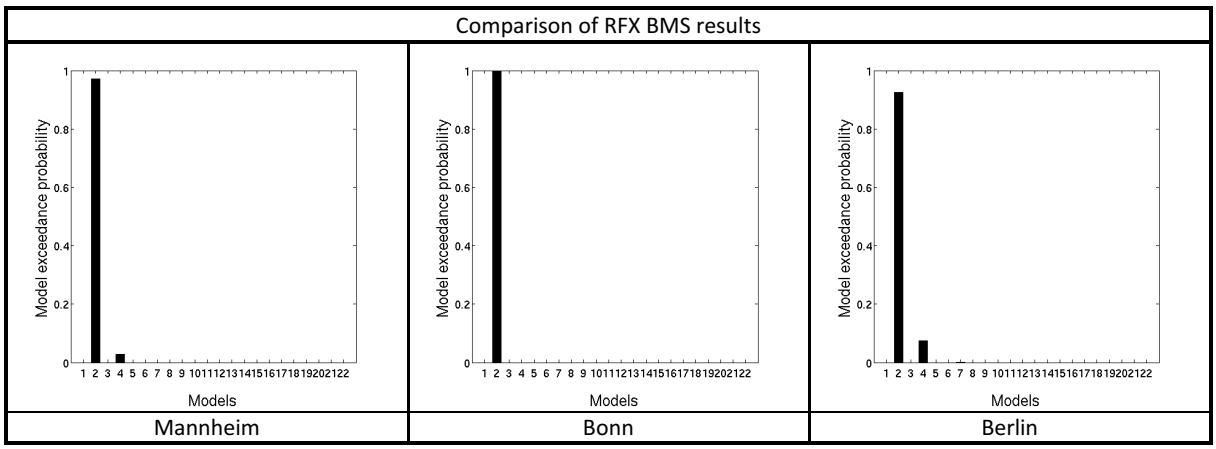

Figure 3.1.2.1. Comparison of RFX BMS results across the three sites

3.1.3. sDCM parameter estimates for each site

As described above, BMS revealed the same winning model in Mannheim, Bonn, and Berlin. For this model, Figure 3.1.3.1 shows the mean sDCM parameter estimates across participants from each site and the grand average across all sites.

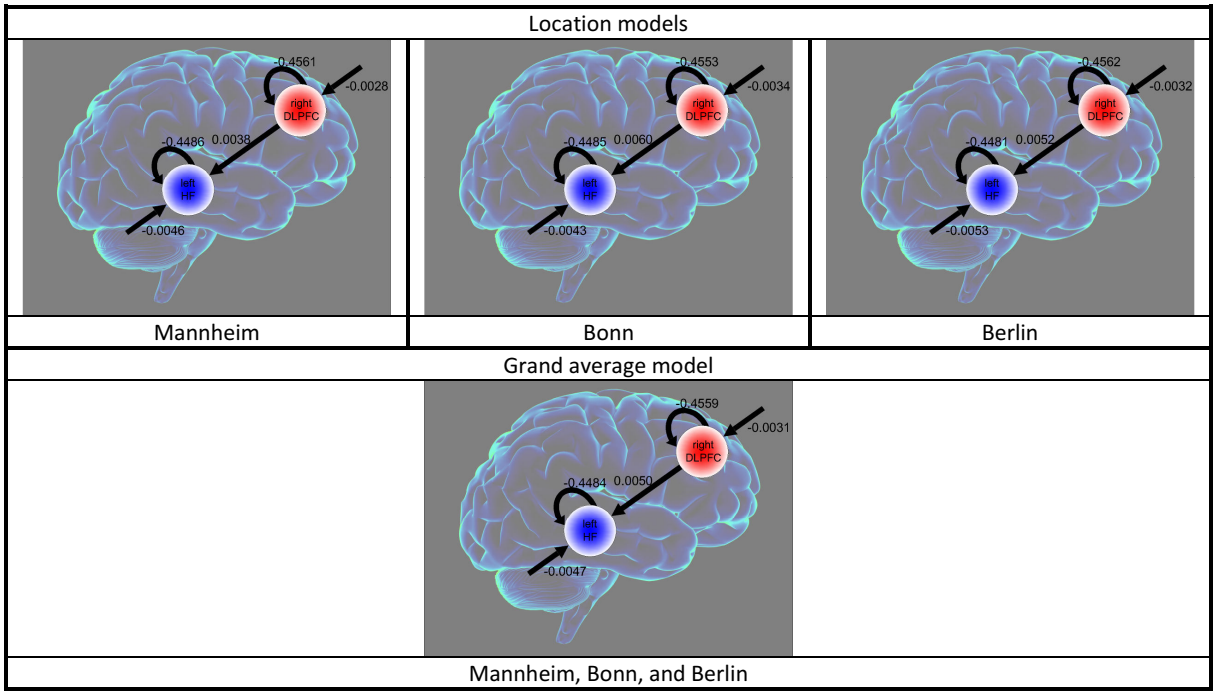

Figure 3.1.3.1. Mean sDCM parameter estimates across participants from each site and the grand average across the three sites

3.1.4. Statistical tests on sDCM parameter estimates across the three sites

As a further test of consistency of sDCM results across the three sites, we examined potential differences in the sDCM parameter estimates of the winning model by performing one-way ANOVA or a Kruskal-Wallis test depending on the distribution of the sDCM parameter estimates previously assessed by a Lilliefors Test, see Figure 3.1.4.1. Even without correction for multiple comparisons, none of the five parameters contained by model 2 were statistically different across sites.

Clearly we cannot infer that there are no differences between the parameter estimates among the sites (because this would rest upon accepting the null hypothesis). For further analysing this effect, we performed two-way analyses of variance, in which the five parameter estimates and the three sites are the two factors. We found no significant differences between sites using non-parametric Friedman-rank test, $\chi^2(2,885) = 3.23$, $p = 0.20$ (normality was rejected according to Lilliefors test only in 3 out of 15 repetitions, $p < 0.01$) and two-way ANOVA, $F(2,885) = 0.67$, $p = 0.51$; neither a significant interaction sites by parameter estimates, $F(8,885) = 0.51$, $p = 0.85$. Nonetheless, differences between the effects of connection strength are highly significant, $p < 0.01$.

Therefore, our two-way analysis of variance (both parametric and non-parametric) enables us to assert that the connection strength summary statistics provides sufficient power to detect differences among connections. This means that the absence of a centre by connection interaction cannot be explained trivially by an under-powered analysis. In other words, our analyses were

sufficiently sensitive to detect departures from the null hypothesis of no connectivity and yet failed to show any differences between centres.

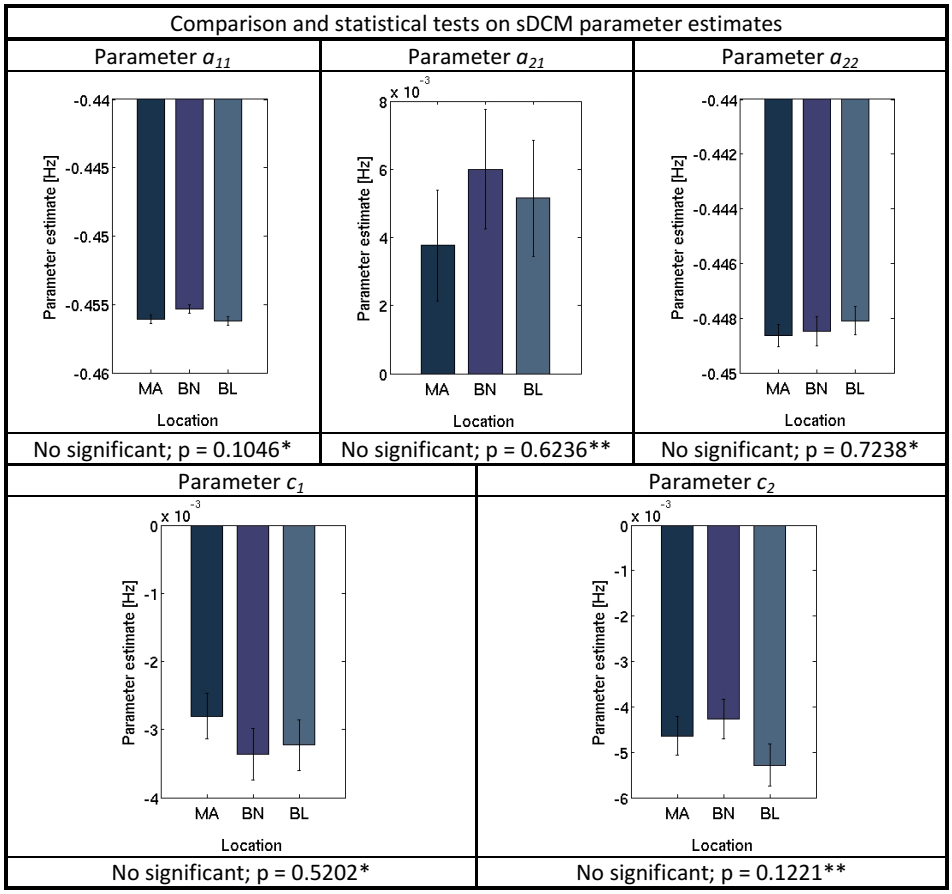

Figure 3.1.4.1. Comparison and statistical tests on sDCM parameter estimates across the three sites: Mannheim (MA), Bonn (BN), and Berlin (BL)
*One-way ANOVA; **Kruskal-Wallis test

3.2. Investigation of relations between sDCM parameter estimates, ZNF804A (rs1344706), and behavior in healthy volunteers

We divided this section into five subsections: sDCM parameter estimates for each genotype group, statistical tests on sDCM parameter estimates across different genetic models, statistical tests on behavior across different genetic models, linear regression of behavior on sDCM parameter estimates across different genetic models, and linear regression of mean performance in the 2-Back on mean reaction time in the 2-Back across different genetic models.

3.2.1. sDCM parameter estimates for each genotype group

As described in Section 3.1.2, BMS revealed the same winning model (model 2; Figure 3.4.2.1) in Mannheim, Bonn, and Berlin. For this model, Figure 4.2.1.1 shows the mean sDCM parameter estimates across participants for each genotype group: AA allele carriers, AC allele carriers, and CC allele carriers.

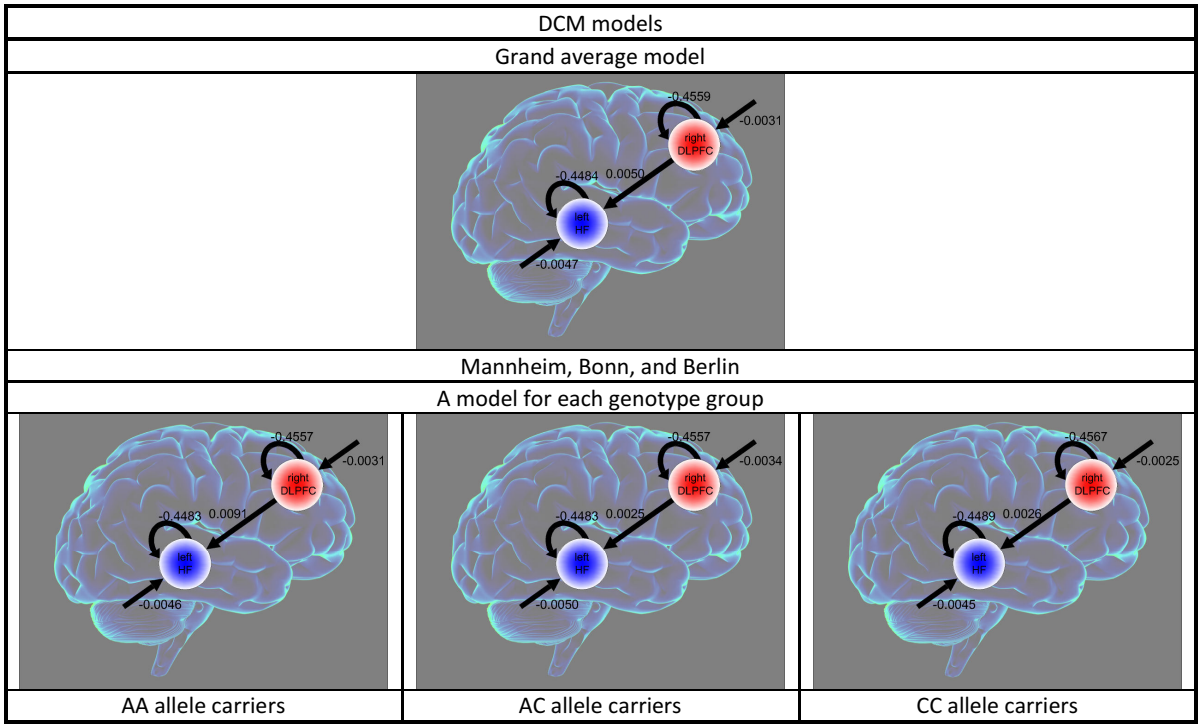

Figure 3.2.1.1. Grand average model across all participants and the mean sDCM parameter estimates across participants for each genotype group: AA, AC, and CC

3.2.2. Statistical tests on sDCM parameter estimates across different genetic models

Figure 3.2.2.1 shows the comparison between sDCM parameter estimates of the winning model for the "AA vs. AC vs. CC" model. We observe a significant effect on the connection from right DLPFC to left HF – parameter a_{21} – between genotype groups ($p = 0.0047$). AA allele carriers show higher prefrontal-hippocampal effective connectivity in comparison to AC+CC allele carriers. Furthermore,

we also observe a tendency on the self-connection in right DLPFC – parameter a_{11} – between genotype groups (n.s., p = 0.1011). AA+AC allele carriers show lower inhibition (higher excitation) per unit of time in right DLPFC in comparison to CC allele carriers.

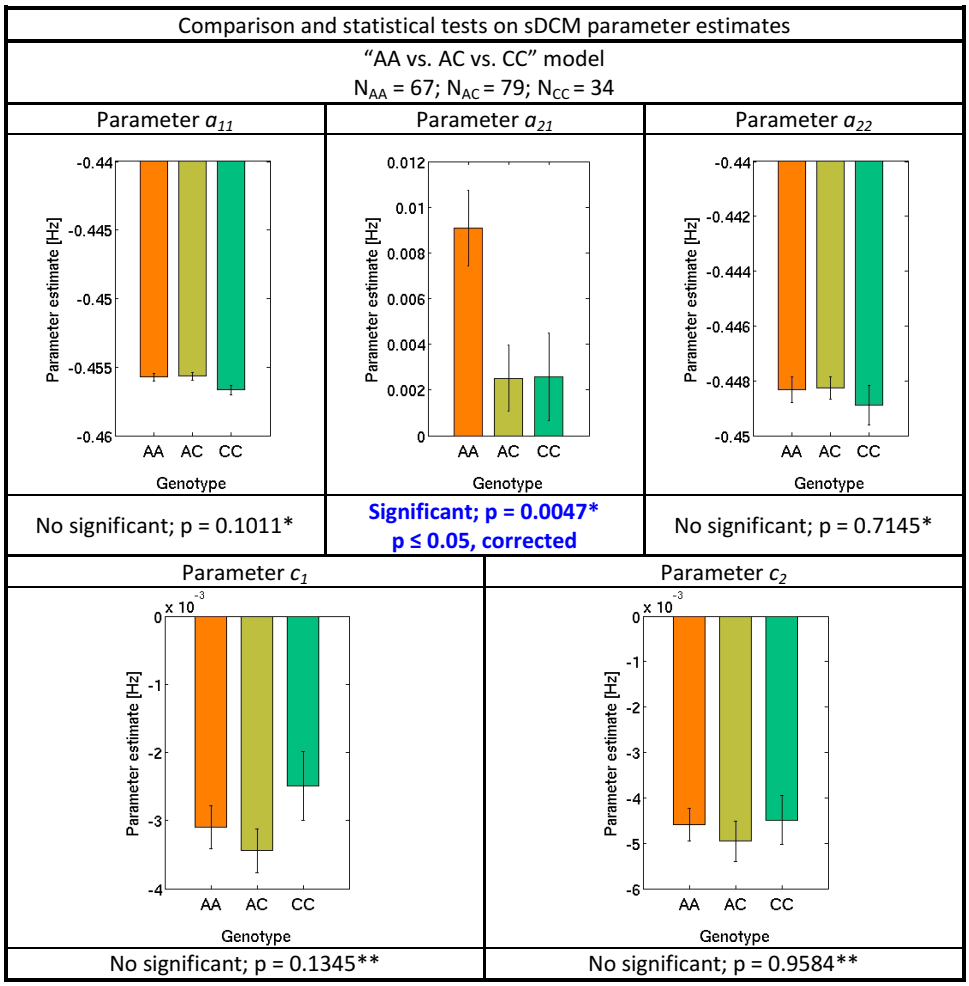

Figure 3.2.2.1. Comparison and statistical tests on sDCM parameter estimates across genotype groups for the "AA vs. AC vs. CC" model
*One-way ANOVA; **Kruskal-Wallis test

Figure 3.2.2.2 shows the comparison between sDCM parameter estimates of the winning model for the "AA vs. AC+CC" genetic model. We observe a significant effect on the connection from right DLPFC to left HF – parameter a_{21} – between genotype groups (p = 0.0011). AA allele carriers show higher prefrontal-hippocampal effective connectivity in comparison to AC+CC allele carriers.

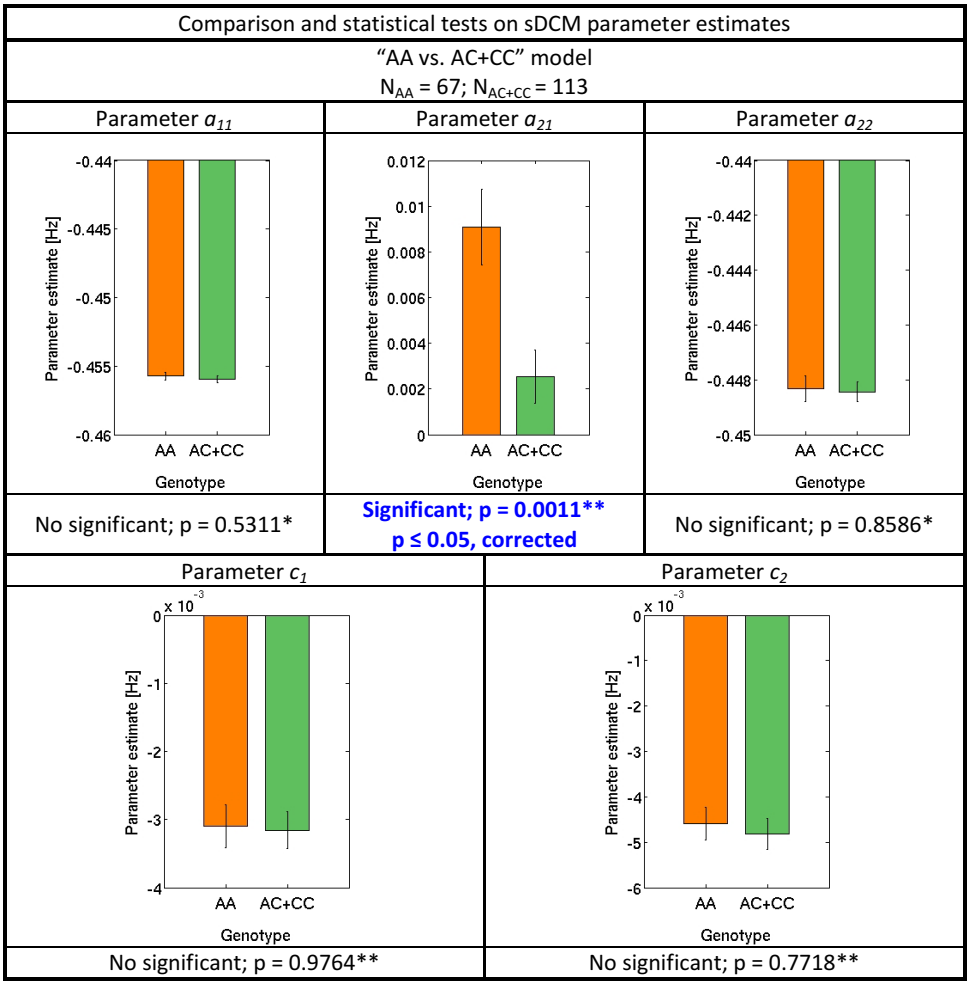

Figure 3.2.2.2. Comparison and statistical tests on sDCM parameter estimates between genotype groups for the "AA vs. AC+CC" model
*Two sample t-test; **Wilcoxon rank sum test

Figure 3.2.2.3 shows the comparison between sDCM parameter estimates of the winning model for the "AC vs. AA+CC" model. We observe a significant effect on the connection from right DLPFC to left HF – parameter a_{21} – between genotype groups (p = 0.0258). AC allele carriers show higher prefrontal-hippocampal effective connectivity in comparison to AA+CC allele carriers.

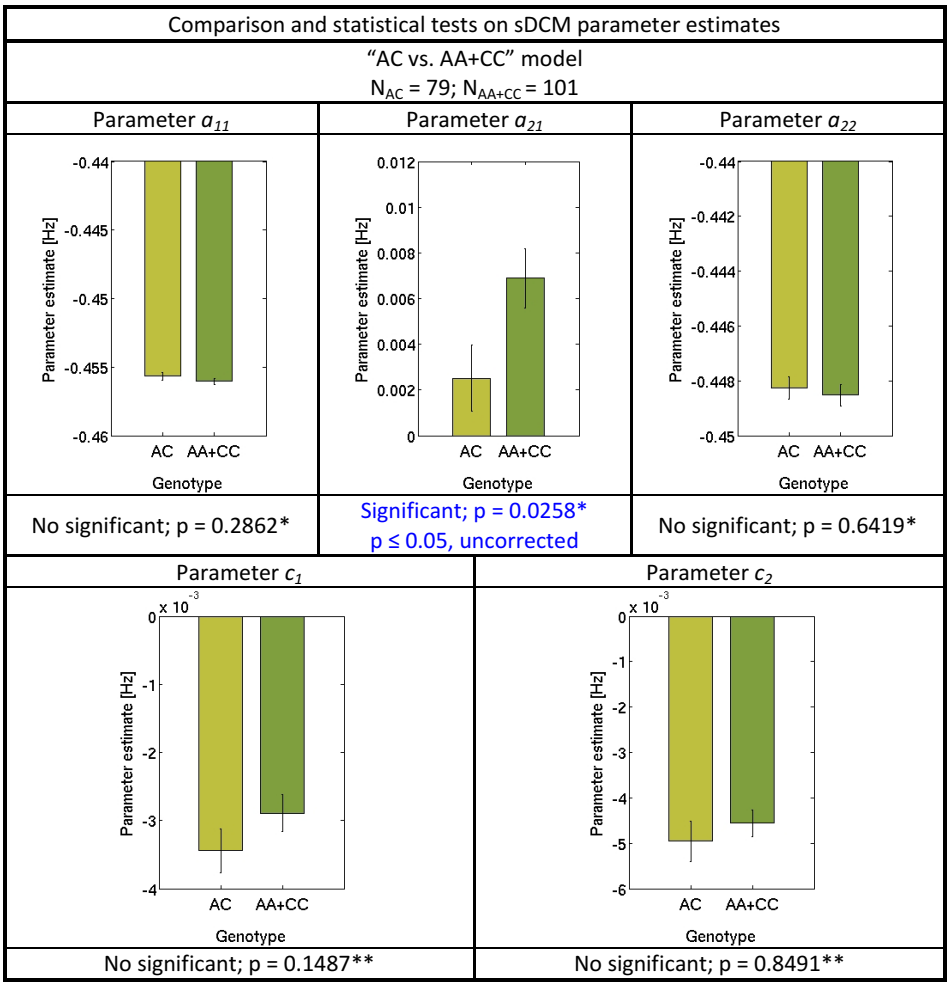

Figure 3.2.2.3. Comparison and statistical tests on sDCM parameter estimates between genotype groups for the "AC vs. AA+CC" model
*Two sample t-test; **Wilcoxon rank sum test

Figure 3.2.2.4 shows the comparison between sDCM parameter estimates of the winning model for the "CC vs. AA+AC" model. We observe a significant effect on the self-connection in right DLPFC – parameter a_{11} – between genotype groups (p = 0.0326). AA+AC allele carriers show lower inhibition (higher excitation) per unit of time in right DLPFC in comparison to CC allele carriers. Furthermore, we do observe a tendency on driven input into right DLPFC – parameter c_1 – between genotype groups (p = 0.0616). AA+AC allele carriers show increased deactivation per unit of time in right DLPFC driven by the 2-Back in comparison to CC allele carriers.

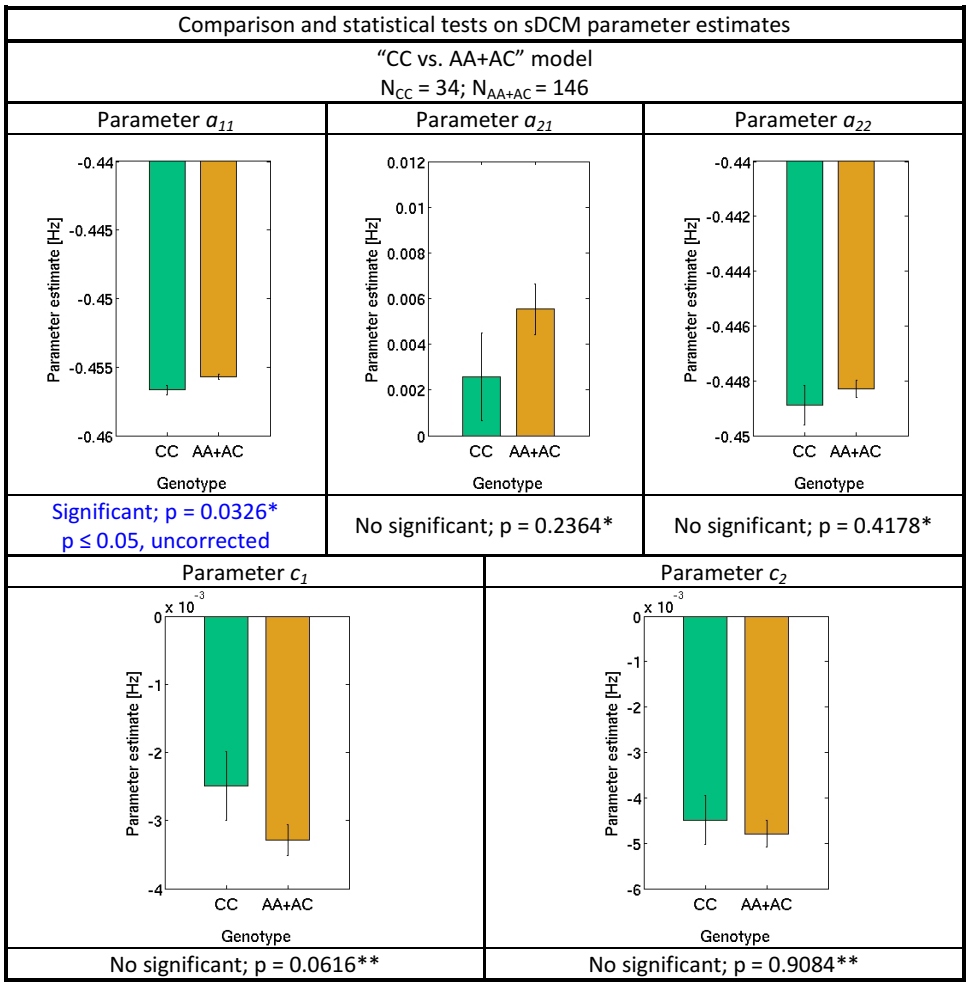

Figure 3.2.2.4. Comparison and statistical tests on sDCM parameter estimates between genotype groups for the "CC vs. AA+AC" model
*Two sample t-test; **Wilcoxon rank sum test

3.2.3. Statistical tests on behavior across different genetic models

(a) Statistical tests on mean performance in the 2-Back across different genetic models

Figure 3.2.3.1 shows the comparison between the mean performances in the 2-Back for each genotype model. We do not observe any statistically significant effect.

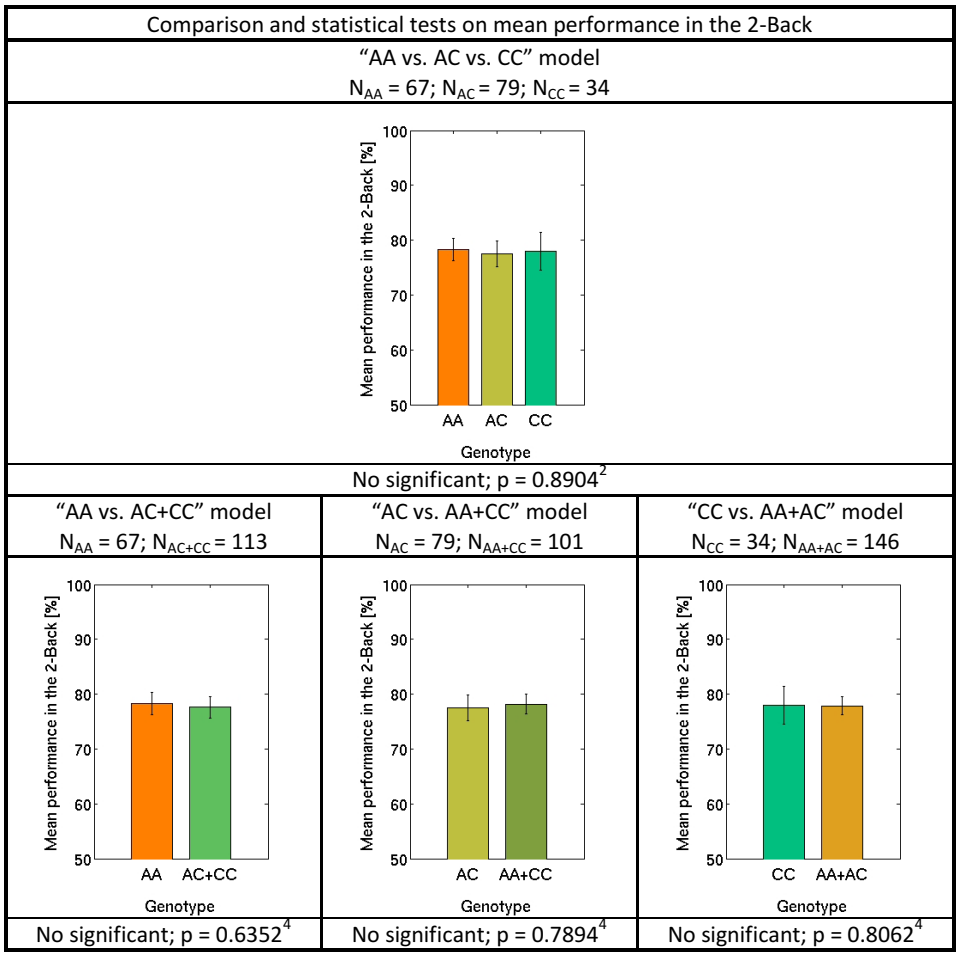

Figure 3.2.3.1. Comparison and statistical tests on mean performance in the 2-Back for each genetic model
[1]One-way ANOVA; [2]Kruskal-Wallis test; [3]Two sample t-test; [4]Wilcoxon rank sum test

(b) Statistical tests on mean reaction time in the 2-Back across different genetic models

Figure 3.2.3.2 shows the comparison between the mean reaction time in the 2-Back for each genetic model. We do not observe any statistically significant effect. Nonetheless, we do observe a slightly tendency in the "CC vs. AA+AC" model (n.s., p = 0.2002). AA+AC allele carriers show higher mean reaction time in the 2-Back in comparison to CC allele carriers.

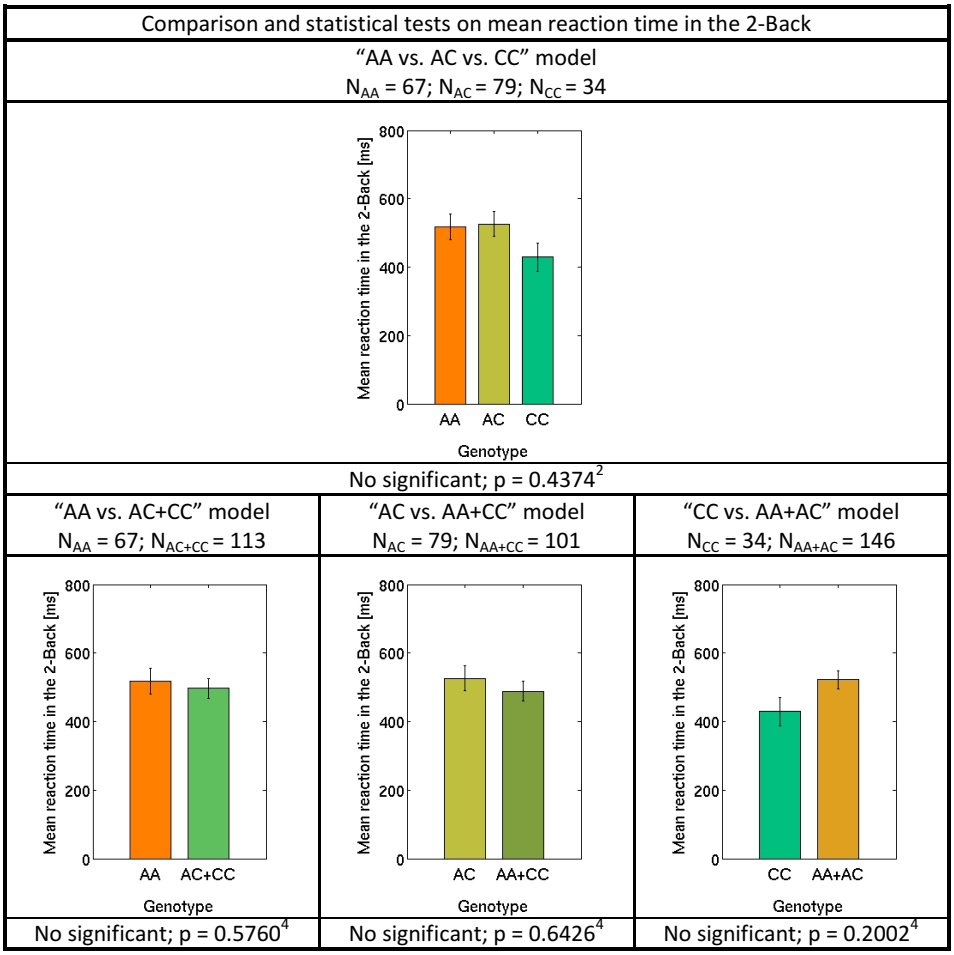

Figure 3.2.3.2. Comparison and statistical tests on mean reaction time in the 2-Back for each genetic model
[1]One-way ANOVA; [2]Kruskal-Wallis test; [3]Two sample t-test; [4]Wilcoxon rank sum test

3.2.4. Linear regression of behavior on sDCM parameter estimates across different genetic models

(a) Linear regression of mean performance in the 2-Back on sDCM parameter estimates across different genetic models

Figure 3.2.4.1 shows the linear regression of mean performance in the 2-Back on sDCM parameter estimates of the winning model for the "AA vs. AC vs. CC" model. We do not observe any statistically significant effect. Nonetheless, we do observe a tendency in AC allele carriers and another tendency in CC allele carriers. On the one hand, self-connection in left HF – parameter a_{22} – seems to predict mean performance in the 2-Back in AC allele carriers (p = 0.0644). The lower the

inhibition (higher excitation) per unit of time in left HF, the higher is the mean performance in the 2-Back in AC allele carriers. On the other hand, driven input into left HF – parameter c_2 – seems to predict mean performance in the 2-Back in CC allele carriers (p = 0.0923). The higher the driven input into left HF, the lower is the mean performance in the 2-Back in CC allele carriers.

<table>
<tr><td colspan="3">Linear regression of mean performance in the 2-Back on sDCM parameter estimates
"AA vs. AC vs. CC" model
N_{AA} = 67; N_{AC} = 79; N_{CC} = 34</td></tr>
<tr><td>Performance = f(Parameter a_{11})</td><td>Performance = f(Parameter a_{21})</td><td>Performance = f(Parameter a_{22})</td></tr>
<tr><td> 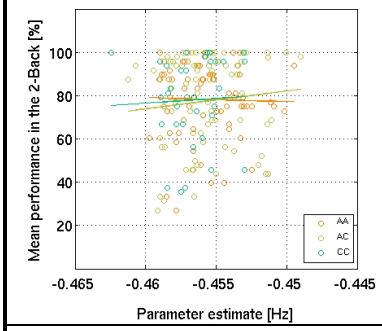
</td><td> 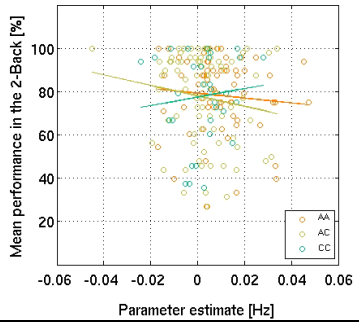
</td><td> 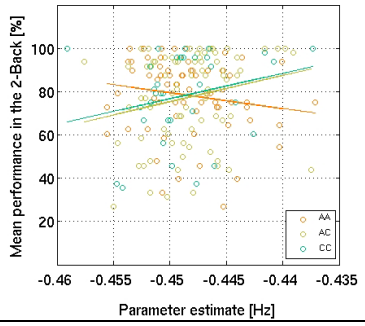
</td></tr>
<tr><td>AA: No significant; p = 0.8381
AC: No significant; p = 0.3912
CC: No significant; p = 0.8123</td><td>AA: No significant; p = 0.4806
AC: No significant; p = 0.1966
CC: No significant; p = 0.5835</td><td>AA: No significant; p = 0.1824
AC: No significant; p = 0.0644
CC: No significant; p = 0.1621</td></tr>
<tr><td colspan="2">Performance = f(Parameter c_1)</td><td>Performance = f(Parameter c_2)</td></tr>
<tr><td colspan="2"> 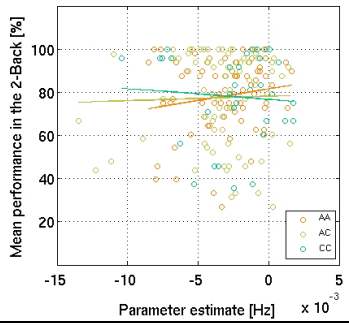
</td><td> 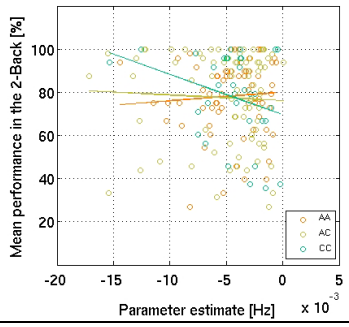
</td></tr>
<tr><td colspan="2">AA: No significant; p = 0.1969
AC: No significant; p = 0.8019
CC: No significant; p = 0.6826</td><td>AA: No significant; p = 0.5926
AC: No significant; p = 0.6754
CC: No significant; p = 0.0923</td></tr>
</table>

Figure 3.2.4.1. Linear regression of mean performance in the 2-Back on sDCM parameter estimates for the "AA vs. AC vs. CC" model

Figure 3.2.4.2 shows the linear regression of mean performance in the 2-Back on sDCM parameter estimates of the winning model for the "AA vs. AC+CC" model. We do observe a significant effect. Self-connection in the left HF – parameter a_{22} – predicts mean performance in the 2-Back in AC+CC allele carriers (p = 0.0202). The lower the inhibition (higher excitation) per unit of time in the left HF, the higher is the mean performance in the 2-Back in AC+CC allele carriers.

<table>
<tr><td colspan="3">Linear regression of mean performance in the 2-Back on sDCM parameter estimates
"AA vs. AC+CC" model
N_{AA} = 67; N_{AC+CC} = 113</td></tr>
<tr><td>Performance = f(Parameter a_{11})</td><td>Performance = f(Parameter a_{21})</td><td>Performance = f(Parameter a_{22})</td></tr>
<tr><td> 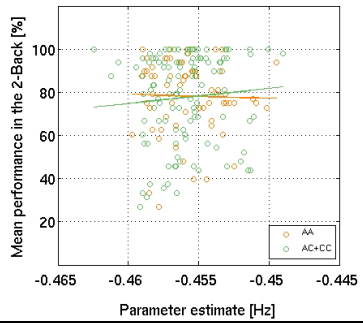
</td><td> 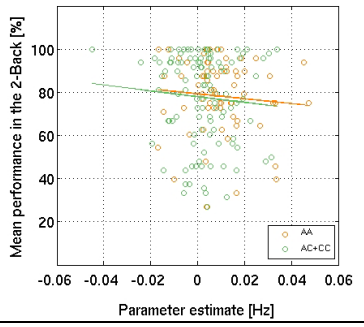
</td><td> 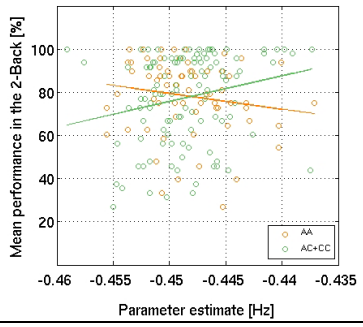
</td></tr>
<tr><td>AA: No significant; p = 0.8381
AC+CC: No significant; p = 0.3971</td><td>AA: No significant; p = 0.4806
AC+CC: No significant; p = 0.4013</td><td>AA: No significant; p = 0.1824
AC+CC: Significant; p = 0.0202
p ≤ 0.05, uncorrected</td></tr>
<tr><td colspan="2">Performance = f(Parameter c_1)</td><td>Performance = f(Parameter c_2)</td></tr>
<tr><td colspan="2"> 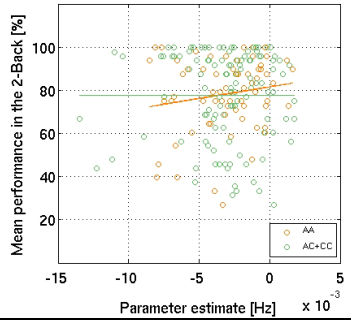
</td><td> 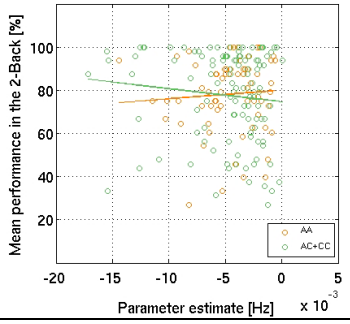
</td></tr>
<tr><td colspan="2">AA: No significant; p = 0.1969
AC+CC: No significant; p = 0.9975</td><td>AA: No significant; p = 0.5926
AC+CC: No significant; p = 0.2571</td></tr>
</table>

Figure 3.2.4.2. Linear regression of mean performance in the 2-Back on sDCM parameter estimates for the "AA vs. AC+CC" model

Figure 3.2.4.3 shows the linear regression of mean performance in the 2-Back on sDCM parameter estimates of the winning model for the "AC vs. AA+CC" model. We do not observe any significant effect. We do observe the same tendency on the self-connection in the left HF – parameter a_{22} – in AC allele carriers, since we are comparing "AC vs. AA+AC".

<table>
<tr><td colspan="3">Linear regression of mean performance in the 2-Back on sDCM parameter estimates
"AC vs. AA+CC" model
N_{AC} = 79; N_{AA+CC} = 101</td></tr>
<tr><td>Performance = f(Parameter a_{11})</td><td>Performance = f(Parameter a_{21})</td><td>Performance = f(Parameter a_{22})</td></tr>
<tr><td> 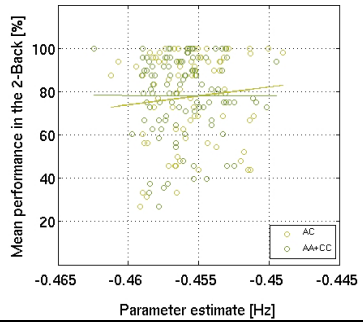
</td><td> 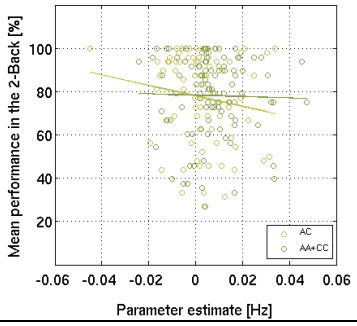
</td><td> 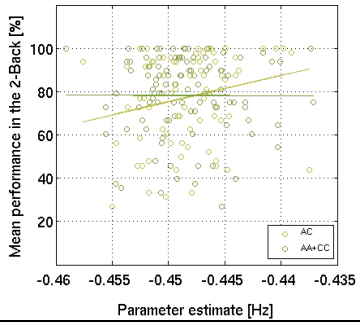
</td></tr>
<tr><td>AC: No significant; p = 0.3912
AA+CC: No significant; p = 0.9883</td><td>AC: No significant; p = 0.1966
AA+CC: No significant; p = 0.8415</td><td>AC: No significant; p = 0.0644
AA+CC: No significant; p = 0.9708</td></tr>
<tr><td colspan="2">Performance = f(Parameter c_1)</td><td>Performance = f(Parameter c_2)</td></tr>
<tr><td colspan="2"> 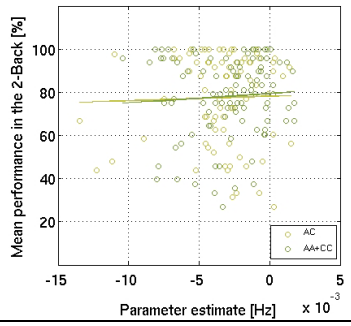
</td><td> 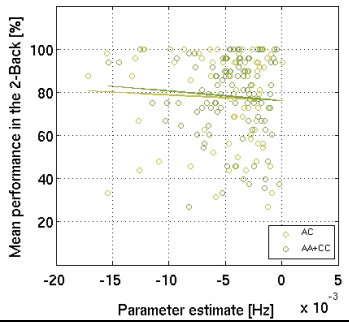
</td></tr>
<tr><td colspan="2">AC: No significant; p = 0.8019
AA+CC: No significant; p = 0.5199</td><td>AC: No significant; p = 0.6754
AA+CC: No significant; p = 0.4597</td></tr>
</table>

Figure 3.2.4.3. Linear regression of mean performance in the 2-Back on sDCM parameter estimates for the "AC vs. AA+CC" model

Figure 3.2.4.4 shows the linear regression of mean performance in the 2-Back on sDCM parameter estimates of the winning model for the "CC vs. AA+AC" model. We do not observe any significant effect. We do observe the same tendency on driven input into left HF – parameter c_2 – in CC allele carriers, since we are comparing "CC vs. AA+AC".

<table>
<tr><td colspan="3">Linear regression of mean performance in the 2-Back on sDCM parameter estimates</td></tr>
<tr><td colspan="3">"CC vs. AA+AC" model
N_{CC} = 34; N_{AA+AC} = 146</td></tr>
<tr><td>Performance = f(Parameter a_{11})</td><td>Performance = f(Parameter a_{21})</td><td>Performance = f(Parameter a_{22})</td></tr>
<tr><td> 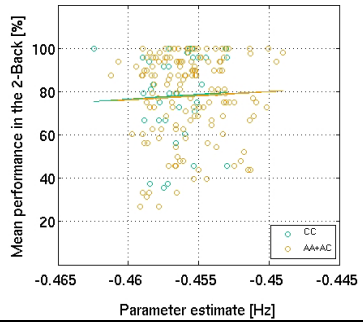
</td><td> 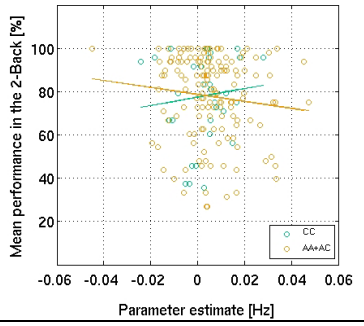
</td><td> 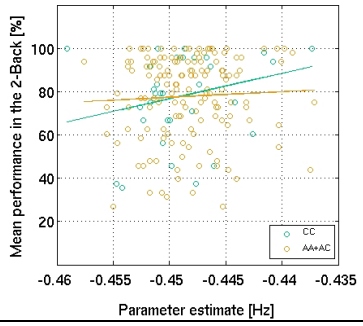
</td></tr>
<tr><td>CC: No significant; p = 0.8123
AA+AC: No significant; p = 0.5554</td><td>CC: No significant; p = 0.5835
AA+AC: No significant; p = 0.1768</td><td>CC: No significant; p = 0.1621
AA+AC: No significant; p = 0.5420</td></tr>
<tr><td colspan="2">Performance = f(Parameter c_1)</td><td>Performance = f(Parameter c_2)</td></tr>
<tr><td colspan="2"> 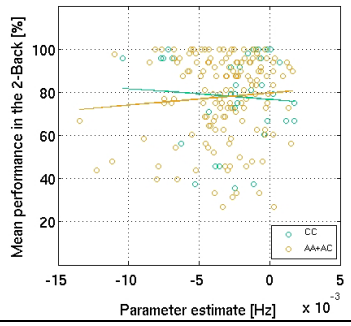
</td><td> 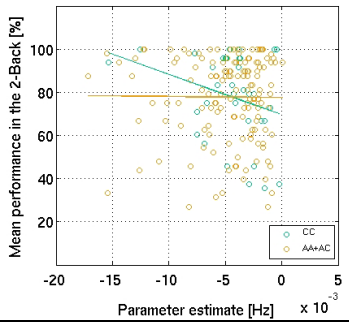
</td></tr>
<tr><td colspan="2">CC: No significant; p = 0.6826
AA+AC: No significant; p = 0.3370</td><td>CC: No significant; p = 0.0923
AA+AC: No significant; p = 0.9226</td></tr>
</table>

Figure 3.2.4.4. Linear regression of mean performance in the 2-Back on sDCM parameter estimates for the "CC vs. AA+AC" model

(b) Linear regression of mean reaction time in the 2-Back on sDCM parameter estimates across different genetic models

Figure 3.2.4.5 shows the linear regression of mean reaction time in the 2-Back on sDCM parameter estimates of the winning model for the "AA vs. AC vs. CC" model. We observe three significant effects. Firstly, self-connection in right DLPFC – parameter a_{11} – predicts mean reaction time in the 2-Back in AA allele carriers (p = 0.0481). The higher the inhibition (lower excitation) per unit of time in right DLPFC, the lower is the mean reaction time in the 2-Back in AA allele carriers. Secondly, connection from right DLPFC to left HF – parameter a_{21} – predicts mean reaction time in the 2-Back in CC allele carriers (p = 0.0457). The higher the prefrontal-hippocampal effective connectivity, the lower is the mean reaction time in the 2-Back in CC allele carriers. Lastly, driven input into right DLPFC - parameter c_1 – predicts mean reaction time in the 2-Back in AA allele carriers (p = 0.0057). The higher the driven input into right DLPFC, the lower is the mean reaction time in the 2-Back in AA allele carriers.

<table>
<tr><td colspan="3">Linear regression of mean reaction time in the 2-Back on sDCM parameter estimates
"AA vs. AC vs. CC" model
N_{AA} = 67; N_{AC} = 79; N_{CC} = 34</td></tr>
<tr><td>Reaction time = f(Parameter a_{11})</td><td>Reaction time = f(Parameter a_{21})</td><td>Reaction time = f(Parameter a_{22})</td></tr>
<tr><td> 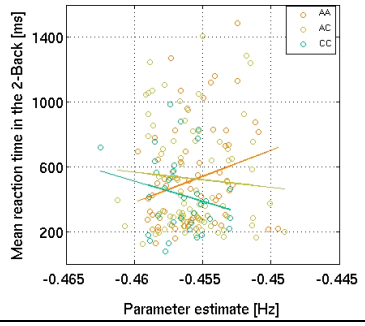
</td><td> 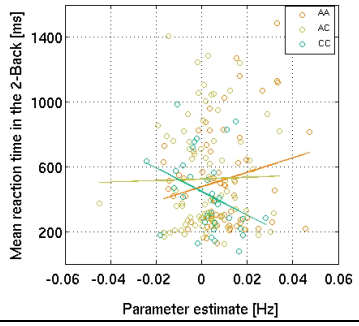
</td><td> 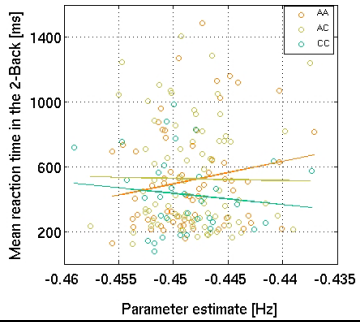
</td></tr>
<tr><td>AA: Significant; p = 0.0481
p ≤ 0.05, uncorrected
AC: No significant; p = 0.5430
CC: No significant; p = 0.2322</td><td>AA: No significant; p = 0.1163
AC: No significant; p = 0.8580
CC: Significant; p = 0.0457
p ≤ 0.05, uncorrected</td><td>AA: No significant; p = 0.1596
AC: No significant; p = 0.8954
CC: No significant; p = 0.4889</td></tr>
<tr><td colspan="2">Reaction time = f(Parameter c_1)</td><td>Reaction time = f(Parameter c_2)</td></tr>
<tr><td colspan="2"> 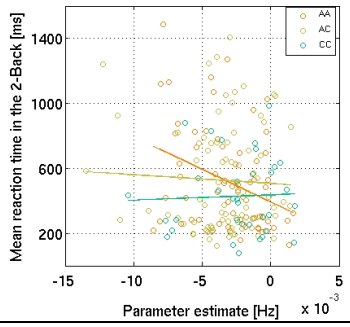
</td><td> 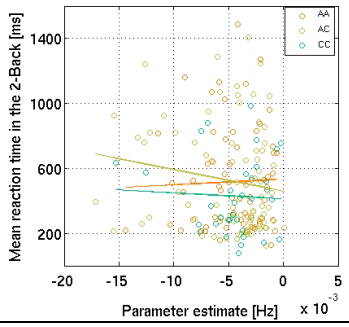
</td></tr>
<tr><td colspan="2">AA: Significant; p = 0.0057
p ≤ 0.05, corrected
AC: No significant; p = 0.6865
CC: No significant; p = 0.8222</td><td>AA: No significant; p = 0.7966
AC: No significant; p = 0.1642
CC: No significant; p = 0.7983</td></tr>
</table>

Figure 3.2.4.5. Linear regression of mean reaction time in the 2-Back on sDCM parameter estimates for the "AA vs. AC vs. CC" model

Figure 3.2.4.6 shows the linear regression of mean reaction time in the 2-Back on sDCM parameter estimates of the winning model for the "AA vs. AC+CC" model. We observe two significant effects, since we are comparing "AA vs. AC+CC". On the one hand, self-connection in right DLPFC – parameter a_{11} – predicts mean reaction time in the 2-Back in AA allele carriers (p = 0.0481). The lower the inhibition (higher excitation) per unit of time in the right DLPFC, the higher is the mean reaction time in the 2-Back in AA allele carriers. On the other hand, driven input into right DLPFC – parameter c_1 – predicts mean reaction time in the 2-Back in AA allele carriers (p = 0.0057). The higher the driven input into the right DLPFC, the lower is the mean reaction time in the 2-Back in AA allele carriers.

<table>
<tr><td colspan="3">Linear regression of mean reaction time in the 2-Back on sDCM parameter estimates</td></tr>
<tr><td colspan="3">"AA vs. AC+CC" model
N_{AA} = 67; N_{AC+CC} = 113</td></tr>
<tr><td>Reaction time = f(Parameter a_{11})</td><td>Reaction time = f(Parameter a_{21})</td><td>Reaction time = f(Parameter a_{22})</td></tr>
<tr><td> 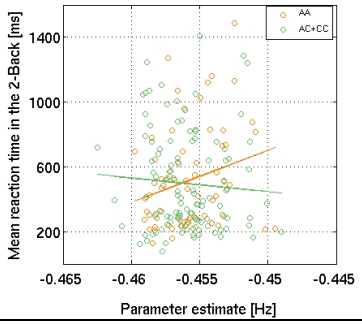
</td><td> 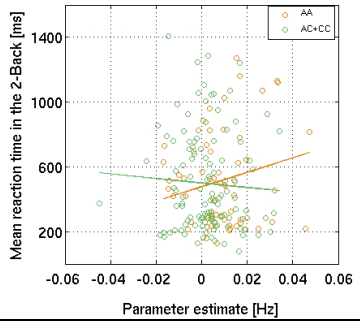
</td><td> 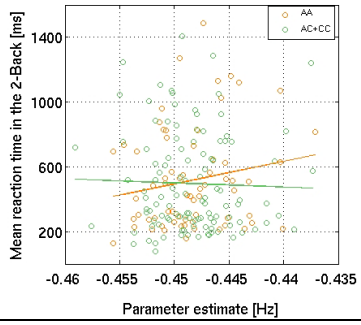
</td></tr>
<tr><td>AA: Significant; p = 0.0481
p ≤ 0.05, uncorrected
AC+CC: No significant; p = 0.4873</td><td>AA: No significant; p = 0.1163
AC+CC: No significant; p = 0.5574</td><td>AA: No significant; p = 0.1596
AC+CC: Significant; p = 0.7471</td></tr>
<tr><td colspan="2">Reaction time = f(Parameter c_1)</td><td>Reaction time = f(Parameter c_2)</td></tr>
<tr><td colspan="2"> 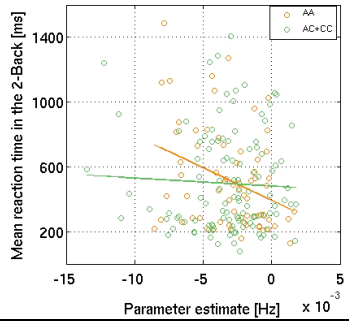
</td><td> 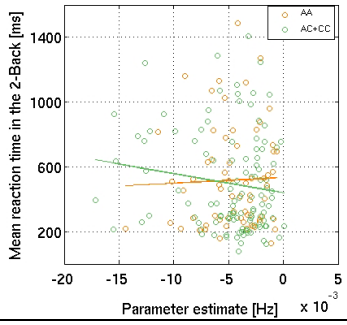
</td></tr>
<tr><td colspan="2">AA: Significant; p = 0.0057
p ≤ 0.05, corrected
AC+CC: No significant; p = 0.6258</td><td>AA: No significant; p = 0.7966
AC+CC: No significant; p = 0.1326</td></tr>
</table>

Figure 3.2.4.6. Linear regression of mean reaction time in the 2-Back on sDCM parameter estimates for the "AA vs. AC+CC" model

Figure 3.2.4.7 shows the linear regression of mean reaction time in the 2-Back on sDCM parameter estimates of the winning model for the "AC vs. AA+CC" model. We observe a significant effect. Driven input into the right DLPFC – parameter c_1 – predicts mean reaction time in the 2-Back in AA+CC allele carriers (p = 0.0221). The higher the driven input into the right DLPFC, the lower is the mean reaction time in the 2-Back in AA+CC allele carriers.

<table>
<tr><td colspan="3">Linear regression of mean reaction time in the 2-Back on sDCM parameter estimates
"AC vs. AA+CC" model
N_{AC} = 79; N_{AA+CC} = 101</td></tr>
<tr><td>Reaction time = f(Parameter a_{11})</td><td>Reaction time = f(Parameter a_{21})</td><td>Reaction time = f(Parameter a_{22})</td></tr>
<tr><td> 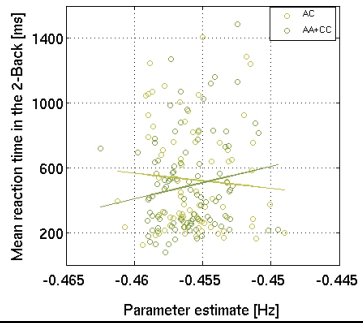
</td><td> 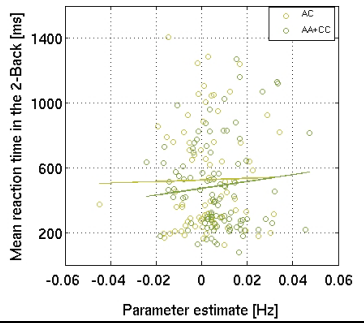
</td><td> 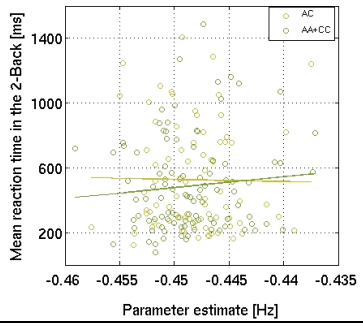
</td></tr>
<tr><td>AC: No significant; p = 0.5430
AA+CC: No significant; p = 0.1192</td><td>AC: No significant; p = 0.8580
AA+CC: No significant; p = 0.3413</td><td>AC: No significant; p = 0.8954
AA+CC: No significant; p = 0.3550</td></tr>
<tr><td colspan="2">Reaction time = f(Parameter c_1)</td><td>Reaction time = f(Parameter c_2)</td></tr>
<tr><td colspan="2"> 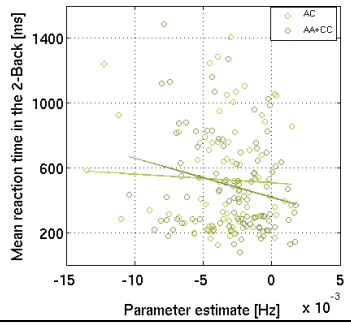
</td><td> 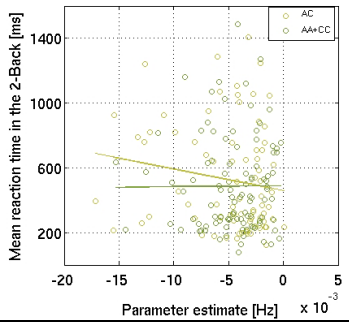
</td></tr>
<tr><td colspan="2">AC: No significant; p = 0.6865
AA+CC: No significant; p = 0.0221
p ≤ 0.05, uncorrected</td><td>AC: No significant; p = 0.1642
AA+CC: No significant; p = 0.9481</td></tr>
</table>

Figure 3.2.4.7. Linear regression of mean reaction time in the 2-Back on sDCM parameter estimates for the "AC vs. AA+CC" model

Figure 3.2.4.8 shows the linear regression of mean reaction time in the 2-Back on sDCM parameter estimates of the winning model for the "CC vs. AA+AC" model. We observe two statistically significant effects. On the one hand, connection from right DLPFC to left HF – parameter a_{21} – predicts mean reaction time in the 2-Back in CC allele carriers (p = 0.0457). The higher the prefrontal-hippocampal effective connectivity, the lower is the mean reaction time in the 2-Back in CC allele carriers. On the other hand, driven input into right DLPFC - parameter c_1 – predicts mean reaction time in the 2-Back in AA+AC allele carriers (p = 0.0440). The higher the driven input into the right DLPFC, the lower is the mean reaction time in the 2-Back in AA+AC allele carriers.

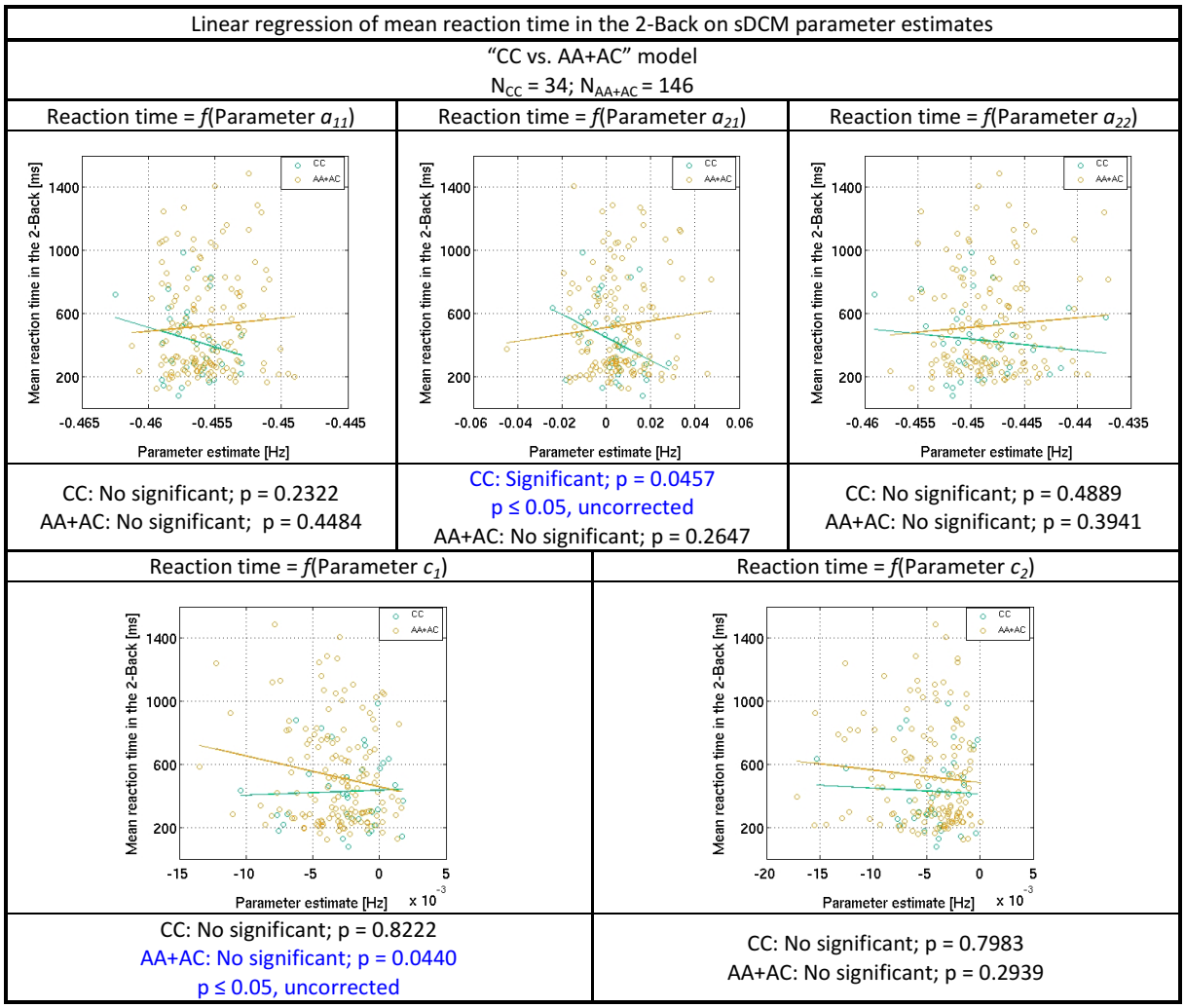

Figure 3.2.4.8. Linear regression of mean reaction time in the 2-Back on sDCM parameter estimates for the "CC vs. AA+AC" model

3.2.5. Linear regression of mean performance in the 2-Back on mean reaction time in the 2-Back across different genetic models

Figure 3.2.5.1 shows the linear regression of mean performance in the 2-Back on mean reaction time in the 2-Back for each genotype model. We observe a statistically significant effect in all subjects independently on genotype. Mean reaction time in the 2-Back predicts mean performance in the 2-Back in AA allele carriers (p = 3.3968e-5), AC allele carriers (p = 3.8194e-10), and CC allele

carriers (p = 0.0096). The lower the reaction time in the 2-Back, the higher is the mean performance in the 2-Back in all subjects.

<table>
<tr><td colspan="3">Linear regression of mean performance in the 2-Back on mean reaction time in the 2-Back</td></tr>
<tr><td colspan="3">“AA vs. AC vs. CC” model
N_{AA} = 67; N_{AC} = 79; N_{CC} = 34</td></tr>
<tr><td colspan="3"> 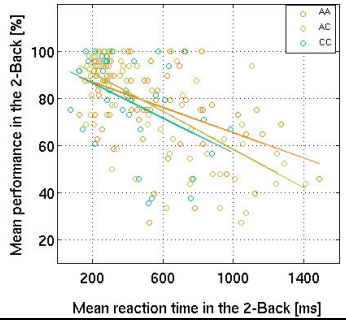
</td></tr>
<tr><td colspan="3">AA: Significant; p = 3.3968e-5
p ≤ 0.05, corrected
AC: Significant; p = 3.8194e-10
p ≤ 0.05, corrected
CC: Significant; p = 0.0096
p ≤ 0.05, corrected</td></tr>
<tr><td>“AA vs. AC+CC” model
N_{AA} = 67; N_{AC+CC} = 113</td><td>“AC vs. AA+CC” model
N_{AC} = 79; N_{AA+CC} = 101</td><td>“CC vs. AA+AC” model
N_{CC} = 34; N_{AA+AC} = 146</td></tr>
<tr><td> 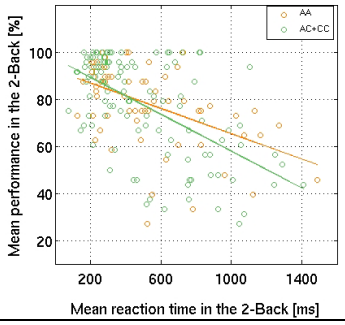
</td><td> 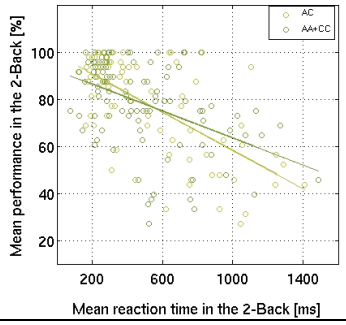
</td><td> 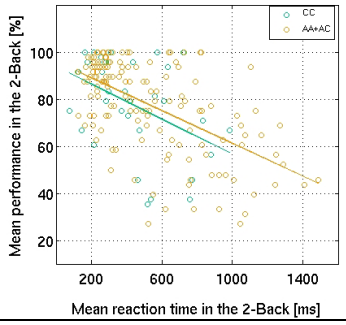
</td></tr>
<tr><td>AA: Significant; p = 3.3968e-5
p ≤ 0.05, corrected
AC+CC: Significant; p = 1.6689e-11
p ≤ 0.05, corrected</td><td>AC: Significant; p = 3.8194e-10
p ≤ 0.05, corrected
AA+CC: Significant; p = 1.8090e-6
p ≤ 0.05, corrected</td><td>CC: Significant; p = 0.0096
p ≤ 0.05, corrected
AA+AC: Significant; p = 4.1417e-14
p ≤ 0.05, corrected</td></tr>
</table>

Figure 3.2.5.1. Linear regression of mean performance in the 2-Back on mean reaction time in the 2-Back for each genetic model

3.3. Investigation of relations between sDCM parameter estimates and behavior in pair-wise matched healthy volunteers and schizophrenia patients

We divided this section into seven subsections: SPM, BMS, DCM parameter estimates for each group, statistical tests on sDCM parameter estimates between groups, statistical tests on behavior between groups, linear regression of behavior on sDCM parameter estimates for each group, and linear regression of mean performance in the 2-Back on mean reaction time in the 2-Back for each group.

3.3.1. SPM for each group

The conjunction maps depicted in Figures 3.3.1.1 and 3.3.1.2 show the common (de)activation pattern across the two groups in our anatomically constrained regions of interest. These conjunction analyses showed a consistent activation in the right DLPFC (*x, y, z* = 45, 11, 35; T = 7.69; p = 0.05, FWE-corrected) and consistent deactivation in the left HF (*x, y, z* = -27, -31, -10; T = 6.80; p = 0.05, FWE-corrected) across the two groups.

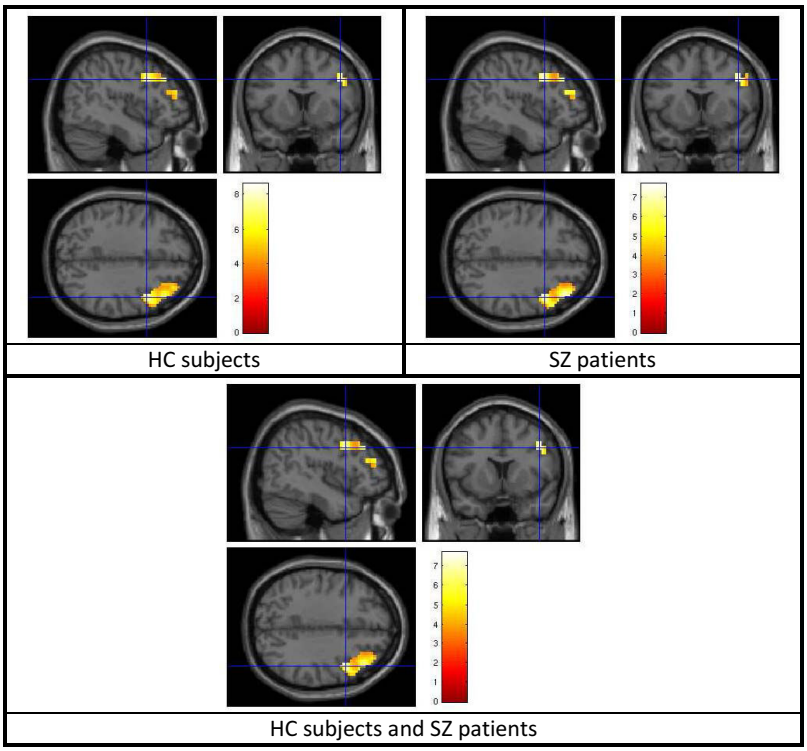

Figure 3.3.1.1. Activation maps for each group and conjunction map in the right DLPFC

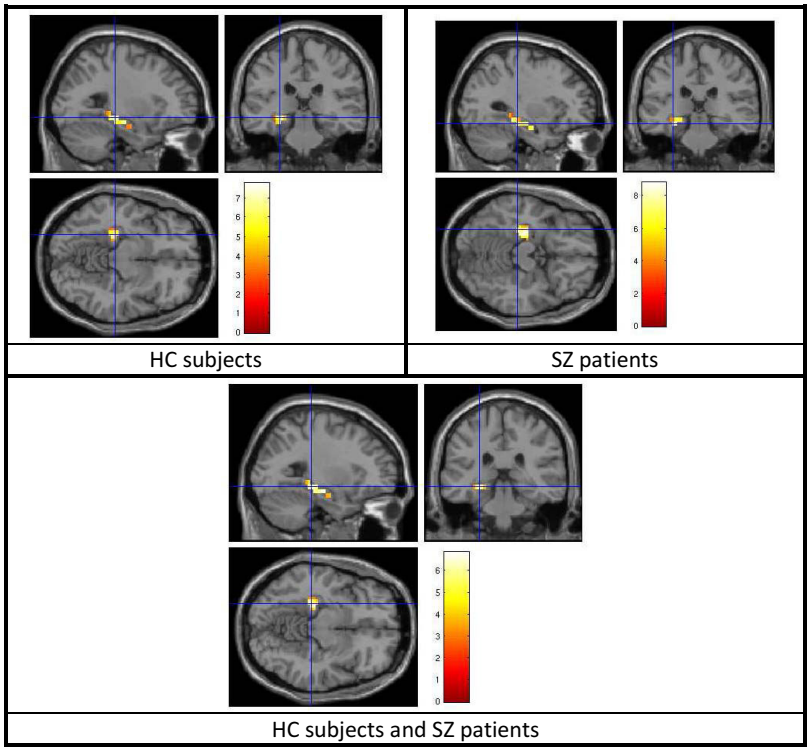

Figure 3.3.1.2. Deactivation maps for each group and conjunction map in the left HF

As described in Chapter 2, these conjunction results were subsequently used as group-level functional ROIs to guide the subsequent time series extraction in the right DLPFC and left HF of each individual subject.

3.3.2. BMS for each group

We used random effects BMS to determine, from our model space of twenty-two alternative sDCMs (Figure 2.5.2.1), the model that provided the best balance between accuracy and complexity for explaining the measured data. The results were fully consistent across the two groups, revealing the same winning model (model 2; Figure 2.5.2.1) in HC subjects and SZ patients. This model includes a driving influence of the 2-Back condition on both DLPFC and HF, and a unidirectional influence from DLPFC to HF.

Figure 3.3.2.1 shows the results of BMS Random Effects (RFX) for each group. The exceedance probability of model 2 (i.e., the probability that this model is a more likely model than any other model considered) was 0.93 (for the healthy control group), and 0.75 (for the schizophrenic group), respectively.

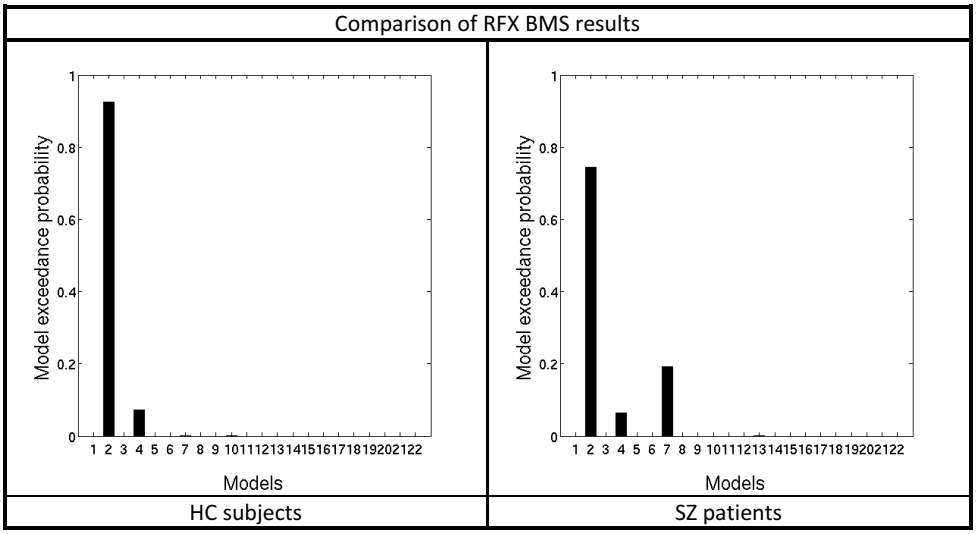

Figure 3.3.2.1. Comparison of RFX BMS results between groups

3.3.3. sDCM parameter estimates for each group

As described above, BMS revealed the same winning model in HC subjects and SZ patients. Figure 3.3.3.1 shows the mean sDCM parameter estimates for each group.

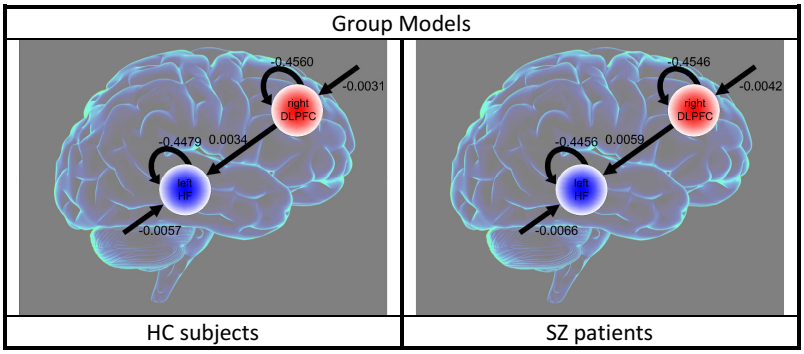

Figure 3.3.3.1. Mean sDCM parameter estimates for each group

3.3.4. Statistical tests on sDCM parameter estimates between groups

Figure 3.3.4.1 shows a comparison between sDCM parameter estimates of the winning model for the "HC vs. SZ" model. We observe two statistically significant effects. On the one hand, we observe a statistically significant effect in the self-connection in right DLPFC – parameter a_{11} – between groups (p = 0.0290). SZ patients show lower inhibition (higher excitation) per unit of time in right DLPFC in comparison to HC subjects. On the other hand, we observe a statistically significant effect in the self-connection in left HF – parameter a_{22} – between groups (p = 0.0159). SZ patients show lower inhibition (higher excitation) per unit of time in the left HF in comparison to HC subjects. Furthermore, we observe two tendencies. On the one hand, we observe a tendency on driven input into right DLPFC – parameter c_1 – between groups (n.s., p = 0.0956). SZ patients show increased deactivation per unit of time in right DLPFC driven by the 2-Back condition in comparison to HC subjects. On the other hand, we observe a tendency on driven input into the left HF – parameter c_2 –

between groups (n.s., p = 0.1437). SZ patients show increased deactivation per unit of time in right DLPFC driven by the 2-Back condition in comparison to HC subjects. We do not observe any tendency on the connection from right DLPFC to left HF – parameter a_{21} – between groups (n.s., p = 0.5548).

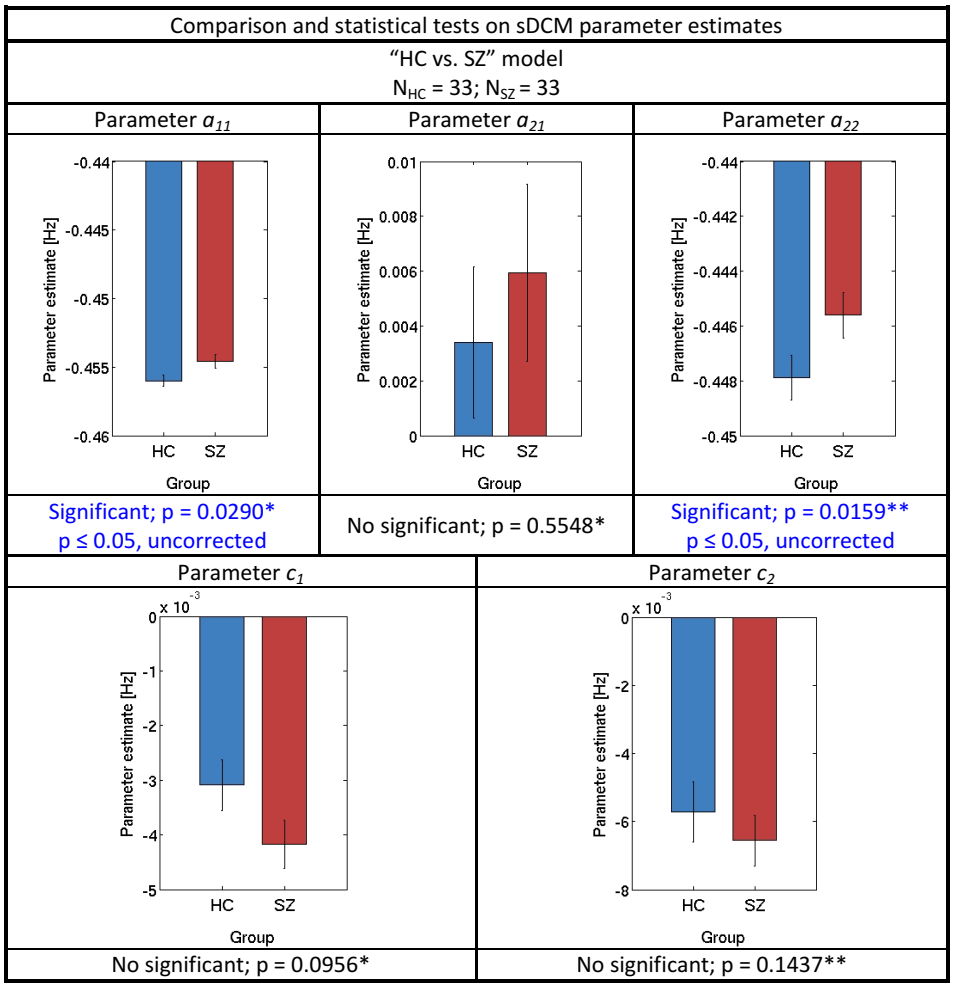

Figure 3.3.4.1. Comparison and statistical tests on sDCM parameter estimates for the "HC vs. SZ" model
*Two sample t-test; **Wilcoxon rank sum test

3.3.5. Statistical tests on behavior between groups

(a) Statistical tests on mean performance in the 2-Back between HC subjects and SZ patients

Figure 3.3.5.1 shows a comparison between mean performances in the 2-Back for the "HC vs. SZ" model. We observe a statistically significant effect in the mean performance in the 2-Back between groups (p = 4.3541e-06). SZ patients show lower mean performance in the 2-Back in comparison to HC subjects.

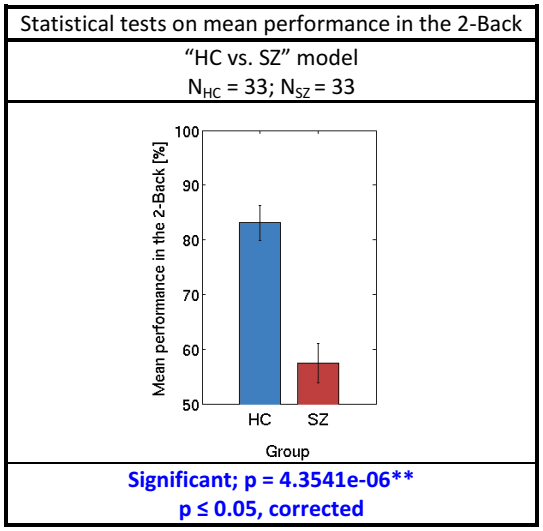

Figure 3.3.5.1. Comparison and statistical tests on mean performance in the 2-Back for the "HC vs. SZ" model *Two sample t-test; **Wilcoxon rank sum test

(b) Statistical tests on mean reaction time in the 2-Back between HC subjects and SZ patients

Figure 3.3.5.2 shows a comparison between mean reaction times in the 2-Back for the "HC vs. SZ" model. We do not observe any statistically significant effect. Nonetheless, we do observe a tendency in the mean reaction time in the 2-Back between groups (n.s., p = 0.1472). SZ patients show higher mean reaction time in the 2-Back in comparison to HC subjects.

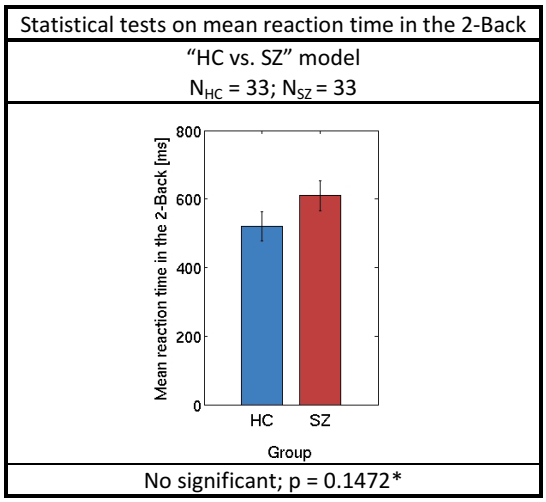

Figure 3.3.5.2. Comparison and statistical tests on mean reaction time in the 2-Back for the "HC vs. SZ" model *Two sample t-test; **Wilcoxon rank sum test

3.3.6. Linear regression of behavior on sDCM parameter estimates for each group

(a) Linear regression of mean performance in the 2-Back on sDCM parameter estimates for each group

Figure 3.3.6.1 shows the linear regression of mean performance in the 2-Back on sDCM parameter estimates of the winning model for the "HC vs. SZ" model. We observe a statistically significant effect. Connection from right DLPFC to left HF – parameter a_{21} – predicts mean performance in the 2-

Back in SZ patients (p = 0.0452). The lower the prefrontal-hippocampal effective connectivity, the higher is the mean performance in the 2-Back in SZ patients. Furthermore, we observe a tendency in HC subjects and another tendency in SZ patients. On the one hand, self-connection in right DLPFC – parameter a_{11} – seems to predict mean performance in the 2-Back in HC subjects (n.s., p = 0.1028). The lower the inhibition (higher excitation) per unit of time in right DLPFC, the higher is the mean performance in the 2-Back in HC subjects. On the other hand, driven input into left HF – parameter c_2 – seems to predict mean performance in the 2-Back in SZ patients (n.s., p = 0.1188). The higher the driven input into the left HF, the higher is the mean performance in the 2-Back in SZ patients.

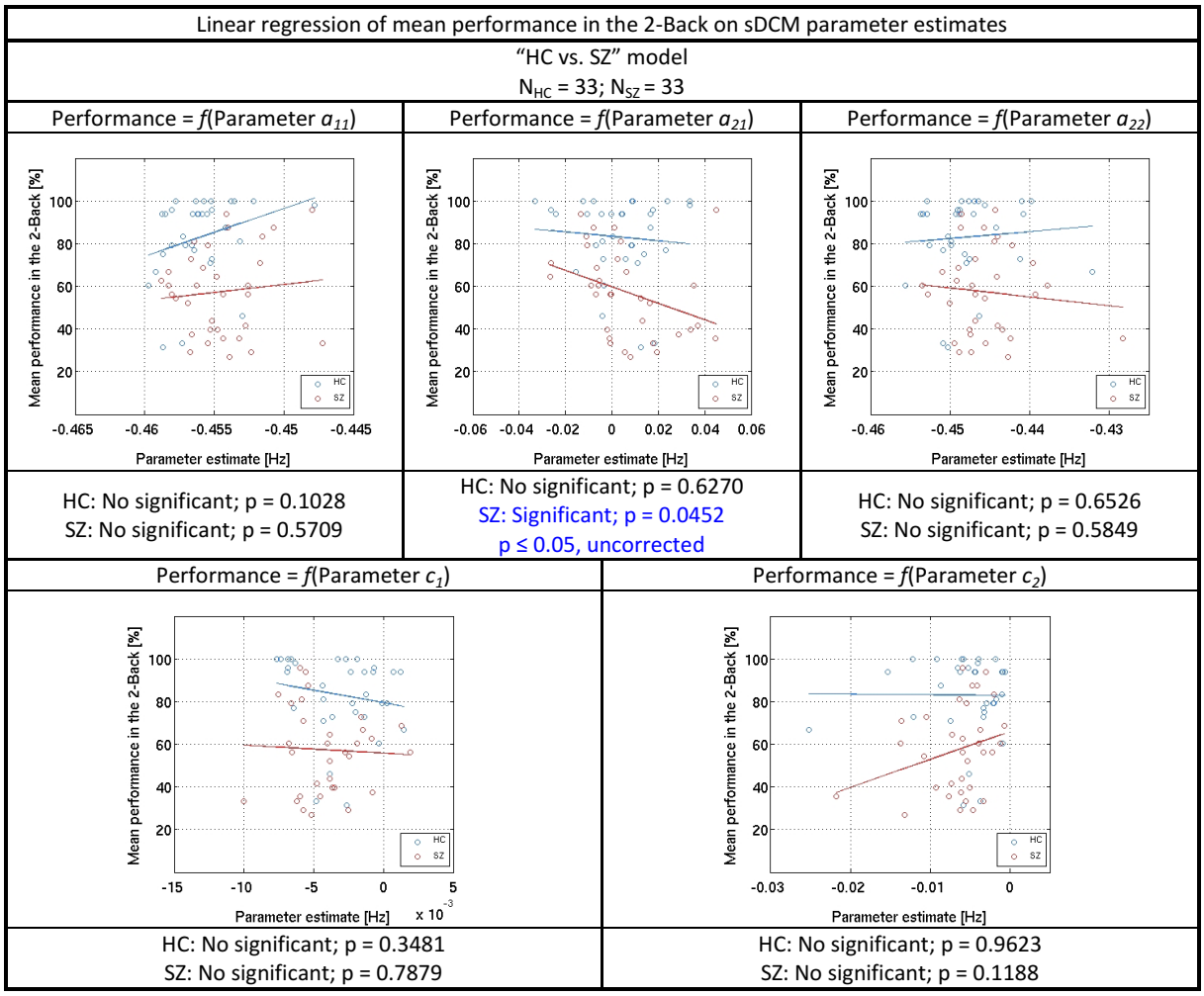

Figure 3.3.6.1. Linear regression of mean performance in the 2-Back on sDCM parameter estimates for the "HC vs. SZ" model

(b) Linear regression of mean reaction time in the 2-Back on sDCM parameter estimates for each group

Figure 3.3.6.2 shows the linear regression of mean reaction time in the 2-Back on sDCM parameter estimates of the winning model for the "HC vs. SZ" model. We do not observe any statistically significant effect. Nonetheless, we observe two tendencies in SZ patients. On the one hand, self-connection in right DLPFC – parameter a_{11} – seems to predict mean reaction time in the 2-

Back in SZ patients (n.s., p = 0.1107). The higher the inhibition (lower excitation) per unit of time in right DLPFC, the lower is the mean reaction time in the 2-Back in SZ patients. On the other hand, driven input into right DLPFC – parameter c_1 – seems to predict mean reaction time in the 2-Back in SZ patients (n.s., p = 0.1360). The higher the driven input into the right DLPFC, the lower is the mean reaction time in the 2-Back in SZ patients.

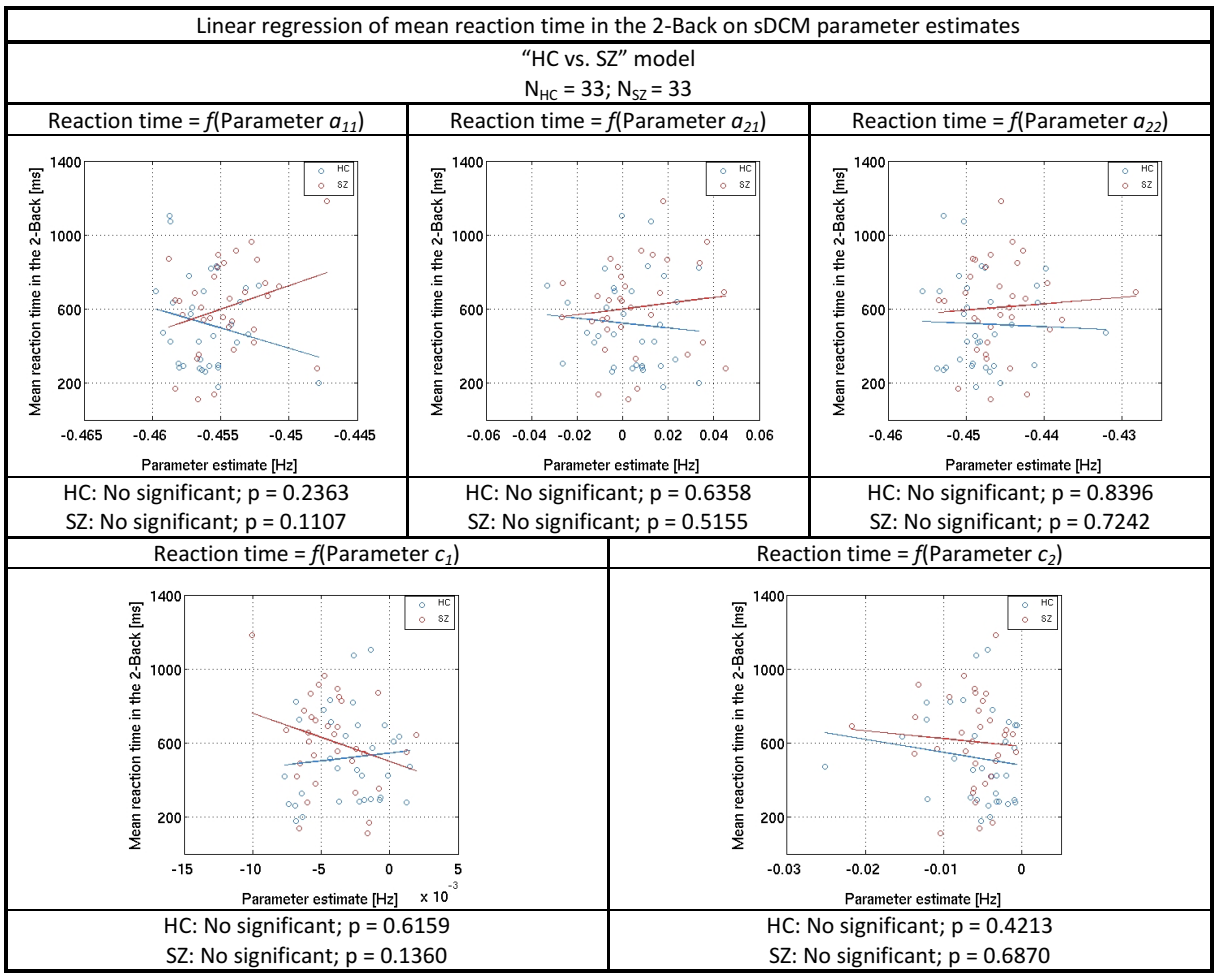

Figure 3.3.6.2. Linear regression of mean reaction time in the 2-Back on sDCM parameter estimates for the "HC vs. SZ" model

3.3.7. Linear regression of mean performance in the 2-Back on mean reaction time in the 2-Back for each group

Figure 3.3.7.1 shows a linear regression of mean performance in the 2-Back on mean reaction time in the 2-Back for the "HC vs. SZ" model. We observe a statistically significant effect. Mean reaction time in the 2-Back predicts mean performance in the 2-Back in SZ patients (p = 0.0035). The lower the reaction time in the 2-Back, the higher is the mean performance in the 2-Back in SZ patients.

Linear regression of mean performance in the 2-Back on mean reaction time in the 2-Back

"HC vs. SZ" model

$N_{HC} = 33$; $N_{SZ} = 33$

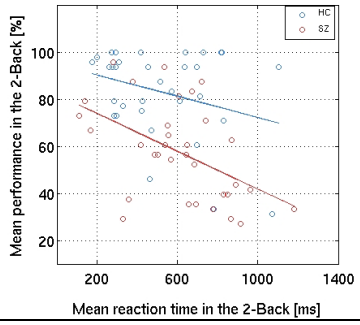

HC: No significant; p = 0.6270

SZ: Significant; p = 0.0035

p ≤ 0.05, corrected

Figure 3.3.7.1. Linear regression of mean performance in the 2-Back on mean reaction time in the 2-Back for the "HC vs. SZ" model

3.4. Comparison of two-group genetic models and healthy vs. schizophrenia model

We qualitatively compare each of the two-group genetic models: "AA vs. AC+CC", "AC vs. AA+CC", and "CC vs. AA+AC" to the "HC vs. SZ" model. We found a high degree of similarity between "CC vs. AA+AC" and "HC vs. SZ" models. Next, we show the similarities between these two models.

3.4.1. Comparison of "CC vs. AA+AC" and "HC vs. SZ" models

We qualitatively compare: (a) sDCM models, (b) Statistical tests on sDCM parameter estimates, (c) Statistical tests on behavior, (d) Linear regression of behavior on sDCM parameter estimates , and (e) Linear regression of mean performance in the 2-Back on mean reaction time in the 2-Back.

(a) Comparison of sDCM models between "CC vs. AA+AC" and "HC vs. SZ" models

Figure 3.4.1.1 shows a comparison of sDCM models between "CC vs. AA+AC" and "HC vs. SZ" models.

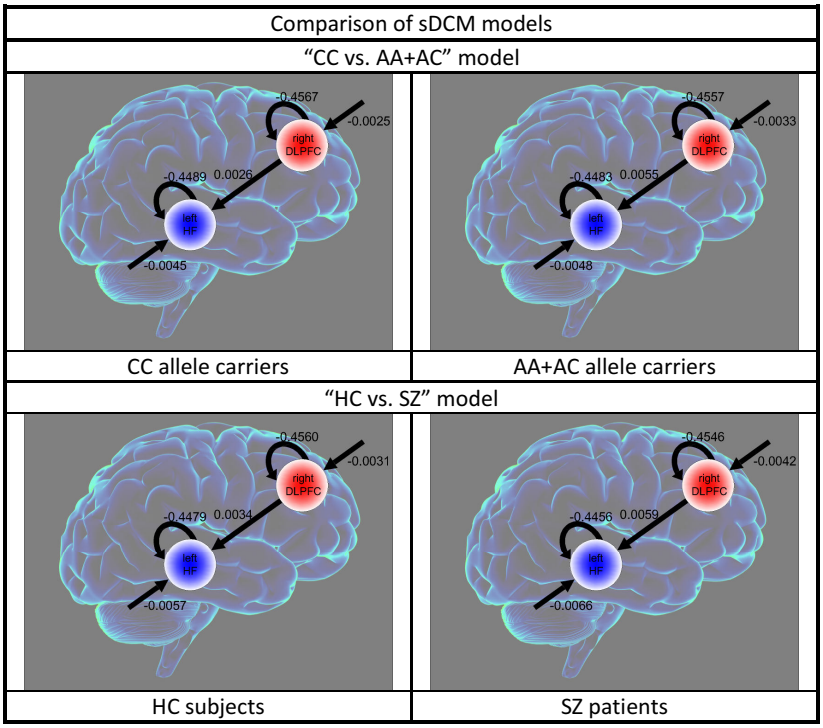

Figure 3.4.1.1. Mean sDCM parameter estimates for the "CC vs. AA+AC" and "HC vs. SZ" models

(b) Comparison of sDCM parameter estimates between "CC vs. AA+AC" and "HC vs. SZ" models

Figure 3.4.1.2 shows a comparison of sDCM parameter estimates of the winning model between "CC vs. AA+AC" and "HC vs. SZ" models. We observe the same phenotype in both models. Self-connection in right DLPFC – parameter a_{11} – increases in AA+AC allele carriers in comparison to CC carriers (p = 0.0326), as do SZ patients in comparison to HC subjects (p = 0.0290). AA+AC allele carriers and SZ patients show lower inhibition (higher excitation) per unit of time in the right DLPFC in comparison to CC allele carriers and HC subjects. Connection from right DLPFC to left HF – parameter a_{21} – increases in AA+AC allele carriers in comparison to CC carriers (n.s., p = 0.2364), as do SZ patients in comparison to HC subjects (n.s., p = 0.5548). AA+AC allele carriers and SZ patients show a greater prefrontal-hippocampal effective connectivity in comparison to CC allele carriers and HC subjects. Self-connection in left HF – parameter a_{22} – increases in AA+AC allele carriers in comparison to CC carriers (n.s., p = 0.4178), as do SZ patients in comparison to HC subjects (p = 0.0159). AA+AC allele carriers and SZ patients show lower inhibition (higher excitation) per unit of time in the left HF in comparison to CC allele carriers and HC subjects. Driven input into right DLPFC – parameter c_1 – decreases in AA+AC allele carriers in comparison to CC carriers (n.s., p = 0.0616), as do SZ patients in comparison to HC subjects (n.s., p = 0.0956). AA+AC allele carriers and SZ patients show increased deactivation per unit of time in the right DLPFC driven by the 2-Back condition in comparison to CC allele carriers and HC subjects. Driven input into left HF – parameter c_2 – decreases in AA+AC allele carriers in comparison to CC carriers (n.s., p = 0.9084), as do SZ patients in comparison to HC subjects (n.s., p = 0.1437). AA+AC allele carriers and SZ patients show increased

deactivation per unit of time in left HF driven by the 2-Back condition in comparison to CC allele carriers and HC subjects.

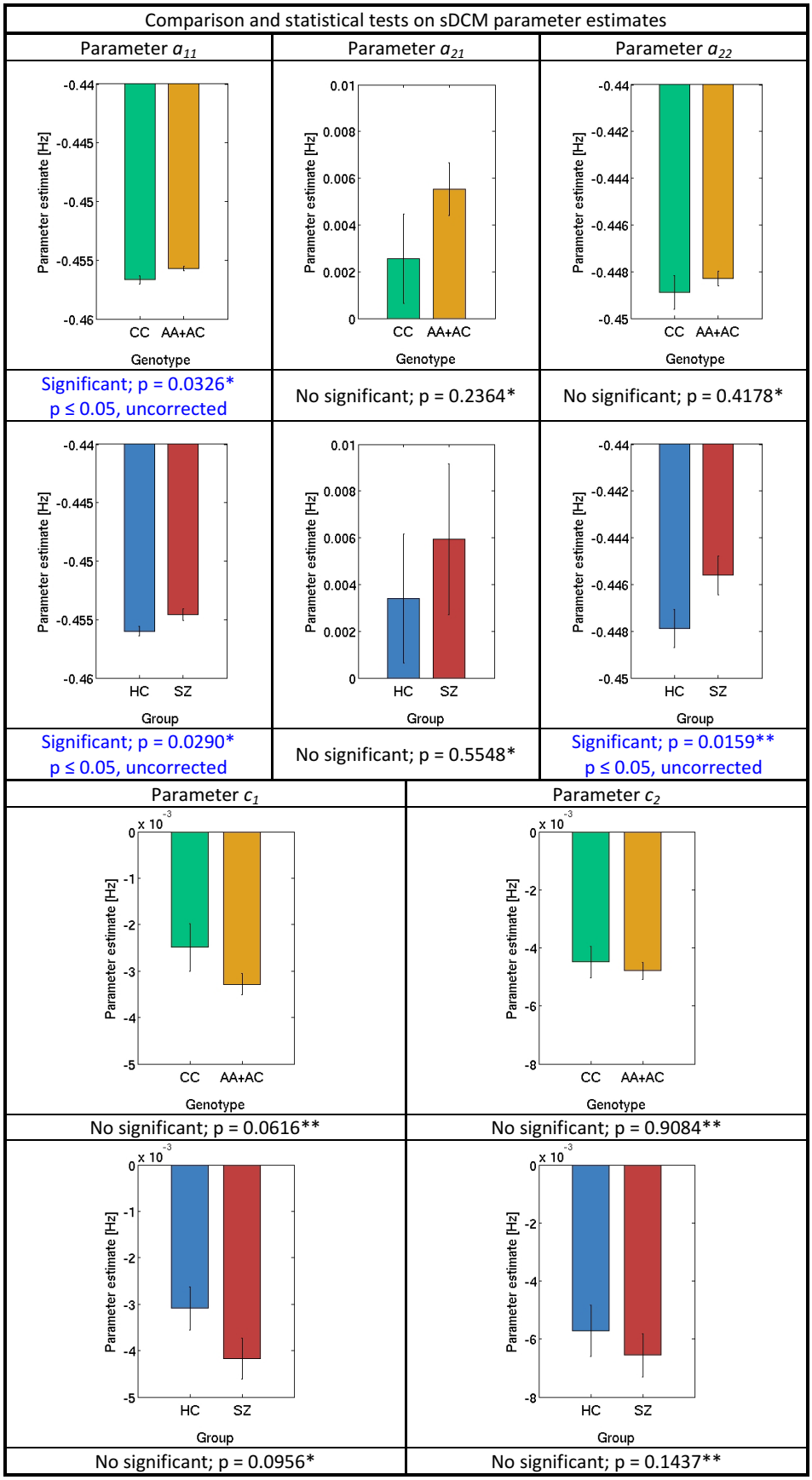

Figure 3.4.1.2. Comparison of sDCM parameter estimates between "CC vs. AA+AC" and "HC vs. SZ" models
*Two sample t-test; **Wilcoxon rank sum test

(c) Comparison of behavior between "CC vs. AA+AC" and "HC vs. SZ" models

Comparison of mean performance in the 2-Back between "CC vs. AA+AC" and "HC vs. SZ" models

Figure 3.4.1.3 shows a comparison of mean performance in the 2-Back between "CC vs. AA+AC" and "HC vs. SZ" models. We observe the same phenotype in both models. We observe that mean performance in the 2-Back decreases in AA+AC allele carriers in comparison to CC carriers (n.s., p = 0.8062), as do SZ patients in comparison to HC subjects (p = 4.3541e-06). AA+AC allele carriers and SZ patients show lower mean performance in the 2-Back in comparison to CC allele carriers and HC subjects.

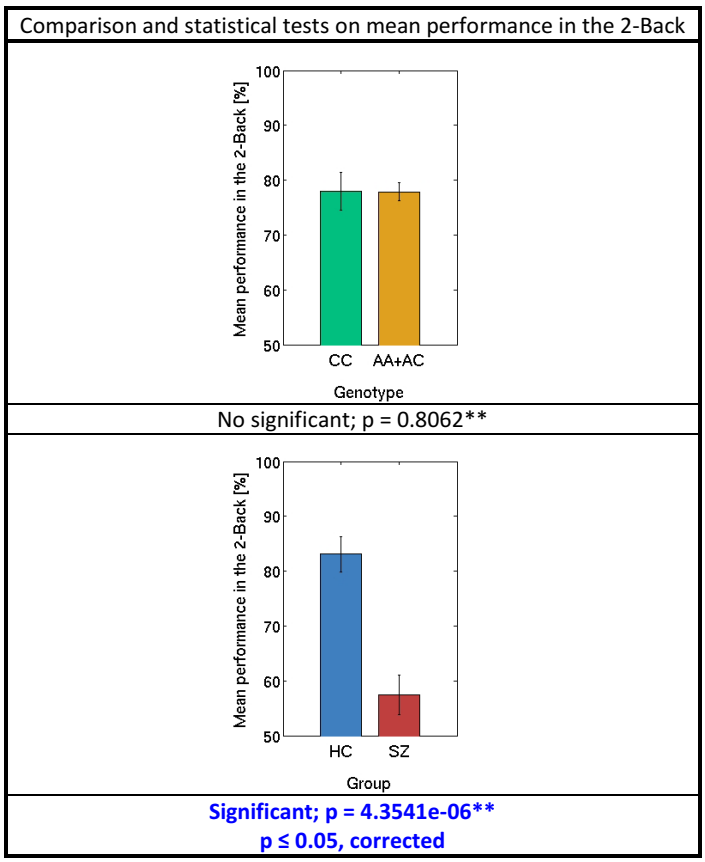

Figure 3.4.1.3. Comparison of mean performance in the 2-Back between "CC vs. AA+AC" and "HC vs. SZ" models
*Two sample t-test; **Wilcoxon rank sum test

Comparison of mean reaction time in the 2-Back between "CC vs. AA+AC" and "HC vs. SZ" models

Figure 3.4.1.4 shows a comparison of mean performance in the 2-Back between "CC vs. AA+AC" and "HC vs. SZ" models. We observe the same phenotype in both models. We observe that mean reaction time in the 2-Back increases in AA+AC allele carriers in comparison to CC carriers (n.s., p = 0.2002), as do SZ patients in comparison to HC subjects (n.s., p = 0.1472). AA+AC allele carriers and SZ patients show higher mean reaction time in the 2-Back in comparison to CC allele carriers and HC subjects.

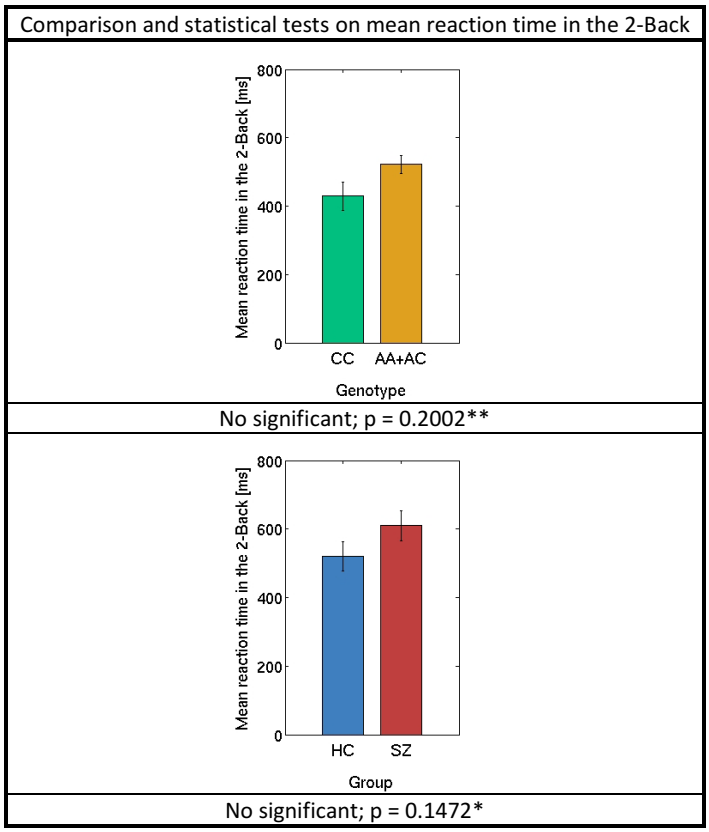

Figure 3.4.1.4. Comparison of mean reaction time in the 2-Back between "CC vs. AA+AC" and "HC vs. SZ" models
*Two sample t-test; **Wilcoxon rank sum test

(d) Comparison of linear regression of behavior on sDCM parameter estimates between "CC vs. AA+AC" and "HC vs. SZ" models

Comparison of linear regression of mean performance in the 2-Back on sDCM parameter estimates between "CC vs. AA+AC" and "HC vs. SZ" models

Figure 3.4.1.5 shows a comparison of the linear regression of mean performance in the 2-Back on sDCM parameter estimates of the winning model between "CC vs. AA+AC" and "HC vs. SZ" models. We observe a comparable linear regression effect of mean performance in the 2-Back within one of the sDCM parameter estimates in both models. Connection from right DLPFC to left HF – parameter a_{21} – seems to predict mean performance in the 2-Back in AA+AC allele carriers (n.s., p = 0.1768), as do in SZ patients (p = 0.0452). The lower the prefrontal-hippocampal effective connectivity, the higher is the mean performance in the 2-Back in both AA+AC allele carriers and SZ patients.

Comparison of linear regression of mean reaction time in the 2-Back on sDCM parameter estimates between "CC vs. AA+AC" and "HC vs. SZ" models

Figure 3.4.1.6 shows a comparison of the linear regression of mean reaction time in the 2-Back on sDCM parameter estimates of the winning model between "CC vs. AA+AC" and "HC vs. SZ" models. We observe a comparable linear regression effect of mean reaction time in the 2-Back within one of the sDCM parameter estimates in both models. Driven input into right DLPFC – parameter c_1 – predicts mean reaction time in the 2-Back in AA+AC allele carriers (p = 0.0440), as seems to do in SZ patients (n.s., p = 0.1360). The higher the driven input into right DLPFC, the lower is the mean reaction time in the 2-Back in AA+AC allele carriers and SZ patients.

Comparison of linear regression of mean performance in the 2-Back on sDCM parameter estimates		
Performance = *f*(Parameter a_{11})	Performance = *f*(Parameter a_{21})	Performance = *f*(Parameter a_{22})
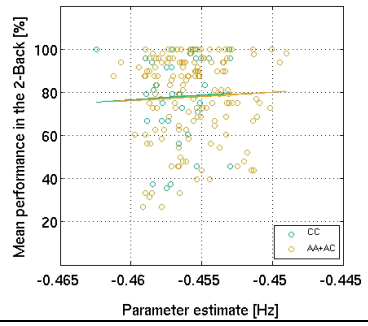	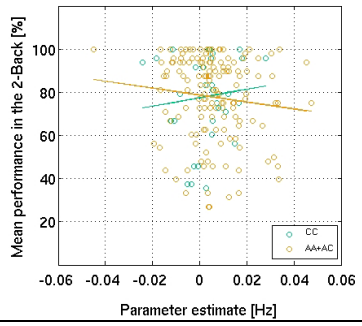	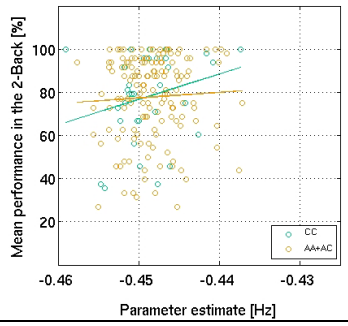
CC: No significant; p = 0.8123 AA+AC: No significant; p = 0.5554	CC: No significant; p = 0.5835 AA+AC: No significant; p = 0.1768	CC: No significant; p = 0.1621 AA+AC: No significant; p = 0.5420
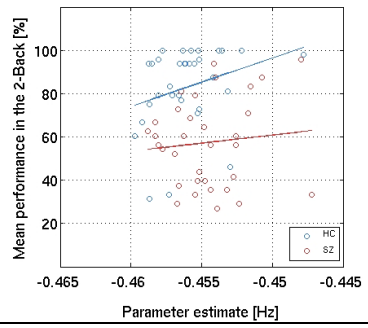	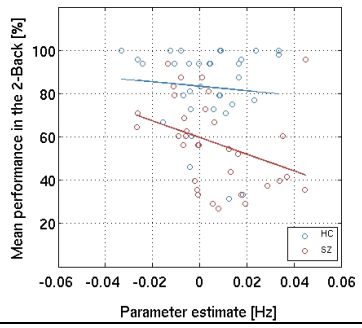	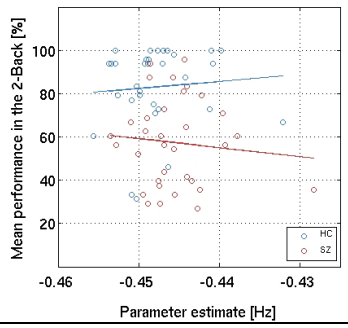
HC: No significant; p = 0.1028 SZ: No significant; p = 0.5709	HC: No significant; p = 0.6270 SZ: Significant; p = 0.0452 p ≤ 0.05, uncorrected	HC: No significant; p = 0.6526 SZ: No significant; p = 0.5849
Performance = *f*(Parameter c_1)	Performance = *f*(Parameter c_2)	
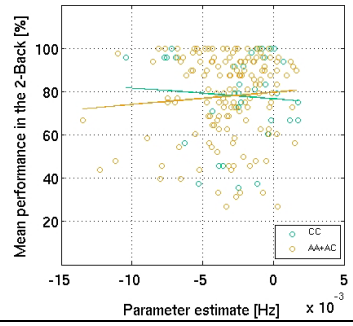	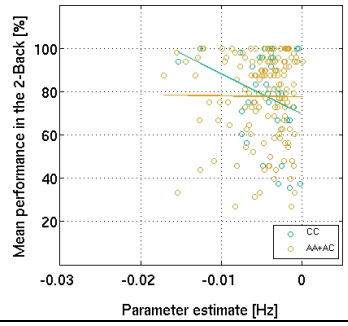	
CC: No significant; p = 0.6826 AA+AC: No significant; p = 0.3370	CC: No significant; p = 0.0923 AA+AC: No significant; p = 0.9226	
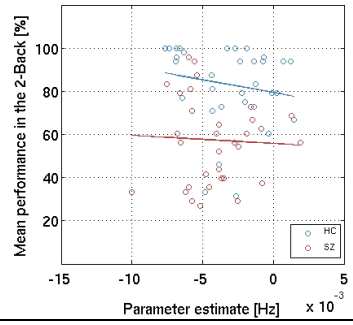	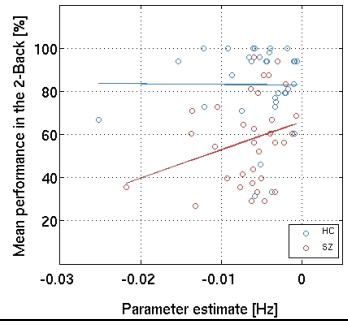	
HC: No significant; p = 0.3481 SZ: No significant; p = 0.7879	HC: No significant; p = 0.9623 SZ: No significant; p = 0.1188	

Figure 3.4.1.5. Comparison of linear regression of mean performance in the 2-Back on sDCM parameter estimates between "CC vs. AA+AC" and "HC vs. SZ" models

<table>
<tr><th colspan="3">Comparison of linear regression of mean reaction time in the 2-Back on sDCM parameter estimates</th></tr>
<tr><th>Reaction time = f(Parameter a_{11})</th><th>Reaction time = f(Parameter a_{21})</th><th>Reaction time = f(Parameter a_{22})</th></tr>
<tr><td> 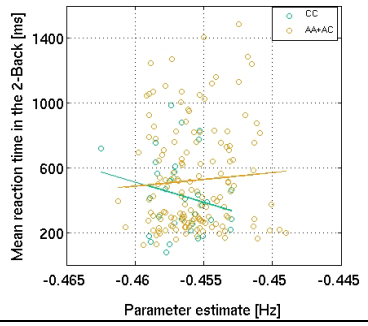
</td><td> 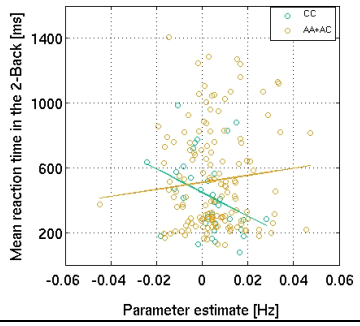
</td><td> 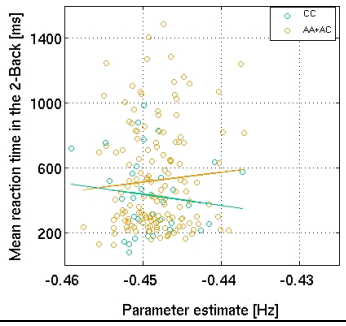
</td></tr>
<tr><td>CC: No significant; p = 0.2322
AA+AC: No significant; p = 0.4484</td><td>CC: Significant; p = 0.0457
p ≤ 0.05, uncorrected
AA+AC: No significant; p = 0.2647</td><td>CC: No significant; p = 0.4889
AA+AC: No significant; p = 0.3941</td></tr>
<tr><td> 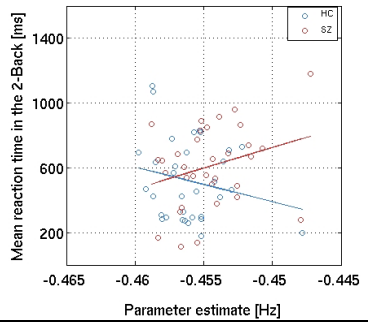
</td><td> 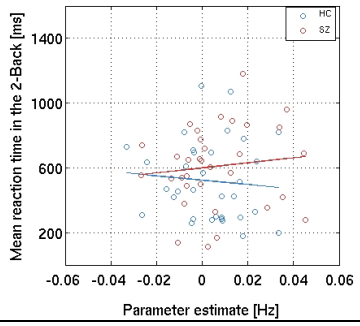
</td><td> 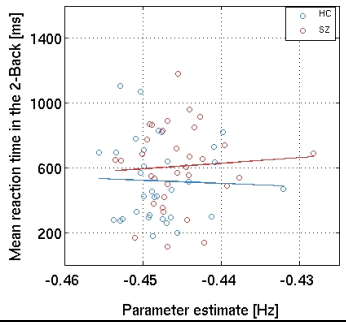
</td></tr>
<tr><td>HC: No significant; p = 0.2363
SZ: No significant; p = 0.1107</td><td>HC: No significant; p = 0.6358
SZ: No significant; p = 0.5155</td><td>HC: No significant; p = 0.8396
SZ: No significant; p = 0.7242</td></tr>
<tr><th colspan="2">Reaction time = f(Parameter c_1)</th><th>Reaction time = f(Parameter c_2)</th></tr>
<tr><td colspan="2"> 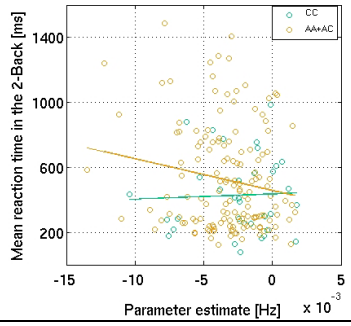
</td><td> 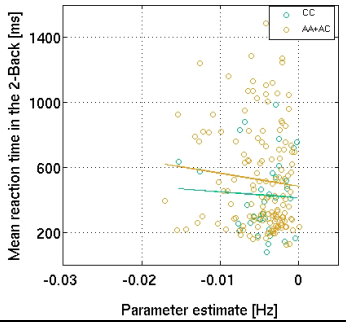
</td></tr>
<tr><td colspan="2">CC: No significant; p = 0.8222
AA+AC: Significant; p = 0.0440
p ≤ 0.05, uncorrected</td><td>CC: No significant; p = 0.7983
AA+AC: No significant; p = 0.2939</td></tr>
<tr><td colspan="2"> 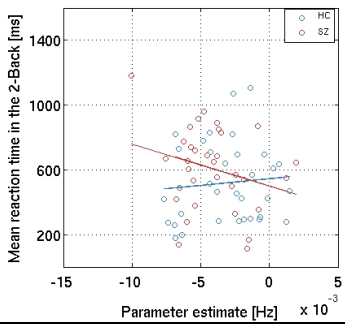
</td><td> 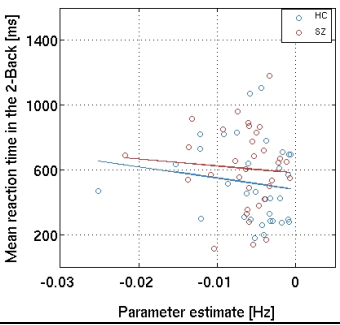
</td></tr>
<tr><td colspan="2">HC: No significant; p = 0.6159
SZ: No significant; p = 0.1360</td><td>HC: No significant; p = 0.4213
SZ: No significant; p = 0.6870</td></tr>
</table>

Figure 3.4.1.6. Comparison of linear regression of mean reaction time in the 2-Back on sDCM parameter estimates between "CC vs. AA+AC" and "HC vs. SZ" models

(e) Comparison of linear regression of mean performance in the 2-Back on mean reaction time in the 2-Back between "CC vs. AA+AC" and "HC vs. SZ" models

Figure 3.4.1.7 shows a comparison of the linear regression of mean performance in the 2-Back on mean reaction time in the 2-Back between "CC vs. AA+AC" and "HC vs. SZ" models. We observe a comparable linear regression effect of mean performance in the 2-Back on mean reaction time in the 2-Back in both models. We observe that mean reaction time in the 2-Back predicts mean performance in the 2-Back in AA+AC allele carriers (p = 4.1417e-14), as do in SZ patients (p = 0.0035). The lower the mean reaction time in the 2-Back, the higher is the mean performance in the 2-Back in AA+AC allele carriers and SZ patients.

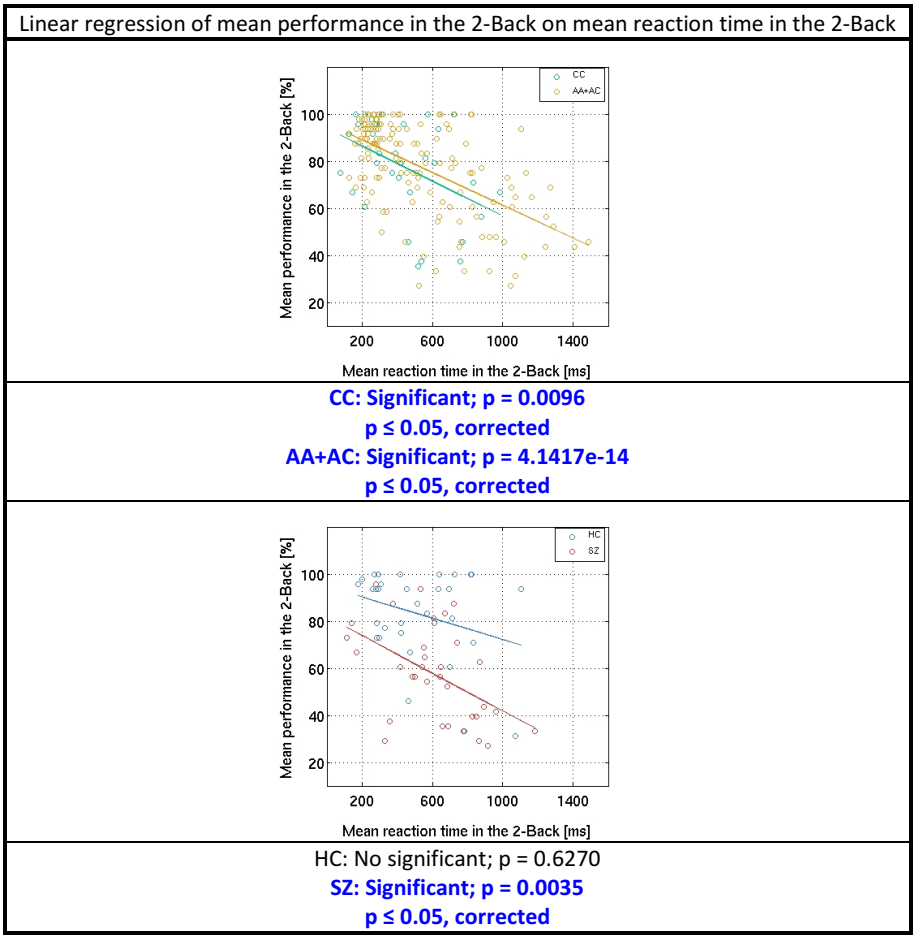

Figure 3.4.1.7. Comparison of linear regression of mean performance in the 2-Back on mean reaction time in the 2-Back between "CC vs. AA+AC" and "HC vs. SZ" models

Chapter 4: Discussion, conclusions and suggestions for future research

"A man can do as he will, but not will as he will."
Arthur Schopenhauer

This chapter discusses the results, reports the conclusions that can be drawn from the results and suggests new approaches for future research.

4.1. Summary

As stated in Section 1.3, we divided the research problem into four stages.

In the first stage, we examined the reproducibility of prefrontal-hippocampal connectivity estimates obtained by stochastic Dynamic Causal Modelling (sDCM). 180 healthy subjects were measured by functional magnetic resonance imaging (fMRI) during a standard working memory N-Back task at three different sites (Mannheim, Bonn, Berlin; each with 60 participants). The reproducibility of regional activations in key regions for working memory (dorsolateral prefrontal cortex, DLPFC; hippocampal formation, HF) was then evaluated using conjunction analyses across locations. For effective connectivity analyses between DLPFC and HF, we used a simple two region sDCM; where the relative plausibility of twenty-two alternative sDCMs for each user was computed using Bayes model selection (BMS). We examined potential differences in the parameter estimates of the winning model by performing statistical tests.

In the second stage, we investigated relations between prefrontal-hippocampal connectivity estimates, a risk genetic variant for schizophrenia: ZNF804A (rs1344706), and behavior in the 180 healthy subjects previously analyzed. We further investigated the modulatory effect of ZNF804A (rs1344706) on the prefrontal-hippocampal network in healthy volunteers. Furthermore, we asked whether specific sDCM parameter estimates contain sufficiently rich discrimination information to enable to predict behavior. Importantly, all genetic models (additive, recessive, co-dominant, and dominant) were explored in order to estimate underlying phenotypic variants.

During the third analysis stage, we applied the same methodology previously described to 33 pair-wise matched healthy volunteers and 33 schizophrenia patients. For each subject, we evaluated the same twenty-two alternative sDCMs and compared their relative plausibility using BMS. We then investigated statistically significant differences on sDCM parameter estimates between healthy control subjects and schizophrenia patients, and relations between the new set of sDCM parameter estimates and behavior. Based on these results, we defined a healthy vs. schizophrenia model.

To conclude in the fourth exploratory analysis stage, we visually compared each of the two-group genetic models (recessive, co-dominant, and dominant) estimated in the second stage to the new healthy vs. schizophrenia model estimated in the third stage. We discussed the similarities and dissimilarities between these models and these comparisons helped to argue the conclusions of this dissertation.

4.2. Discussion

4.2.1. Multi-site reproducibility of prefrontal-hippocampal connectivity estimates by sDCM in healthy volunteers

For deterministic DCM, two studies of reliability exist, showing high reproducibility of parameter estimates (Schuyler et al., 2010) and model selection (Rowe et al., 2010) respectively. While reliability tests do not directly address questions of model validity, reliability is an important prerequisite for validity. For deterministic DCM, several studies have been performed that assessed different aspect of its validity. For example, construct validity of deterministic DCM for fMRI has been demonstrated in relation to SEM (Penny et al., 2004b) or large-scale neuronal models (Lee et al., 2006). Predictive validity has been demonstrated in a multimodal rodent study, showing that regional origins of epilepsy spread can be detected (David et al., 2008), and in studies of stroke patients where DCM applied to data from non-lesioned parts of the brain could predict, with nearly perfect accuracy, the absence or presence of a "hidden" lesion, i.e., out of the field of view (Brodersen et al., 2011). Stochastic DCM for fMRI is a more recent development, and so far, only one validation study exists (Daunizeau et al., 2013).

Remarkably, in our winning model the maximum a posteriori (MAP) estimates of both our inter-regional connection strengths and driving inputs are rather small (Figure 3.1.3.1), while visual inspection of our models shows good fit to data. This implies that the activity in DLPFC and HF can be largely explained by the stochastic innovations (fluctuation terms) that drive activity in DLPFC and HF; and suggests that future refinements of sDCM in SPM should consider the relative precision of priors on stochastic innovations and connectivity parameters.

Nevertheless, the additional (small) explanatory contribution of inter-regional connectivity is very stable across subjects, as demonstrated by our analyses (Figure 3.1.4.1). Furthermore, both removing the influence of task as driving input (models 8-22) or disallowing for the endogenous connection from DLPFC to HF (in models 1-7) clearly deteriorated model goodness, as shown by the results of our BMS analyses. This means that despite their small MAP values, both driving inputs and inter-

regional connections play a sufficiently important role in explaining regional activity (in DLPFC and HF) that the respective models can be clearly distinguished in terms of their model evidence.

Another interesting (and unexpected) aspect of the quantitative results was that the parameters that scale experimental input (2-Back) were negative for both regions - despite the fact that one region activated and the other deactivated. This again speaks to the subtleties of stochastic DCM, in which experimental effects can be modelled by condition-specific fluctuations in hidden neuronal states. In other words, despite the fact that the cognitive set associated with task performance appears to produce an inhibitory afferent drive to both regions, the estimated changes in neuronal activity must more than compensate in the prefrontal region showing an activation (which drives the hippocampal region showing a deactivation). In future work, it may be interesting to test this conjecture using the estimates of hidden neuronal activity in the two regions, as opposed to the observed hemodynamic responses. Our hypothesis here would be that the estimated activity in the prefrontal region would be higher, on average, during working memory and the converse for the hippocampal region.

To conclude, it may be helpful to remember that the lumped neuronal activity modelled by DCM for fMRI does not correspond to evoked responses in electrophysiology; rather, it probably reflects very slow fluctuations in the power of high frequency dynamics - that have much slower rate constants than the underlying neuronal activity itself.

4.2.2. Investigation of relations between sDCM parameter estimates, ZNF804A (rs1344706), and behavior in healthy volunteers

In this section, we will frame the second analysis results in terms of effective connectivity and functional (E-I) balance highlighting the crucial role that plays in our research the disconnection hypothesis and dysfunctional (E-I) balance. These two concepts were introduced in Chapter 1 and will serve as a guide to discuss our research findings and compare them to the discoveries published by other colleagues.

As described in Chapter 1, recently neuroimaging studies started to link ZNF804A (rs1344706) to the prefrontal-hippocampal network. Furthermore, some molecular biology studies, investigated the influence of ZNF804A (rs1344706) on DLPFC and HF. Please see Chapter 1 for further details; Table 4.2.2.1 summarizes these research findings.

Neuroimaging studies on ZNF804A (rs1344706)	→	↑ Risk allele "A"	→	DLPFC-HF network	→	↑ Functional connectivity between DLPFC-HF		
Molecular biology studies on ZNF804A (rs1344706)	→	↑ Risk allele "A"	→	DLPFC	→	↑ ZNF804A	→	↑ COMT
Molecular biology studies on ZNF804A (rs1344706)	→	↑ Risk allele "A"	→	HF	→	It seems ZNF804A (rs1344706) does not play any role within the HF		

Table 4.2.2.1. Recent discoveries of ZNF804A (rs1344706) within the DLPFC-HF network

Here, we performed statistical tests on sDCM parameter estimates of the winning model and behavior to examine potential differences across different genetic models.

We observed a statistical difference on the connection from right DLPFC to left HF within the recessive model (see Figure 3.2.2.2). AA allele carriers show greater prefrontal-hippocampal effective connectivity or higher functional (E-I) balance (lower inhibition) in comparison to AC+CC allele carriers. This result is fully consistent with (Rasetti et al., 2011). In this study, the researchers revealed that subjects homozygous for the risk-associated allele (AA allele carriers) showed a disruption in task-related modulation of right DLPFC-left HC coupling in the PPI analysis. Moreover, is partially consistent with (Esslinger et al., 2009; Paulus et al., 2013). In these studies, the researchers revealed a gene-dose effect of the genotype on the prefrontal-hippocampal connectivity in seeded connectivity analysis. The functional connectivity between the right DLPFC and the left HF statistically increased with the number of rs1344706 risk alleles.

In addition, we also observed a statistical difference on the self-connection in the right DLPFC within the dominant model (see Figure 3.2.2.4). AA+AC allele carriers show higher functional (E-I) balance (lower inhibition) per unit of time in right DLPFC in comparison to CC allele carriers. We do not have any reference to compare our results with; nonetheless some molecular biology studies already reported a pretty similar research finding showing that ZNF804A (rs1344706) seems to play a very crucial role within the DLPFC (see Chapter 1; i.e. Girgenti et al., 2012).

Following on these results, we further investigate the biological implications of ZNF804A (rs1344706) on the DLPFC-HF network by reviewing some other molecular biology studies. Table 4.2.2.2 summarizes the research findings reported by other studies in relation to increased COMT within the DLPFC:

Molecular biology studies on ZNF804A (rs1344706)	→	↑ Risk allele "A"	→	DLPFC	→	↑ ZNF804A	→	↑ COMT	→	…
Other molecular biology studies	→	↓ DA	→ Via D1	↓ NMDAR-mediated currents on GABA interneurons	→	↓ Overall network inhibition	→	↑ Excitation primary corticolimbic networks		

Table 4.2.2.2. Summary of implications of increased COMT within the DLPFC

In view of these research findings, considering the winning model with a directed connection from DLPFC to HF (see above), we hypothesize the next functional pathway of ZNF804A (rs1344706) on the prefrontal-hippocampal network.

The rs1344706 risk allele has been associated with increased expression in the DLPFC (Riley et al., 2010). ZNF804A regulates transcription levels of four SZ associated genes: PRSS16 and COMT by increasing transcript levels; and PDE4B and DRD2 by decreasing transcript levels (Girgenti et al., 2012). For instance, increased transcript levels of COMT lead to higher degradation of dopamine in the synaptic cleft in the PFC (Karoum et al., 1994; Matsumoto et al., 2003). Dopamine, in particular D1 receptors, in the PFC is profoundly implicated in the control of cognition, e.g. working memory (Goldman-Rakic et al., 2004). Reduced dopamine via D1 reduces NMDA receptor-activated synaptic currents (Tseng and O'Donnell, 2004). A consequence of NMDA-hypofunction is an extensive release of glutamate in cortical regions, i.e. DLPFC (Adams and Moghaddam, 1998; Moghaddam et al., 1997). One assumption of the NMDA-hypofunction model is that this increased release of excitatory neurotransmitter leads to an overstimulation of downstream excitatory neurons, as well as to a further disinhibition through a lack of NMDA receptor excitation on interneurons and a consequent loss in overall network inhibition (Homayoun and Moghaddam, 2007). According to this model, this complex disinhibitory phenomenon results in hyperstimulation of primary corticolimbic networks, i.e. DLPFC-HF network. This excessive release of glutamate in the DLPFC and in primary corticolimbic networks may lead to a net excitatory activity that can be observed by fMRI (Figure 2.1.3.1; Logothetis, 2008; Logothetis and Wandell, 2004). This cascade of phenomena might be a plausible explanation for observing, in a first step, a higher functional (E-I) balance (lower inhibition) per unit of time in the right DLPFC in AA+AC allele carriers in comparison to CC allele carriers, and in a second step, a higher prefrontal-hippocampal effective connectivity or higher functional (E-I) balance (lower inhibition) per unit of time in AA allele carriers in comparison to AC+CC allele carriers.

In the same vein, the rs1344706 risk allele has not been associated with increased expression in the HF and that might be a plausible explanation for not observing this phenomenon in the HF.

Table 4.2.2.3 illustrates the research findings reported by other studies in comparison to our second analysis results.

<table>
<tr><td>Neuroimaging studies on ZNF804A (rs1344706)</td><td>→</td><td>↑ Risk allele “A”</td><td>→</td><td>DLPFC-HF network</td><td>→</td><td colspan="3">↑ Functional connectivity between DLPFC-HF</td></tr>
<tr><td rowspan="2">Our second analysis</td><td rowspan="2">→</td><td rowspan="2">↑ Risk allele “A”</td><td rowspan="2">→</td><td rowspan="2">DLPFC-HF network</td><td rowspan="2">→</td><td colspan="3">↑ Effective connectivity between DLPFC-HF</td></tr>
<tr><td colspan="3"> 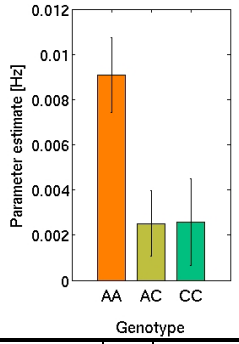
</td></tr>
<tr><td>Molecular biology studies on ZNF804A (rs1344706)</td><td>→</td><td>↑ Risk allele “A”</td><td>→</td><td>DLPFC</td><td>→</td><td>↓ Overall network inhibition</td><td>→</td><td>↑ Excitation primary corticolimbic networks</td></tr>
<tr><td rowspan="2">Our second analysis</td><td rowspan="2">→</td><td rowspan="2">↑ Risk allele “A”</td><td rowspan="2">→</td><td rowspan="2">DLPFC</td><td rowspan="2">→</td><td>↑ Functional (E-I) balance per unit of time in the DLPFC</td><td rowspan="2">→</td><td>↑ Functional (E-I) balance per unit of time between DLPFC-HF</td></tr>
<tr><td> 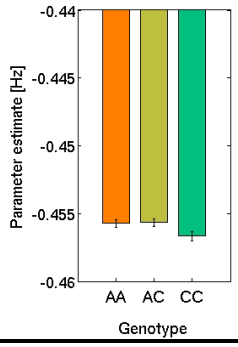
</td><td> 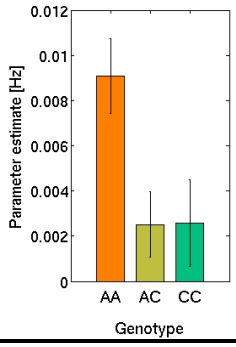
</td></tr>
<tr><td>Molecular biology studies on ZNF804A (rs1344706)</td><td>→</td><td>↑ Risk allele “A”</td><td>→</td><td>HF</td><td>→</td><td colspan="3">It seems ZNF804A (rs1344706) does not play any role within the HF</td></tr>
<tr><td rowspan="2">Our second analysis</td><td rowspan="2">→</td><td rowspan="2">↑ Risk allele “A”</td><td rowspan="2">→</td><td rowspan="2">HF</td><td rowspan="2">→</td><td colspan="3">↑ Functional (E-I) balance per unit of time in the HF (n.s.)</td></tr>
<tr><td colspan="3"> 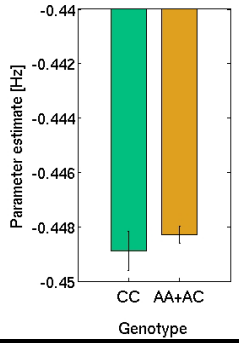
</td></tr>
</table>

Table 4.2.2.3. Comparison of recent discoveries of ZNF804A (rs1344706) within the DLPFC-HF network and our second analysis results

Regarding the statistical tests on behavior, we did not observe any statistical difference across different genetic models within the mean performance nor within the mean reaction time in the 2-

Back. Nonetheless, we do observed a slight tendency within the mean reaction time in the 2-Back in the dominant model (see Figure 3.2.3.2). AA+AC allele carriers show higher mean reaction time in the 2-Back in comparison to CC allele carriers. These results are fully in line with previous studies (Esslinger et al., 2009; Paulus et al., 2013; Rasetti et al., 2011). In these works, the influence of the genotype on mean performance or mean reaction time in the 2-Back was not found.

We also investigated relations between sDCM parameter estimates and behavior by means of linear regression.

First, we performed linear regression of mean performance in the 2-Back on sDCM parameter estimates of the winning model. We observed that self-connection in the left HF predicts mean performance in the 2-Back in AC+CC allele carriers (Figure 3.2.4.2). The higher the functional (E-I) balance (lower inhibition) per unit of time in the left HF, the higher is the mean performance in the 2-Back in AC+CC allele carriers.

Second, we computed linear regression of mean reaction time in the 2-Back on sDCM parameter estimates of the winning model. Firstly, we observed that self-connection in the right DLPFC predicts mean reaction time in the 2-Back in AA allele carriers (see Figure 3.2.4.5). The lower the functional (E-I) balance (higher inhibition) per unit of time in the right DLPFC, the lower is the mean reaction time in the 2-Back in AA allele carriers. Secondly, connection from right DLPFC to left HF predicts mean reaction time in the 2-Back in CC allele carriers (see Figure 3.2.4.5). The greater the prefrontal-hippocampal effective connectivity or higher the functional (E-I) balance (lower inhibition); the lower is the mean reaction time in the 2-Back in CC allele carriers. Finally, we observed that the driven input into the right DLPFC predicts mean reaction time in the 2-Back in AA allele carriers (see Figure 3.2.4.5). The higher the driven input into the right DLPFC, the lower is the mean reaction time in the 2-Back in AA allele carriers.

To conclude, we performed linear regression of mean performance in the 2-Back on mean reaction time in the 2-Back. We observed that mean reaction time in the 2-Back predicts mean performance in the 2-Back in all genotype groups (see Figure 3.2.5.1). The lower the mean reaction time in the 2-Back, the higher is the mean performance in the 2-Back in all subjects independently on the genotype.

Despite all these discoveries, we do not have any reference to compare our regression analyses results with. Nonetheless, all these observations will be very important for the conclusions of this dissertation as will be discussed in short.

4.2.3. Investigation of relations between sDCM parameter estimates and behavior in pair-wise matched healthy volunteers and schizophrenia patients

In this section, we will also frame the third analysis results in terms of effective connectivity and functional (E-I) balance emphasizing the fundamental role that plays the disconnection hypothesis and dysfunctional (E-I) balance in our dissertation.

As described in Chapter 1, the prefrontal-hippocampal network has been extensively analysed in neuroimaging studies of schizophrenia. Furthermore, recent reports reviewed strong evidence of altered functional (E-I) balance within brain regions associated with the disease, i.e. DLPFC and HF. (please see Chapter 1 for further details). Table 4.2.3.1 shows a simplified schema of the recent findings in the topic.

Neuroimaging studies of schizophrenia	→	DLPFC-HF network	→	↑ Functional connectivity between DLPFC-HF						
Molecular biology studies of schizophrenia	→	DLPFC	→	NMDAR hypofunction model	→	↓ NMDAR-mediated currents on GABA interneurons	→	↓ Overall network inhibition	→	↑ Excitation primary corticolimbic networks
Molecular biology studies of schizophrenia	→	HF	→	NMDAR hypofunction model	→	↓ NMDAR-mediated currents on GABA interneurons	→	↓ Overall network inhibition		

Table 4.2.3.1. Recent discoveries of schizophrenia within the DLPFC-HF network

Using BMS, we revealed the same connectivity pattern or winning model between DLPFC and HF during WM in controls and patients. Furthermore, we performed statistical tests on sDCM parameter estimates of the winning model and behavior to examine potential differences between healthy control subjects and schizophrenia patients. Two main results were obtained:

First, we observed a statistical difference in the self-connection in the right DLPFC (see Figure 3.3.4.1). Schizophrenia patients have higher functional (E-I) balance (lower inhibition) per unit of time in the right DLPFC in comparison to healthy control subjects. This result is fully consistent with the literature review published by (Kehrer et al., 2008). In this study, the researchers reviewed strong evidence for altered functional (E-I) balance in the NMDA-hypofunction model of schizophrenia within brain regions associated with the disease (PFC and HF among others). Furthermore, this research finding is also consistent with (Yizhar et al., 2011). In this study, the authors provided support for the elevated cellular (E-I) balance hypothesis within neocortical regions of severe neuropsychiatric disease-related symptoms.

Second, we reported a statistical difference in the self-connection in the left HF (see Figure 3.3.4.1). Schizophrenia patients have higher functional (E-I) balance (lower inhibition) per unit of time in left HF in comparison to healthy control subjects. Once again, this result is fully consistent with the NMDA-hypofunction model of schizophrenia depicted by (Kehrer et al., 2008).

Remarkably, we did not observe any tendency on the causal connection from right DLPFC to left HF between groups (see Figure 3.3.4.1). This result is not consistent with (Meyer-Lindenberg et al., 2005). Nonetheless, in this work, the authors show a statistical difference on the "functional connectivity" between right DLPFC and left HF when comparing healthy control subjects and schizophrenia patients. Nonetheless, we must stress that functional connectivity between two variables, e.g. brain regions, does not necessarily imply that one causes the other (Aldrich, 1995). Furthermore, in our study, we disentangle one parameter – the original functional connectivity estimate – into five parameters, the five sDCM parameter estimates of the winning model. Thus, these facts might be plausible reasons that explain the observed effects on both self-connection parameter estimates, but not on the connection from right DLPFC to left HF as described earlier by (Meyer-Lindenberg et al., 2005).

In view of these research findings, considering the winning model with a directed connection from DLPFC to HF (see above), we hypothesize the next underlying neurobiology of the prefrontal-hippocampal network in schizophrenia:

On the one hand, the NMDA-hypofunction model of schizophrenia within the DLPFC leads to an extensive release of glutamate (Adams and Moghaddam, 1998; Moghaddam et al., 1997). As stated above, this increased release of excitatory neurotransmitter leads to an overstimulation of downstream excitatory neurons, as well as to a further disinhibition through a lack of NMDA receptor excitation on interneurons and a consequent loss in overall network inhibition (Homayoun and Moghaddam, 2007). This complex disinhibitory syndrome seems to lead to hyperstimulation in primary corticolimbic networks, i.e. DLPFC-HF network. On the other hand, the NMDA-hypofunction model of schizophrenia within the HF might also lead to a loss in overall network inhibition. This cascade of phenomena might be a plausible explanation for observing, in a first step, higher functional (E-I) balance (lower inhibition) per unit of time in the right DLPFC in patients in comparison to controls, in a second step, a higher prefrontal-hippocampal effective connectivity or higher functional (E-I) balance (lower inhibition) per unit of time in patients in comparison to controls, and in a last stage, a higher functional (E-I) balance (lower inhibition) per unit of time in the right DLPFC in patients in comparison to controls.

Table 4.2.3.2 illustrates the research findings reported by other studies in comparison to our third analysis results.

<table>
<tr><td>Neuroimaging studies of schizophrenia</td><td>→</td><td>DLPFC-HF network</td><td>→</td><td colspan="3">↑ Functional connectivity between DLPFC-HF</td></tr>
<tr><td rowspan="2">Our third analysis</td><td rowspan="2">→</td><td rowspan="2">DLPFC-HF network</td><td rowspan="2">→</td><td colspan="3">↑ Effective connectivity between DLPFC-HF (n.s.)</td></tr>
<tr><td colspan="3"> 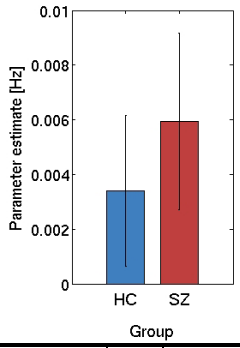
</td></tr>
<tr><td>Molecular biology studies of schizophrenia</td><td>→</td><td>DLPFC</td><td>→</td><td>↓ Overall network inhibition</td><td>→</td><td>↑ Excitation primary corticolimbic networks</td></tr>
<tr><td rowspan="2">Our third analysis</td><td rowspan="2">→</td><td rowspan="2">DLPFC</td><td rowspan="2">→</td><td>↑ Functional (E-I) balance per unit of time in the DLPFC</td><td rowspan="2">→</td><td>↑ Functional (E-I) balance per unit of time between DLPFC-HF (n.s.)</td></tr>
<tr><td> 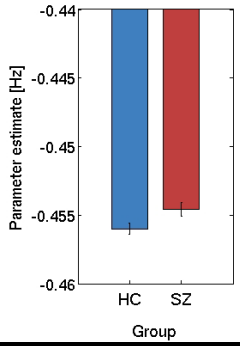
</td><td> 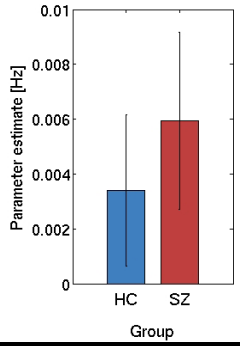
</td></tr>
<tr><td>Molecular biology studies of schizophrenia</td><td>→</td><td>HF</td><td>→</td><td colspan="3">↓ Overall network inhibition</td></tr>
<tr><td rowspan="2">Our third analysis</td><td rowspan="2">→</td><td rowspan="2">HF</td><td rowspan="2">→</td><td colspan="3">↑ Functional (E-I) balance per unit of time in the HF</td></tr>
<tr><td colspan="3"> 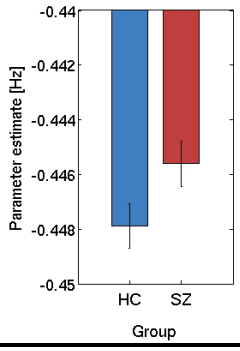
</td></tr>
</table>

Table 4.2.3.2. Comparison of recent discoveries of schizophrenia within the DLPFC-HF network and our third analysis results

Concerning the statistical tests on behavior, we observed a statistical difference in the mean performance in the 2-Back between groups (see Figure 3.3.5.1). Schizophrenia patients show lower

mean performance in the 2-Back in comparison to healthy control subjects. Furthermore, we observed a slight tendency in the mean reaction time in the 2-Back (see Figure 3.3.5.2). Schizophrenia patients show higher mean reaction time in the 2-Back in comparison to healthy control subjects. These results are fully consistent with (Goldman-Rakic, 1994; He et al., 2012; Manoach et al., 1999; Park and Holzman, 1992). In these studies, the authors reported longer mean reaction time and lower mean performance in patients in comparison to controls during working memory tasks.

In this section, we also investigated relations between sDCM parameter estimates and behavior by means of linear regression.

In a first step, we performed linear regression of mean performance in the 2-Back on sDCM parameter estimates of the winning model. The analysis revealed that connection from right DLPFC to left HF predicts mean performance in the 2-Back in schizophrenia patients (see Figure 3.3.6.1). The lower the prefrontal-hippocampal effective connectivity or the lower the functional (E-I) balance (higher inhibition), the higher is the mean performance in the 2-Back in schizophrenia patients.

In a second step, we computed linear regression of mean reaction time in the 2-Back on sDCM parameter estimates of the winning model. We observed a slight tendency in the self-connection in the right DLPFC in schizophrenia patients (see Figure 3.3.6.2). The lower the functional (E-I) balance (higher inhibition) per unit of time in the right DLPFC, the lower is the mean reaction time in the 2-Back in schizophrenia patients.

To conclude, in the last analysis step, we performed linear regression of mean performance in the 2-Back on mean reaction time in the 2-Back. The results revealed that mean reaction time in the 2-Back predicts mean performance in the 2-Back in schizophrenia patients (see Figure 3.3.7.1). The lower the reaction time in the 2-Back, the higher is the mean performance in the 2-Back in schizophrenia patients.

Despite all these research findings, we do not have any reference to compare our regression analyses results with. However, all these observations will be relevant for the conclusions of this dissertation as will be discussed in short.

4.2.4. Comparison of two-group genetic models and healthy vs. schizophrenia model

In this section, we will compare each the two-group genetic models (recessive, co-dominant, and dominant) to the healthy vs. schizophrenia model in relation to the underlying neurobiology and

behavior. We visually observed a high degree of similarity between the dominant and the healthy vs. schizophrenia models. As discussed in previous sections, we will frame these comparisons in terms of effective connectivity and functional (E-I) balance.

Comparisons of sDCM parameter estimates between the dominant and the healthy vs. schizophrenia models revealed some interesting similarities. On the one hand, we observed that self-connection in the right DLPFC increases in AA+AC allele carriers in comparison to CC, as do schizophrenia patients in comparison to healthy control subjects (see Figure 3.4.1.2). AA+AC allele carriers and patients have higher functional (E-I) balance (lower inhibition) per unit of time in the right DLPFC in comparison to CC allele carriers and controls. This difference is statistically significant in both models. On the other hand, we observed that self-connection in left HF increases in AA+AC allele carriers in comparison to CC carriers, as do schizophrenia patients in comparison to healthy control subjects (see Figure 3.4.1.2). AA+AC allele carriers and patients show higher functional (E-I) balance (lower inhibition) per unit of time in the left HF in comparison to CC allele carriers and controls. Nonetheless, this difference is only statistically significant in the healthy vs. schizophrenia model.

The comparison of mean performance in the 2-Back between the dominant and the healthy vs. schizophrenia models was performed next. We observed that mean performance in the 2-back decreases in AA+AC allele carriers in comparison to CC carriers, as do schizophrenia patients in comparison to healthy control subjects (see Figure 3.4.1.3). AA+AC allele carriers and patients show lower mean performance in the 2-Back in comparison to CC allele carriers and controls. Nonetheless, this difference is only statistically significant in the healthy vs. schizophrenia model. Concerning the comparison of mean reaction time in the 2-Back between both models, we observed that mean reaction time in the 2-back increases in AA+AC allele carriers in comparison to CC carriers, as do schizophrenia patients in comparison to healthy control subjects (see Figure 3.4.1.4). AA+AC allele carriers and patients show higher mean reaction time in the 2-Back in comparison to CC allele carriers and controls. This difference is not statistically significant in either model, but shows a tendency in both of them.

We also observed a similarity when comparing linear regression analysis of mean performance in the 2-Back on sDCM parameter estimates between the dominant and the healthy vs. schizophrenia model. Connection from right DLPFC to left HF seems to predict mean performance in the 2-Back in AA+AC allele carriers, as do in schizophrenia patients (see Figure 3.4.1.5). The lower the prefrontal-hippocampal effective connectivity or the lower the functional (E-I) balance (higher excitation) per

unit of time, the higher is the mean performance in the 2-Back in both AA+AC allele carriers and patients. Nonetheless, this statistical effect is only significant in the healthy vs. schizophrenia model.

Concerning the comparison of linear regression analysis of mean reaction time in the 2-Back on sDCM parameter estimates between both models, we observed that the driven input into the right DLPFC predicts mean reaction time in the 2-Back in AA+AC allele carriers, as seems to do in schizophrenia patients (see Figure 3.4.1.6). The higher the driven input into the right DLPFC, the lower is the mean reaction time in the 2-Back in AA+AC allele carriers and patients. Nonetheless, this statistical effect is only significant in the dominant model.

To conclude this section, when comparing linear regression analysis of mean performance in the 2-Back on mean reaction time in the 2-Back, we found that mean reaction time in the 2-Back predicts mean performance in the 2-Back in AA+AC allele carriers and schizophrenia patients (see Figure 3.4.1.7). The lower the mean reaction time in the 2-Back, the higher is the mean performance in the 2-Back in AA+AC allele carriers and patients. This statistical effect is significant in the dominant and the healthy vs. schizophrenia models.

4.3. Conclusions

4.3.1. Multi-site reproducibility of prefrontal-hippocampal connectivity estimates by sDCM in healthy volunteers

This initial analysis demonstrated a consistent pattern of activation in the right DLPFC and deactivation in the left HF across the three locations. Moreover, BMS revealed the same connectivity pattern or winning model between DLPFC and HF during WM in Mannheim, Bonn, and Berlin, and statistical tests on sDCM parameter estimates of the winning model did not reveal any statistical difference across sites.

While certainly not an exhaustive test of the robustness of sDCM, this initial reproducibility analysis speaks favourably to the reliability of sDCM as a method for assessing effective connectivity from fMRI data. This analysis of sDCM provided a basis for next stages. After demonstrating that sDCM provides reliable estimates of prefrontal-hippocampal interactions, we used this modelling approach to identify connectivity alterations in genetic risk carriers and schizophrenia patients.

4.3.2. Investigation of relations between sDCM parameter estimates, ZNF804A (rs1344706), and behavior in healthy volunteers

This second analysis provided strong support for the genetic influence of ZNF804A (rs1344706) on the prefrontal-hippocampal network and revealed some relations between sDCM parameter estimates, ZNF804A (rs1344706), and behavior.

Statistical tests on sDCM parameter estimates of the winning model revealed a statistical difference on the connection from right DLPFC to left HF within the recessive model: increased effective connectivity and functional (E-I) balance in risk homozygotes; and a statistical difference on the self-connection in right DLPFC within the dominant model: increased functional (E-I) balance in risk allele carriers. In summary, we observed that AA allele carriers have a higher functional (E-I) balance (lower inhibition) within the prefrontal-hippocampal network in comparison to AC allele carriers and these, in turn, have a higher functional (E-I) balance (lower inhibition) within the network in comparison to CC allele carriers.

Statistical tests on behavior did not reveal any statistical difference across genetic models within the mean performance in the 2-Back nor within the mean reaction time in the 2-Back. Nonetheless, these analyses revealed a non-statistical effect but tendency in the mean reaction time in the 2-Back within the dominant model: higher reaction time in the 2-Back in risk allele carriers. Table 4.3.2.1 summarizes the research findings of this second analysis.

<table>
<tr><td rowspan="2">↑ Risk allele “A”</td><td rowspan="2">→</td><td rowspan="2">DLPFC-HF network</td><td rowspan="2">→</td><td></td><td></td><td>↑ Effective connectivity between DLPFC-HF</td><td></td><td></td></tr>
<tr><td>↑ Functional (E-I) balance in the DLPFC</td><td>→</td><td>↑ Functional (E-I) balance between DLPFC-HF</td><td>→</td><td>↑ Functional (E-I) balance in the HF (n.s.)</td></tr>
<tr><td></td><td></td><td>Behavior in the 2-Back</td><td>→</td><td colspan="5">= Mean performance in the 2-Back (n.s.)
&
↑ Mean reaction time in the 2-Back (n.s. but tendency)</td></tr>
</table>

Table 4.3.2.1. Summary results of the second analysis

In view of these research findings, we hypothesize a mechanistic causal model between self-connection in the right DLPFC and mean reaction time in the 2-Back within the dominant model. Figure 4.3.2.1 illustrates this mechanistic account. According to this model, higher functional (E-I) balance (lower inhibition) on self-connection in the right DLPFC (premise **P**) seems to lead to a higher mean reaction time in the 2-Back (premise **S**). Thus, this causal relationship can be translated into the next mathematical logic expression: **P → S**.

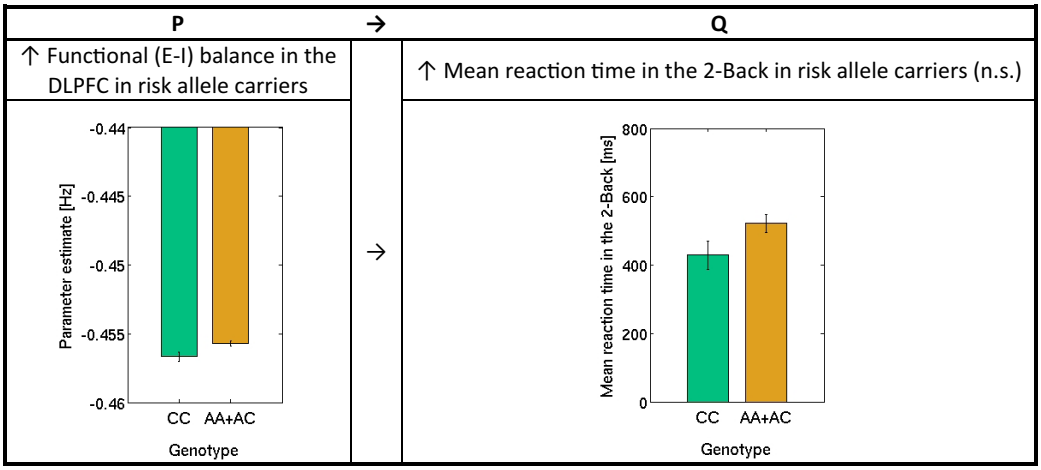

Figure 4.3.2.1. Graphical representation of the proposed causal relationship: **P → S**

Regression analyses revealed statistical effects across different genetic models. First of all, these analyses showed that self-connection in right DLPFC seems to contain sufficiently rich information for predicting mean reaction time in the 2-Back in AA allele carriers. Secondly, we observed that connection from right DLPFC to left HF seems to contain sufficiently rich information for predicting mean reaction time in the 2-Back in CC allele carriers. In a third step, these analyses showed that self-connection in left HF seems to contain sufficiently rich information for predicting mean performance in the 2-Back in AC+CC allele carriers. To conclude, we observed that mean reaction time in the 2-Back seems to contain sufficiently rich information for predicting mean performance in the 2-Back in all subjects independently on the genotype.

In view of these results, we assume that the prefrontal-hippocampal network is modulated by the genotype and each genotype individual requires of a small perturbation on the mean genotype parameter estimates in order to achieve the optimal behavior. Figure 4.3.2.2 illustrates this mechanistic account. Therefore, this perturbation depends on the genotype of each individual. AA allele carriers, who as depicted in Figure 4.3.2.2, have the highest functional (E-I) balance (lowest inhibition) within the prefrontal-hippocampal network (left side of Figure 4.3.2.2), require the lowest functional (E-I) balance on the prefrontal-hippocampal network in order to achieve the optimal behavior (right side of Figure 4.3.2.2). AC allele carriers, who as depicted below, have an intermediate functional (E-I) balance (intermediate inhibition) within the prefrontal-hippocampal network, require lower functional (E-I) balance on the prefrontal-hippocampal network in order to achieve the optimal behavior. CC allele carriers, who as described below, have the lowest functional (E-I) balance (highest inhibition) within the prefrontal-hippocampal network, require the highest functional (E-I) balance on the prefrontal-hippocampal network in order to achieve the optimal behavior.

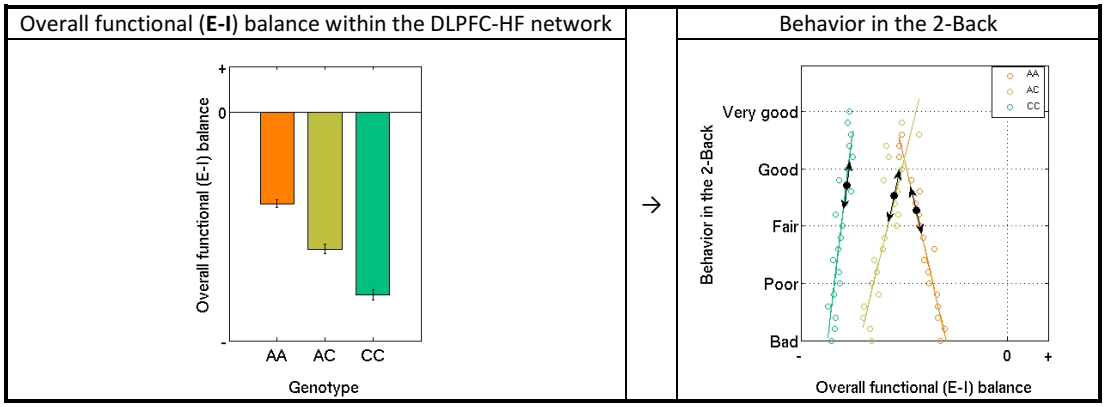

Figure 4.3.2.2. Simplified scheme of the influence of the overall functional (E-I) balance within the DLPFC-HF network on behavior for each genotype group: AA, AC, and CC

4.3.3. Investigation of relations between sDCM parameter estimates and behavior in pair-wise matched healthy volunteers and schizophrenia patients

This analysis demonstrated a consistent pattern of activation in the right DLPFC and deactivation in the left HF in healthy control subjects and schizophrenia patients. Moreover, BMS revealed the same connectivity pattern or winning model between DLPFC and HF during WM in controls and patients. However, statistical tests on model parameter estimates revealed statistical differences across groups.

More precisely, statistical tests on sDCM parameter estimates of the winning model revealed differences on the self-connection in the right DLPFC and in the self-connection in left HF between groups. Schizophrenia patients have higher functional (E-I) balance (lower inhibition) in right DLPFC and left HF in comparison to healthy control subjects. In summary, we observed that patients have a higher functional (E-I) balance (lower inhibition) within the prefrontal-hippocampal network in comparison to controls.

In addition, statistical tests on behavior indicated differences in the mean performance in the 2-Back and a slight tendency in the mean reaction time in the 2-Back. Schizophrenia patients showed lower mean performance in the 2-Back and higher mean reaction time in the 2-Back in comparison to healthy control subjects. Table 4.3.3.1 summarizes the research findings of this third analysis.

<table>
<tr><td rowspan="2">Schizophrenia</td><td rowspan="2">→</td><td rowspan="1">DLPFC-HF network</td><td>→</td><td colspan="5">↑ Effective connectivity between DLPFC-HF (n.s.)</td></tr>
<tr><td>Behavior in the 2-Back</td><td>→</td><td colspan="5">↓ Mean performance in the 2-Back
&
↑ Mean reaction time in the 2-Back (n.s. but tendency)</td></tr>
<tr><td colspan="4"></td><td>↑ Functional (E-I) balance in the DLPFC</td><td>→</td><td>↑ Functional (E-I) balance between DLPFC-HF (n.s.)</td><td>→</td><td>↑ Functional (E-I) balance in the HF</td></tr>
</table>

Table 4.3.3.1. Summary results of the third analysis

In view of these research findings, we hypothesize a mechanistic causal relationship between self-connection in the right DLPFC and self-connection in the left HF, on the one hand, and mean performance in the 2-Back and mean reaction time in the 2-Back, on the other hand. Figure 4.3.3.1 illustrates this mechanistic model. According to this model, higher functional (E-I) balance (lower inhibition) of self-connection in the right DLPFC (premise **P**) and higher functional (E-I) balance (lower inhibition) of self-connection in the left HF (premise **Q**) seems to lead to a lower mean performance in the 2-Back (premise **R**) and a higher mean reaction time in the 2-Back (premise **S**). Thus, this causal relationship can be translated into the next mathematical logic expression: **(P & Q) → (R & S)**.

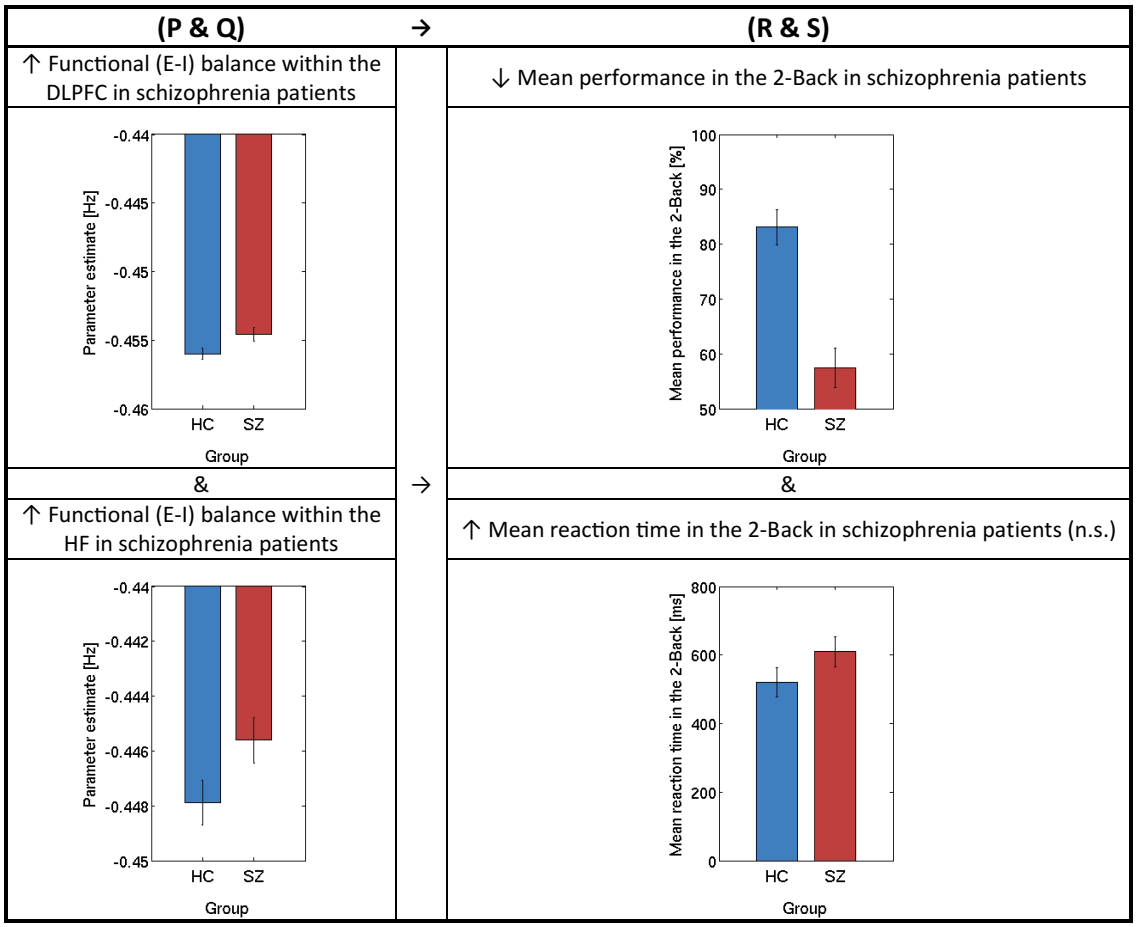

Figure 4.3.3.1. Graphical representation of the proposed causal relationship: **(P & Q) → (R & S)**

Furthermore, regression analysis revealed some statistical effects. On the one hand, the analyses revealed that connection from right DLPFC to left HF seems to contain sufficiently rich information for predicting mean performance in the 2-Back in schizophrenia patients. The lower the prefrontal-hippocampal effective connectivity, the higher is the mean performance in the 2-Back in schizophrenia patients. On the other hand, the analysis revealed that mean reaction time in the 2-Back seems to contain sufficiently rich information for predicting mean performance in the 2-Back in schizophrenia patients. The lower the reaction time in the 2-Back, the higher is the mean performance in the 2-Back in schizophrenia patients.

Taken together, these results suggest that the prefrontal-hippocampal network is modulated by each group: controls and patients, and each group individual require of a perturbation on the mean group parameter estimates in order to achieve the optimal behavior. Figure 4.3.3.2 illustrates this mechanistic account. Thus, this perturbation depends on the group of each individual. On the one hand, schizophrenia patients, who as depicted in Figure 4.3.3.2, have a higher functional (E-I) balance (lower inhibition) within the prefrontal-hippocampal network (left side of Figure 4.3.3.2), require lower functional (E-I) balance on the prefrontal-hippocampal network in order to achieve the optimal behavior (right side of Figure 4.3.3.2). One the other hand, healthy control subjects, who as depicted below, have a lower functional (E-I) balance (higher inhibition) within the prefrontal-hippocampal network, require higher functional (E-I) balance on prefrontal-hippocampal network in order to achieve the optimal behavior.

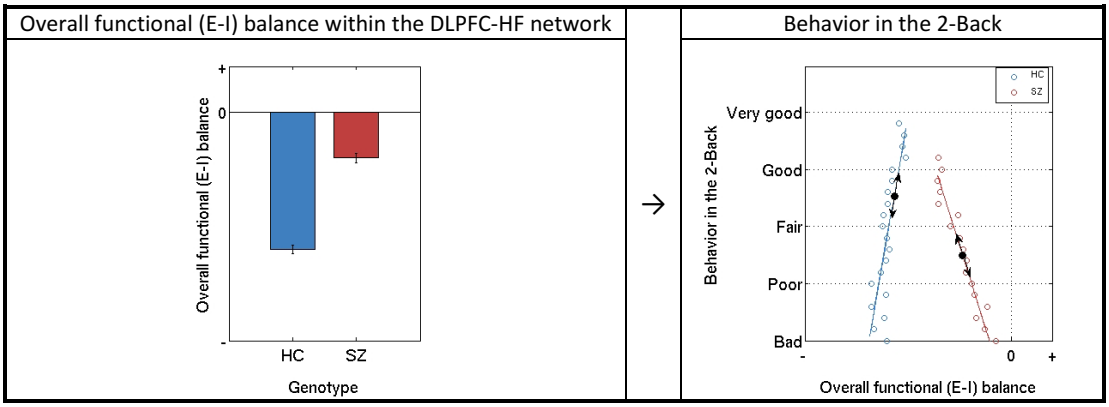

Figure 4.3.3.2. Simplified scheme of the influence of overall functional (E-I) balance within the DLPFC-HF network on behavior for healthy volunteers and schizophrenia patients

4.3.4. Comparison of two-group genetic models and healthy vs. schizophrenia model

We compared each of the two-group genetic models: recessive, co-dominant, and dominant to the healthy vs. schizophrenia model. We visually observed a high degree of similarity between the dominant and the healthy vs. schizophrenia models in relation to the underlying neurobiology and behavior. In summary, our comparisons showed that risk allele carriers have higher functional (E-I) balance (lower inhibition) within the prefrontal-hippocampal network in comparison to non-risk allele carriers, as do schizophrenia patients in comparison to healthy control subjects. Furthermore, we reported that some of the sDCM parameter estimates contained sufficiently rich information for predicting mean performance in the 2-Back and mean reaction time in the 2-Back in risk allele carriers and patients.

Taking into consideration these comparisons, the winning model with a directed connection from DLPFC to HF, and the two plausible causal relationships: **P → S** within the dominant model, and **(P & Q) → (R & S)** within the healthy vs. schizophrenia model, we hypothesize the following functionality of the prefrontal-hippocampal network in genetic risk carriers and patients. In the dominant model,

dysfunction of the right DLPFC in risk allele carriers or increased functional (E-I) balance within the right DLPFC leads to a higher mean reaction time in the 2-Back; but mean performance in the 2-Back is not affected because the left HF in risk allele carriers seems to work properly. Nonetheless, in the healthy vs. schizophrenia model, dysfunction of the right DLPFC in patients or increased functional (E-I) balance within the right DLPFC leads to a higher mean reaction time in the 2-Back, and mean performance in the 2-Back is affected because the left HF in patients is disrupted.

Recapitulating, we conclude that the prefrontal-hippocampal network is modulated by each genotype and group. Schizophrenia patients require lower functional (E-I) balance on the prefrontal-hippocampal network in order to achieve the optimal behavior and these findings are consistent with the similarities observed between the dominant and healthy vs. schizophrenia models by assuming that their phenotypes can be approximated by a weighted sum of AA and AC phenotypes. Pair-wise healthy volunteers with genotype frequencies: N_{AA} = 11; N_{AC} = 14; N_{CC} = 8; require higher functional (E-I) balance on the prefrontal-hippocampal network in order to achieve the optimal behavior and these findings are consistent with the conclusions of second analysis by assuming that their phenotypes can be approximated by a weighted sum of AA, AC, and CC phenotypes.

Therefore, our analyses revealed that ZNF804A (rs1344706) genotype contributes to the phenotype expressed in schizophrenia patients. Better understanding of the biology of ZNF804A (rs1344706) is necessary to clarify the nature of this observation. Nonetheless, it is quite remarkable that a risk genetic variant for schizophrenia can so clearly show a predicted illness circuit phenotype in this way.

4.4. Final conclusions and suggestions for future research

● In a first sample, 180 healthy subjects were measured by fMRI during a standard working memory N-Back task at three different sites (Mannheim, Bonn, Berlin; each with 60 participants). The effective connectivity between key regions for working memory: DLPFC and HF, was analyzed using a simple two-region sDCM. BMS revealed the same causal pattern or winning model across the three sites, with the 2-Back working memory condition as driving input to both DLPFC and HF and with a connection from DLPFC to HF. Furthermore, a genome-wide risk variant for schizophrenia: ZNF804A (rs1344706), showed a strong impact on the DLPFC-HF network. On the one hand, risk homozygotes showed higher effective connectivity or higher functional (E-I) balance between DLPFC and HF. On the other hand, risk allele carriers showed higher functional (E-I) balance on the self-connection in the DLPFC. In summary, we observed that risk allele carriers have a higher functional (E-I) balance within the DLPFC-HF network in comparison to non-risk allele carriers.

● In a second sample, 33 schizophrenia patients were measured by fMRI during the same working memory N-Back task. We pair-wise matched healthy volunteers of the first sample and patients and applied the same methodology. BMS revealed the same winning model in patients but sDCM parameter estimates differed significantly between groups. Patients showed higher functional (E-I) balance on the self-connection in the DLPFC, as we had previously observed in risk allele carriers, but also showed higher functional (E-I) balance on the self-connection in the HF. In summary, we observed that patients have a higher functional (E-I) balance within the DLPFC-HF network, as we had previously observed in risk allele carriers, in comparison to controls.

● In view of these research findings, we concluded a possible biological functioning of ZNF804A (rs1344706) within the DLPFC-HF network:

The risk allele rs1344706 increases the expression of ZNF804A in the DLPFC, and this, in turn, up-regulates transcripts levels of COMT. Increased transcript levels of COMT lead to higher degradation of dopamine, and reduced dopamine via D1 reduces NMDA receptor-activated synaptic currents. A consequence of NMDA-hypofunction is an extensive release of glutamate in the DLPFC. This increased release of glutamate leads to a hyperstimulation of downstream excitatory neurons, and to a further disinhibition through a lack of NMDA receptor excitation on interneurons and a consequent loss in overall network inhibition within the DLPFC. This disinhibitory phenomenon leads to overstimulation of the DLPFC-HF network. In the same vein, the risk allele rs1344706 has not been associated with increased expression in the HF and that might explain the reason for not observing this phenomenon within the HF.

● Furthermore, we also suggested a model for explaining the underlying neurobiology of schizophrenia within the DLPFC-HF network:

On the one hand, as explained above, increased release of glutamate within the DLPFC due to genetic variants, i.e. ZNF804A (rs1344706), leads to an overstimulation of downstream excitatory neurons, as well as to a further disinhibition through a lack of NMDA receptor excitation on interneurons and a consequent loss in overall network inhibition within the DLPFC. This complex disinhibitory phenomenon results in hyperstimulation of the DLPFC-HF network. On the other hand, a lack of NMDA receptor excitation due to genetic variants for schizophrenia other than ZNF804A (rs1344706) might lead as well to a loss in overall network inhibition within the HF.

● Then, we reported causal relations between some sDCM parameter estimates and behavior in terms of functional (E-I) balance in both samples:

Dysfunction of the DLPFC in risk allele carriers or increased functional (E-I) balance within the DLPFC leads to a higher mean reaction time in the 2-Back; but mean performance in the 2-Back is not

affected because the HF in risk allele carriers seems to work properly. In contrast, dysfunction of the DLPFC in schizophrenia patients or increased functional (E-I) balance within the DLPFC leads as well to a higher mean reaction time in the 2-Back, but mean performance in the 2-Back is affected because of dysfunction in the HF or increased functional (E-I) balance.

● Finally, we reported a series of interesting observations between the DLPFC-HF network and the optimal behavior during working memory in both samples:

On the one hand, we observed that risk allele carriers and patients, who as noted above have a higher functional (E-I) balance within the DLPFC-HF network, require lower functional (E-I) balance on the DLPFC-HF network in order to achieve the best performance during the task. On the other hand, we found that healthy volunteers, who as noted above have a higher functional (E-I) balance within the DLPFC-HF network, require higher functional (E-I) balance on the network in order to achieve the optimal behavior.

● This study investigated the applicability of computational models like sDCM to establish the functional significance of specific genetic polymorphisms for schizophrenia and identify causal mechanisms associated with the disease in relation to the underlying neurobiology and behavior. In forthcoming studies, we plan to investigate whether subject-specific directed connections strengths between DLPFC and HF, and genotype, contain sufficiently rich information to enable accurate predictions of behavior. In order to study how temporal patterns in the neuronal ensembles and genotype convey robust information about behavior, multivariate regressors or statistical decoding algorithms will be used in both samples.

Appendix

Acronyms

5-HT	5-hydroxytryptamine
ACh	Acetylcholine
AC-PC line	Anterior commissure-posterior commissure line
AMPAR	α-amino-3-hydroxy-5-methyl-4-isoxazolepropionic acid receptor
BMS	Bayes model selection
BOLD	Blood oxygenation level dependent
BL	Berlin
BN	Bonn
COMT	Catechol-O-methyltransferase
DA	Dopamine
DCM	Dynamic causal modelling
DLPFC	Dorsolateral prefrontal cortex
DRD2	Dopamine receptor D2 isoform
EEG	Electroencephalography
fMRI	Functional magnetic resonance imaging
FOV	The field of view
GWAS	Genome wide association study
HC	Healthy control
HF	Hippocampal formation
MA	Mannheim
MEG	Magnetoencephalography
MRI	Magnetic resonance imaging
mGluR	Metabotropic glutamate receptor
NE	Norepinephrine

NIRS	Near-infrared spectroscopy
NMDAR	N-methyl D-aspartate
NMR	Nuclear magnetic resonance
PDE4B	Phosphodiesterase 4B
PET	Positron emission tomography
PFC	Prefrontal cortex
PPI	Psychophysiological interaction
PRSS16	Thymus-specific serine protease
SNP	Single nucleotide polymorphism
SPECT	Single photon emission computed tomography
SPM	Statistical parametric mapping
SZ	Schizophrenia
sDCM	Stochastic dynamic causal modelling
TE	Echo Time
TMS	Transcranial magnetic stimulation
TR	Repetition Time
WM	Working memory

List of figures

List of tables

References

Adali, T., Wang, Z.J., McKeown, M.J., Ciuciu, P., Hansen, L.K., Cichocki, A., Calhoun, V.D., 2008. Introduction to the Issue on fMRI Analysis for Human Brain Mapping. IEEE J Sel Top Signal Process 2, 813.

Adams, B., Moghaddam, B., 1998. Corticolimbic dopamine neurotransmission is temporally dissociated from the cognitive and locomotor effects of phencyclidine. J Neurosci 18, 5545-5554.

Aertsen, A., Preissl, H., 1991. Dynamics of activity and connectivity in physiological neuronal networks. In: Schuster, H.G. (Ed.), Non Linear Dynamics and Neuronal Networks. VCH Publishers Inc., New York, pp. 281-302.

Aldrich, J., 1995. Correlations Genuine and Spurious in Pearson and Yule. Statistical Science 10, 364-376.

Ashburner, J., Friston, K.J., 2005. Unified segmentation. Neuroimage 26, 839-851.

Baddeley, A., 1992. Working memory. Science 255, 556-559.

Barch, D.M., 2005. The cognitive neuroscience of schizophrenia. Annu Rev Clin Psychol 1, 321-353.

Belliveau, J.W., Kennedy, D.N., Jr., McKinstry, R.C., Buchbinder, B.R., Weisskoff, R.M., Cohen, M.S., Vevea, J.M., Brady, T.J., Rosen, B.R., 1991. Functional mapping of the human visual cortex by magnetic resonance imaging. Science 254, 716-719.

Benetti, S., Mechelli, A., Picchioni, M., Broome, M., Williams, S., McGuire, P., 2009. Functional integration between the posterior hippocampus and prefrontal cortex is impaired in both first episode schizophrenia and the at risk mental state. Brain 132, 2426-2436.

Biswal, B., Yetkin, F.Z., Haughton, V.M., Hyde, J.S., 1995. Functional connectivity in the motor cortex of resting human brain using echo-planar MRI. Magn Reson Med 34, 537-541.

Biswal, B.B., Mennes, M., Zuo, X.N., Gohel, S., Kelly, C., Smith, S.M., Beckmann, C.F., Adelstein, J.S., Buckner, R.L., Colcombe, S., Dogonowski, A.M., Ernst, M., Fair, D., Hampson, M., Hoptman, M.J., Hyde, J.S., Kiviniemi, V.J., Kotter, R., Li, S.J., Lin, C.P., Lowe, M.J., Mackay, C., Madden, D.J., Madsen, K.H., Margulies, D.S., Mayberg, H.S., McMahon, K., Monk, C.S., Mostofsky, S.H., Nagel, B.J., Pekar, J.J., Peltier, S.J., Petersen, S.E., Riedl, V., Rombouts, S.A., Rypma, B., Schlaggar, B.L., Schmidt, S., Seidler,

R.D., Siegle, G.J., Sorg, C., Teng, G.J., Veijola, J., Villringer, A., Walter, M., Wang, L., Weng, X.C., Whitfield-Gabrieli, S., Williamson, P., Windischberger, C., Zang, Y.F., Zhang, H.Y., Castellanos, F.X., Milham, M.P., 2010. Toward discovery science of human brain function. Proc Natl Acad Sci U S A 107, 4734-4739.

Bleuler, E., 1911. Dementia praecox, oder Gruppe der Schizophrenien. Deuticke, Leipzig.

Brodersen, K.H., Schofield, T.M., Leff, A.P., Ong, C.S., Lomakina, E.I., Buhmann, J.M., Stephan, K.E., 2011. Generative embedding for model-based classification of fMRI data. PLoS Comput Biol 7, e1002079.

Buckner, R.L., 2010. Human functional connectivity: new tools, unresolved questions. Proc Natl Acad Sci U S A 107, 10769-10770.

Craddock, N., O'Donovan, M.C., Owen, M.J., 2005. The genetics of schizophrenia and bipolar disorder: dissecting psychosis. J Med Genet 42, 193-204.

Crossley, N.A., Mechelli, A., Fusar-Poli, P., Broome, M.R., Matthiasson, P., Johns, L.C., Bramon, E., Valmaggia, L., Williams, S.C., McGuire, P.K., 2009. Superior temporal lobe dysfunction and frontotemporal dysconnectivity in subjects at risk of psychosis and in first-episode psychosis. Hum Brain Mapp 30, 4129-4137.

Daunizeau, J., Friston, K.J., Kiebel, S.J., 2009. Variational Bayesian identification and prediction of stochastic nonlinear dynamic causal models. Physica D 238, 2089-2118.

Daunizeau, J., Lemieux, L., Vaudano, A.E., Friston, K.J., Stephan, K.E., 2013. An electrophysiological validation of stochastic DCM for fMRI. Frontiers in Computational Neuroscience 6.

Daunizeau, J., Stephan, K.E., Friston, K.J., 2012. Stochastic dynamic causal modelling of fMRI data: should we care about neural noise? Neuroimage 62, 464-481.

David, O., Guillemain, I., Saillet, S., Reyt, S., Deransart, C., Segebarth, C., Depaulis, A., 2008. Identifying neural drivers with functional MRI: an electrophysiological validation. PLoS Biol 6, 2683-2697.

Esslinger, C., Walter, H., Kirsch, P., Erk, S., Schnell, K., Arnold, C., Haddad, L., Mier, D., Opitz von Boberfeld, C., Raab, K., Witt, S.H., Rietschel, M., Cichon, S., Meyer-Lindenberg, A., 2009. Neural mechanisms of a genome-wide supported psychosis variant. Science 324, 605.

Fletcher, P., 1998. The missing link: a failure of fronto-hippocampal integration in schizophrenia. Nat Neurosci 1, 266-267.

Forbes, N.F., Carrick, L.A., McIntosh, A.M., Lawrie, S.M., 2009. Working memory in schizophrenia: a meta-analysis. Psychol Med 39, 889-905.

Fornito, A., Zalesky, A., Pantelis, C., Bullmore, E.T., 2012. Schizophrenia, neuroimaging and connectomics. Neuroimage 62, 2296-2314.

Friston, K., Mattout, J., Trujillo-Barreto, N., Ashburner, J., Penny, W., 2007. Variational free energy and the Laplace approximation. Neuroimage 34, 220-234.

Friston, K., Stephan, K., Li, B., Daunizeau, J., 2010. Generalised Filtering. Mathematical Problems in Engineering 2010.

Friston, K.J., 1994. Functional and effective connectivity in neuroimaging: A synthesis. Hum. Brain Mapp. Human Brain Mapping 2, 56-78.

Friston, K.J., 1998. The disconnection hypothesis. Schizophr Res 30, 115-125.

Friston, K.J., Frith, C.D., 1995. Schizophrenia: a disconnection syndrome? Clin Neurosci 3, 89-97.

Friston, K.J., Frith, C.D., Frackowiak, R.S.J., 1993a. Time-dependent changes in effective connectivity measured with PET. Hum. Brain Mapp. Human Brain Mapping 1, 69-79.

Friston, K.J., Frith, C.D., Liddle, P.F., Frackowiak, R.S., 1993b. Functional connectivity: the principal-component analysis of large (PET) data sets. J Cereb Blood Flow Metab 13, 5-14.

Friston, K.J., Harrison, L., Penny, W., 2003. Dynamic causal modelling. Neuroimage 19, 1273-1302.

Friston, K.J., Li, B., Daunizeau, J., Stephan, K.E., 2011. Network discovery with DCM. Neuroimage 56, 1202-1221.

Friston, K.J., Trujillo-Barreto, N., Daunizeau, J., 2008. DEM: a variational treatment of dynamic systems. Neuroimage 41, 849-885.

Gerstein, G.L., Bedenbaugh, P., Aertsen, M.H., 1989. Neuronal assemblies. IEEE Trans Biomed Eng 36, 4-14.

Gerstein, G.L., Perkel, D.H., 1969. Simultaneously recorded trains of action potentials: analysis and functional interpretation. Science 164, 828-830.

Girgenti, M.J., LoTurco, J.J., Maher, B.J., 2012. ZNF804a regulates expression of the schizophrenia-associated genes PRSS16, COMT, PDE4B, and DRD2. PLoS One 7, e32404.

Gochin, P.M., Miller, E.K., Gross, C.G., Gerstein, G.L., 1991. Functional interactions among neurons in inferior temporal cortex of the awake macaque. Exp Brain Res 84, 505-516.

Goldman-Rakic, P.S., 1994. Working memory dysfunction in schizophrenia. J Neuropsychiatry Clin Neurosci 6, 348-357.

Goldman-Rakic, P.S., Castner, S.A., Svensson, T.H., Siever, L.J., Williams, G.V., 2004. Targeting the dopamine D1 receptor in schizophrenia: insights for cognitive dysfunction. Psychopharmacology (Berl) 174, 3-16.

Gu, Q., 2002. Neuromodulatory transmitter systems in the cortex and their role in cortical plasticity. Neuroscience 111, 815-835.

Harrison, P.J., Weinberger, D.R., 2005. Schizophrenia genes, gene expression, and neuropathology: on the matter of their convergence. Mol Psychiatry 10, 40-68; image 45.

He, H., Sui, J., Yu, Q., Turner, J.A., Ho, B.C., Sponheim, S.R., Manoach, D.S., Clark, V.P., Calhoun, V.D., 2012. Altered small-world brain networks in schizophrenia patients during working memory performance. PLoS One 7, e38195.

Hill, M.J., Bray, N.J., 2011. Allelic differences in nuclear protein binding at a genome-wide significant risk variant for schizophrenia in ZNF804A. Mol Psychiatry 16, 787-789.

Hill, M.J., Jeffries, A.R., Dobson, R.J., Price, J., Bray, N.J., 2012. Knockdown of the psychosis susceptibility gene ZNF804A alters expression of genes involved in cell adhesion. Hum Mol Genet 21, 1018-1024.

Hoffman, R.E., Buchsbaum, M.S., Escobar, M.D., Makuch, R.W., Nuechterlein, K.H., Guich, S.M., 1991. EEG coherence of prefrontal areas in normal and schizophrenic males during perceptual activation. J Neuropsychiatry Clin Neurosci 3, 169-175.

Homayoun, H., Moghaddam, B., 2007. NMDA receptor hypofunction produces opposite effects on prefrontal cortex interneurons and pyramidal neurons. J Neurosci 27, 11496-11500.

Karoum, F., Chrapusta, S.J., Egan, M.F., 1994. 3-Methoxytyramine is the major metabolite of released dopamine in the rat frontal cortex: reassessment of the effects of antipsychotics on the dynamics of dopamine release and metabolism in the frontal cortex, nucleus accumbens, and striatum by a simple two pool model. J Neurochem 63, 972-979.

Kehrer, C., Maziashvili, N., Dugladze, T., Gloveli, T., 2008. Altered Excitatory-Inhibitory Balance in the NMDA-Hypofunction Model of Schizophrenia. Front Mol Neurosci 1, 6.

Kruger, G., Glover, G.H., 2001. Physiological noise in oxygenation-sensitive magnetic resonance imaging. Magn Reson Med 46, 631-637.

Lee, J., Park, S., 2005. Working memory impairments in schizophrenia: a meta-analysis. J Abnorm Psychol 114, 599-611.

Lee, L., Friston, K., Horwitz, B., 2006. Large-scale neural models and dynamic causal modelling. Neuroimage 30, 1243-1254.

Li, B., Daunizeau, J., Stephan, K.E., Penny, W., Hu, D., Friston, K., 2011a. Generalised filtering and stochastic DCM for fMRI. Neuroimage 58, 442-457.

Li, M., Luo, X.J., Xiao, X., Shi, L., Liu, X.Y., Yin, L.D., Diao, H.B., Su, B., 2011b. Allelic differences between Han Chinese and Europeans for functional variants in ZNF804A and their association with schizophrenia. Am J Psychiatry 168, 1318-1325.

Logothetis, N.K., 2008. What we can do and what we cannot do with fMRI. Nature 453, 869-878.

Logothetis, N.K., Wandell, B.A., 2004. Interpreting the BOLD signal. Annu Rev Physiol 66, 735-769.

Malinow, R., Malenka, R.C., 2002. AMPA receptor trafficking and synaptic plasticity. Annu Rev Neurosci 25, 103-126.

Manoach, D.S., Press, D.Z., Thangaraj, V., Searl, M.M., Goff, D.C., Halpern, E., Saper, C.B., Warach, S., 1999. Schizophrenic subjects activate dorsolateral prefrontal cortex during a working memory task, as measured by fMRI. Biol Psychiatry 45, 1128-1137.

Massey, P.V., Bhabra, G., Cho, K., Brown, M.W., Bashir, Z.I., 2001. Activation of muscarinic receptors induces protein synthesis-dependent long-lasting depression in the perirhinal cortex. Eur J Neurosci 14, 145-152.

Matsumoto, M., Weickert, C.S., Beltaifa, S., Kolachana, B., Chen, J., Hyde, T.M., Herman, M.M., Weinberger, D.R., Kleinman, J.E., 2003. Catechol O-methyltransferase (COMT) mRNA expression in the dorsolateral prefrontal cortex of patients with schizophrenia. Neuropsychopharmacology 28, 1521-1530.

Meyer-Lindenberg, A., Weinberger, D.R., 2006. Intermediate phenotypes and genetic mechanisms of psychiatric disorders. Nat Rev Neurosci 7, 818-827.

Meyer-Lindenberg, A.S., Olsen, R.K., Kohn, P.D., Brown, T., Egan, M.F., Weinberger, D.R., Berman, K.F., 2005. Regionally specific disturbance of dorsolateral prefrontal-hippocampal functional connectivity in schizophrenia. Arch Gen Psychiatry 62, 379-386.

Moghaddam, B., Adams, B., Verma, A., Daly, D., 1997. Activation of glutamatergic neurotransmission by ketamine: a novel step in the pathway from NMDA receptor blockade to dopaminergic and cognitive disruptions associated with the prefrontal cortex. J Neurosci 17, 2921-2927.

Montgomery, J.M., Madison, D.V., 2004. Discrete synaptic states define a major mechanism of synapse plasticity. Trends Neurosci 27, 744-750.

Nichols, T., Brett, M., Andersson, J., Wager, T., Poline, J.B., 2005. Valid conjunction inference with the minimum statistic. Neuroimage 25, 653-660.

O'Donovan, M.C., Craddock, N., Norton, N., Williams, H., Peirce, T., Moskvina, V., Nikolov, I., Hamshere, M., Carroll, L., Georgieva, L., Dwyer, S., Holmans, P., Marchini, J.L., Spencer, C.C., Howie, B., Leung, H.T., Hartmann, A.M., Moller, H.J., Morris, D.W., Shi, Y., Feng, G., Hoffmann, P., Propping, P., Vasilescu, C., Maier, W., Rietschel, M., Zammit, S., Schumacher, J., Quinn, E.M., Schulze, T.G., Williams, N.M., Giegling, I., Iwata, N., Ikeda, M., Darvasi, A., Shifman, S., He, L., Duan, J., Sanders, A.R., Levinson, D.F., Gejman, P.V., Cichon, S., Nothen, M.M., Gill, M., Corvin, A., Rujescu, D., Kirov, G., Owen, M.J., Buccola, N.G., Mowry, B.J., Freedman, R., Amin, F., Black, D.W., Silverman, J.M., Byerley, W.F., Cloninger, C.R., 2008. Identification of loci associated with schizophrenia by genome-wide association and follow-up. Nat Genet 40, 1053-1055.

Owen, A.M., McMillan, K.M., Laird, A.R., Bullmore, E., 2005. N-back working memory paradigm: a meta-analysis of normative functional neuroimaging studies. Hum Brain Mapp 25, 46-59.

Park, S., Holzman, P.S., 1992. Schizophrenics show spatial working memory deficits. Arch Gen Psychiatry 49, 975-982.

Paulus, F.M., Krach, S., Bedenbender, J., Pyka, M., Sommer, J., Krug, A., Knake, S., Nothen, M.M., Witt, S.H., Rietschel, M., Kircher, T., Jansen, A., 2013. Partial support for ZNF804A genotype-dependent alterations in prefrontal connectivity. Hum Brain Mapp 34, 304-313.

Penny, W.D., Stephan, K.E., Daunizeau, J., Rosa, M.J., Friston, K.J., Schofield, T.M., Leff, A.P., 2010. Comparing families of dynamic causal models. PLoS Comput Biol 6, e1000709.

Penny, W.D., Stephan, K.E., Mechelli, A., Friston, K.J., 2004a. Comparing dynamic causal models. Neuroimage 22, 1157-1172.

Penny, W.D., Stephan, K.E., Mechelli, A., Friston, K.J., 2004b. Modelling functional integration: a comparison of structural equation and dynamic causal models. Neuroimage 23 Suppl 1, S264-274.

Pitt, M.A., Myung, I.J., 2002. When a good fit can be bad. Trends Cogn Sci 6, 421-425.

Rasetti, R., Sambataro, F., Chen, Q., Callicott, J.H., Mattay, V.S., Weinberger, D.R., 2011. Altered cortical network dynamics: a potential intermediate phenotype for schizophrenia and association with ZNF804A. Arch Gen Psychiatry 68, 1207-1217.

Riera, J.J., Watanabe, J., Kazuki, I., Naoki, M., Aubert, E., Ozaki, T., Kawashima, R., 2004. A state-space model of the hemodynamic approach: nonlinear filtering of BOLD signals. Neuroimage 21, 547-567.

Riley, B., Thiselton, D., Maher, B.S., Bigdeli, T., Wormley, B., McMichael, G.O., Fanous, A.H., Vladimirov, V., O'Neill, F.A., Walsh, D., Kendler, K.S., 2010. Replication of association between schizophrenia and ZNF804A in the Irish Case-Control Study of Schizophrenia sample. Mol Psychiatry 15, 29-37.

Rowe, J.B., Hughes, L.E., Barker, R.A., Owen, A.M., 2010. Dynamic causal modelling of effective connectivity from fMRI: are results reproducible and sensitive to Parkinson's disease and its treatment? Neuroimage 52, 1015-1026.

Schuyler, B., Ollinger, J.M., Oakes, T.R., Johnstone, T., Davidson, R.J., 2010. Dynamic Causal Modeling applied to fMRI data shows high reliability. Neuroimage 49, 603-611.

Shibasaki, H., 2008. Human brain mapping: hemodynamic response and electrophysiology. Clin Neurophysiol 119, 731-743.

Sigurdsson, T., Stark, K.L., Karayiorgou, M., Gogos, J.A., Gordon, J.A., 2010. Impaired hippocampal-prefrontal synchrony in a genetic mouse model of schizophrenia. Nature 464, 763-767.

Silver, H., Feldman, P., Bilker, W., Gur, R.C., 2003. Working memory deficit as a core neuropsychological dysfunction in schizophrenia. Am J Psychiatry 160, 1809-1816.

Steinberg, S., Mors, O., Borglum, A.D., Gustafsson, O., Werge, T., Mortensen, P.B., Andreassen, O.A., Sigurdsson, E., Thorgeirsson, T.E., Bottcher, Y., Olason, P., Ophoff, R.A., Cichon, S., Gudjonsdottir, I.H., Pietilainen, O.P., Nyegaard, M., Tuulio-Henriksson, A., Ingason, A., Hansen, T., Athanasiu, L., Suvisaari, J., Lonnqvist, J., Paunio, T., Hartmann, A., Jurgens, G., Nordentoft, M., Hougaard, D., Norgaard-Pedersen, B., Breuer, R., Moller, H.J., Giegling, I., Glenthoj, B., Rasmussen, H.B., Mattheisen, M., Bitter, I., Rethelyi, J.M., Sigmundsson, T., Fossdal, R., Thorsteinsdottir, U., Ruggeri, M., Tosato, S., Strengman, E., Kiemeney, L.A., Melle, I., Djurovic, S., Abramova, L., Kaleda, V., Walshe, M., Bramon, E., Vassos, E., Li, T., Fraser, G., Walker, N., Toulopoulou, T., Yoon, J., Freimer, N.B., Cantor, R.M., Murray, R., Kong, A., Golimbet, V., Jonsson, E.G., Terenius, L., Agartz, I., Petursson, H., Nothen, M.M., Rietschel, M., Peltonen, L., Rujescu, D., Collier, D.A., Stefansson, H., St Clair, D., Stefansson, K., 2011. Expanding the range of ZNF804A variants conferring risk of psychosis. Mol Psychiatry 16, 59-66.

Stephan, K.E., Baldeweg, T., Friston, K.J., 2006. Synaptic plasticity and dysconnection in schizophrenia. Biol Psychiatry 59, 929-939.

Stephan, K.E., Friston, K.J., Frith, C.D., 2009a. Dysconnection in schizophrenia: from abnormal synaptic plasticity to failures of self-monitoring. Schizophr Bull 35, 509-527.

Stephan, K.E., Penny, W.D., Daunizeau, J., Moran, R.J., Friston, K.J., 2009b. Bayesian model selection for group studies. Neuroimage 46, 1004-1017.

Stephan, K.E., Penny, W.D., Moran, R.J., den Ouden, H.E., Daunizeau, J., Friston, K.J., 2010. Ten simple rules for dynamic causal modeling. Neuroimage 49, 3099-3109.

Stephan, K.E., Weiskopf, N., Drysdale, P.M., Robinson, P.A., Friston, K.J., 2007. Comparing hemodynamic models with DCM. Neuroimage 38, 387-401.

Tseng, K.Y., O'Donnell, P., 2004. Dopamine-glutamate interactions controlling prefrontal cortical pyramidal cell excitability involve multiple signaling mechanisms. The Journal of neuroscience : the official journal of the Society for Neuroscience 24, 5131-5139.

Volkow, N.D., Wolf, A.P., Brodie, J.D., Cancro, R., Overall, J.E., Rhoades, H., Van Gelder, P., 1988. Brain interactions in chronic schizophrenics under resting and activation conditions. Schizophr Res 1, 47-53.

Weinberger, D.R., Berman, K.F., Suddath, R., Torrey, E.F., 1992. Evidence of dysfunction of a prefrontal-limbic network in schizophrenia: a magnetic resonance imaging and regional cerebral blood flow study of discordant monozygotic twins. Am J Psychiatry 149, 890-897.

Wernicke, C., 1906. Grundriss der Psychiatrie in klinischen Vorlesungen. Thieme, Leipzig.

Williams, H.J., Norton, N., Dwyer, S., Moskvina, V., Nikolov, I., Carroll, L., Georgieva, L., Williams, N.M., Morris, D.W., Quinn, E.M., Giegling, I., Ikeda, M., Wood, J., Lencz, T., Hultman, C., Lichtenstein, P., Thiselton, D., Maher, B.S., Malhotra, A.K., Riley, B., Kendler, K.S., Gill, M., Sullivan, P., Sklar, P., Purcell, S., Nimgaonkar, V.L., Kirov, G., Holmans, P., Corvin, A., Rujescu, D., Craddock, N., Owen, M.J., O'Donovan, M.C., 2011. Fine mapping of ZNF804A and genome-wide significant evidence for its involvement in schizophrenia and bipolar disorder. Mol Psychiatry 16, 429-441.

Wolf, M.E., Mangiavacchi, S., Sun, X., 2003. Mechanisms by which dopamine receptors may influence synaptic plasticity. Ann N Y Acad Sci 1003, 241-249.

Wolf, R.C., Vasic, N., Sambataro, F., Hose, A., Frasch, K., Schmid, M., Walter, H., 2009. Temporally anticorrelated brain networks during working memory performance reveal aberrant prefrontal and hippocampal connectivity in patients with schizophrenia. Prog Neuropsychopharmacol Biol Psychiatry 33, 1464-1473.

Xiao, B., Li, W., Zhang, H., Lv, L., Song, X., Yang, Y., Yang, G., Jiang, C., Zhao, J., Lu, T., Zhang, D., Yue, W., 2011. Association of ZNF804A polymorphisms with schizophrenia and antipsychotic drug efficacy in a Chinese Han population. Psychiatry Res 190, 379-381.

Yizhar, O., Fenno, L.E., Prigge, M., Schneider, F., Davidson, T.J., O'Shea, D.J., Sohal, V.S., Goshen, I., Finkelstein, J., Paz, J.T., Stehfest, K., Fudim, R., Ramakrishnan, C., Huguenard, J.R., Hegemann, P., Deisseroth, K., 2011. Neocortical excitation/inhibition balance in information processing and social dysfunction. Nature 477, 171-178.

Zhang, R., Lu, S.M., Qiu, C., Liu, X.G., Gao, C.G., Guo, T.W., Valenzuela, R.K., Deng, H.W., Ma, J., 2011. Population-based and family-based association studies of ZNF804A locus and schizophrenia. Mol Psychiatry 16, 360-361.

Zhou, Y., Liang, M., Jiang, T., Tian, L., Liu, Y., Liu, Z., Liu, H., Kuang, F., 2007. Functional dysconnectivity of the dorsolateral prefrontal cortex in first-episode schizophrenia using resting-state fMRI. Neurosci Lett 417, 297-302.

Zhou, Y., Shu, N., Liu, Y., Song, M., Hao, Y., Liu, H., Yu, C., Liu, Z., Jiang, T., 2008. Altered resting-state functional connectivity and anatomical connectivity of hippocampus in schizophrenia. Schizophr Res 100, 120-132.

Acknowledgements

Writing this dissertation has been a great learning experience for me both academically and personally. A large number of people have contributed to make this possible.

I am greatly indebted to my supervisor Prof. Dr. Peter Kirsch for opening the door of neuroscience. His knowledge and experience helped in nourishing my interest in neuroscience as well as in conceptualising this dissertation. I take immense pleasure in thanking Prof. Dr. Klaas Enno Stephan for his valuable inputs and motivation through the methodology used in this study. I would also like to thank to Dr. Emili Balaguer for his guidance through my research and for valuable suggestions which contributed greatly towards developing this dissertation. I would like to express my gratitude to Prof. Dr. Andreas Meyer-Lindenberg for opening the door of the methodology with his recommendation letter. Finally, I would like to take this opportunity to thank to Prof. Dr. Rainer Spanagel for being my tutor at the University of Heidelberg.

My thanks and appreciations also go to my colleagues at the Department of Clinical Psychology at the Central Institute for Mental Health in Mannheim for their support during my work as well as for sharing their experiences. I would also like to thank to my colleagues at the Universities of Heidelberg, Zürich, and Barcelona for giving me valuable inputs that helped in improving my research.

I would like to express my sincere gratitude to the German Government for providing me with the financial assistance which made it possible for me to undertake my PhD studies. This work was funded by grants from the German ministry for Education and Research through the Bernstein Center for Computational Neuroscience (BMBF, 01GQ1003B) initiative and through the National Genome Research Network (NGFN plus MOODS).

I wish to thank my Friends at home and Ilvesheim. To my Friends in Ilvesheim, thank you for your time and companion. Special thanks to Claudio Sebastian Quiroga Lombard. I do not have words to convey my great respect and appreciation to you. Thank you very much for all your teachings. My appreciations also go to Anna Zarembo, Dennis Wolf, Stephan Richard Huber, Marco Grollmus, Dr. Juan De Álvaro, Behnaz Gholami, Olga Kornienko, Oliver Sukrow, Ms. Roswitha Rawle, and Mr. Matthias Ruf for sharing their experiences, understanding, patience, and providing me valuable information. Thank you very much for all you have done. I would also like to express my deepest gratitude to all Huber's Family members for their hospitality. Thank you very much for taking care of my personal situation. You will be always in my heart. To my Friends at home, thank you very much for your calls, e-mails, texts, visits and being there for me always. Special thanks to Jaime Gallego

Vila, David Matas Navarro, and Marc Poch Riera for your support. Thank you very much for organizing the very best trip ever. My appreciations also go to Gianfranco Andía Vera, Selva Vía Labrada, Tiago Marini Steck, and Shambhu Nath Jha for their advices and teachings. Finally, I would also like to thank to all the other Friends I did not mention but supported me in these years. Thank you very much to all of you for your time.

I would like to thank to my Family for always believing in me and wanting the best for me. To my Mom and Dad, thank you very much for making me who I am. You have shaped every personal value I have. To my Brother, thank you very much for your advices, talks, Figures, love… You know you are the number one. To my Sister-in-law, thank you for your support and T-Shirt. To my Parents-in-law thank you for your understanding and patience. To my Brother-in-law thank you for your kindness. To my Aunt Montse and Uncle Jorge thank you for your constructive advices. Finally, I would also like to thank the rest of my Family for their love. Thank you very much to all of you for your time. This journey would not have been possible without you.

Last but not least, I wish to avail myself of this opportunity to express my deepest gratitude and love to my Wife. I hope you know that without your tireless support, energy, and understanding I would have never written this dissertation. Y qué más puedo decirte… Sólo espero poder decírtelo cada día de mi vida.

Concluiré simplemente con lo siguiente: **“Somos un equipo”**